TECHNISCHE UNIVERSITÄT MÜNCHEN

TUM School of Life Sciences

Cholesterol-gut microbiome interactions as drivers of obesity and colorectal cancer

Akim Strohmeyer

Vollständiger Abdruck der von der TUM School of Life Sciences der Technischen Universität München zur Erlangung des akademischen Grade eines

Doktors der Naturwissenschaften

(Dr.rer.nat.)

genehmigten Dissertation.

Vorsitzender: Prof Dr. Dietmar Zehn

Prüfer der Dissertation:

1. Prof. Dr. Martin Klingenspor
2. apl. Prof. Dr. Klaus-Peter Janssen

Die Dissertation wurde am 13.07.2023 bei der Technischen Universität eingereicht und durch die TUM School of Life Sciences am 27.10.2023 angenommen

Table of Content

Abbrevations

AbX	Antibiotic treated
ANCOVA	Analysis of co-variance
ANOVA	Analysis of variance
AOM	Azoxymethane
Apc	Adenomatous polyposis coli
ATP	Adenosine triphosphate
BA	Bile acid
Chol	Cholesterol
Conv	Conventional
CRC	Colorectal cancer
DGE	Differential gene expression
DIO	Diet induced obesity
DIO2	Iodothyronnine deiodinase
DSS	Dextran sodium sulfate
ECM	Extracellular matrix
EMT	Epithelium to mesenchyme transformation
eWAT	Epidydimal white adipose tissue
FA	Fatty acid
FAME	Fatty acid methyl ester
FDR	False discovery rate
FFA	Free fatty acid
FXR	Farnesoid x receptor
GC-MS	Gas chromatography – mass spectrometry
GF	Germ free
GIT	Gastrointestinal tract
GSEA	Gene set enrichment analysis
HFD	High-fat diet
iWAT	Ingenual white adipose tissue
KRAS	Kirsten rat sarcoma
LOX	Lysyl oxidase
MK8	Menaquinol 8
MMP	Matrix Metalloproteinase
MUFA	Mono unsaturated fatty acid
NAFLD	Non-alcoholic fatty liver disease
NGS	Next generation sequencing
NMR	Nuclear magnetic resonance
OTU	Operational taxonomic unit
PCA	Principal component analysis
PCoA	Principal coordinate analysis
pgWAT	Perigonadal white adipose tissue
PICRUSt2	Phylogenetic investigation of communities by reconstruction of unobserved States

PLS-DA	Partial least squares – discriminant analysis
PUFA	Polyunsaturated fatty acid
RIN	RNA integrity number
ROS	Reactive oxygen species
SAFA	Saturated fatty acid
SCD1	Stearoyl coenzyme A desaturase 1
SCFA	Short chain fatty acid
SD	Standard deviation
Sele	Selectin E
Selp	Selectin P
SEM	Standard error of the mean
SNP	Single nucleotide polymorphism
SPF	Specific pathogen free
T2D	Type 2 diabetes
TGR5	G protein coupled bile acid receptor
WT	Wild type
CVD	Cardiovascular disease
TG	Triglyceride
DG	Diglyceride
MG	Monoglyceride
ER	Endoplasmatic reticulum
CD36	Cluster of differentiation 36
CD	Control diet
FATP4	Fatty acid transport protein 4
NPC1L1	Niemann pick 1 like 1
SR-BI	Scavenger Receptor BI
ABCG5	ATP-binding cassette subfamily G member 5
ABCG8	ATP-binding cassette subfamily G member 8
ApoB48	Apolipoprotein B48
ACAT	Acyl-CoA:cholesterol acyltransferases
TICE	Transintestinal cholesterol influx
BMI	Body mass index
ROS	Reactive oxygen species
RNS	Reactive nitrogen species
TME	Tumor microenvironment

List of figures

Main figures

Supplemental figures

List of tables

Abstract

Increasing numbers in global cases of overweight and obesity pose a high burden for healthcare systems. Not only metabolic diseases like type 2 diabetes or cardiovascular diseases but also several types of cancers are closely connected. Excess intake of dietary lipids is a major factor contributing to this development and has a direct impact on the microorganisms inhabiting the gastrointestinal system. In both obesity and colorectal cancer, distinct changes in these microorganisms, referred to as the microbiome, have been identified.

The present study aims at the comprehensive characterization of the molecular interplay between dietary fat, cholesterol, and the intestinal microbiome. A first employed dose-response experiment identified the lipid species cholesterol as driver of resistance to diet induced obesity in germ free mice. This resistance proved to be specific to microbiome deficient mouse models, which indicated that cholesterol-gut microbiome interactions are decisive. A targeted metabolomics analysis based on mass spectrometry then identified changes in the intestinal bile acid pool, which were connected microbial dysbiosis. By combining these findings with 16S sequencing in a multi-omics manner, the glyoxylate shunt, a metabolic adaptation with implications in metabolic diseases, was identified as a possible driver.

In a further approach, cholesterol and gut microbiota-driven carcinogenicity were investigated in a mouse model of intestinal tumors. Germ-free mice exhibited an overall increased tumor burden. A merged transcriptomics and stable isotope tracking analysis uncovered elevated fatty acid uptake and desaturation as possible metabolic drivers of tumorigenesis. Additionally, cholesterol-gut microbiota interactions were capable of ameliorating high-fat diet-induced tumorigenesis. In the absence of cholesterol, the cell surface proteins Selectin E and P stood out as top candidates with elevated expression. Beyond this, sequencing-based analysis of tumor-adjacent bacterial communities with modulatory influence on the identified candidate proteins in response to cholesterol was revealed.

Conclusively, the present work established a platform to study the interactions of the lipid cholesterol and gut microbial species with relevance to the diseases obesity and colorectal cancer. By extensively using germ-free mouse models and multi-omics technology, novel bacterial pathways and metabolites with potential implications were characterized.

Zusammenfassung

Die weltweit steigende Zahl der Fälle von Übergewicht und Adipositas stellt eine große Belastung für die Gesundheitssysteme dar. Nicht nur Stoffwechselkrankheiten wie Herz-Kreislauf-Erkrankungen oder Typ-2-Diabetes, sondern auch verschiedene Krebsarten stehen in engem Zusammenhang. Die übermäßige Aufnahme von Nahrungsfetten ist ein wichtiger Faktor, der zu dieser Entwicklung beiträgt und sich direkt auf die Mikroorganismen im Magen-Darm-Trakt auswirkt. Sowohl bei Adipositas als auch bei Darmkrebs wurden deutliche Veränderungen dieser Mikroorganismen, des so genannten Mikrobioms, festgestellt.

Die vorliegende Studie zielt auf die umfassende Charakterisierung des molekularen Zusammenspiels zwischen Nahrungsfett, Cholesterin und dem intestinalen Mikrobiom ab. Ein Dosis-Wirkungs-Experiment identifizierte die Lipidspezies Cholesterin als treibende Kraft für die Resistenz gegen ernährungsbedingte Fettleibigkeit bei keimfreien Mäusen. Diese Resistenz erwies sich als spezifisch für mikrobiomdefiziente Mausmodelle, was darauf hindeutet, dass die Wechselwirkungen zwischen Cholesterin und Darmmikrobiom ausschlaggebend sind. Eine gezielte Metabolomanalyse identifizierte dann Veränderungen im intestinalen Gallensäurepool, die mit einer mikrobiellen Dysbiose in Verbindung gebracht wurden. Durch die Kombination dieser Ergebnisse mit der 16S-Sequenzierung in einer Multi-omics-Analyse wurde der Glyoxylat-Beipass, eine Stoffwechselanpassung mit Auswirkungen auf Stoffwechselkrankheiten, als mögliche Ursache identifiziert. In einem weiteren Ansatz wurden dann Auswirkung von Cholesterin –Darmmikrobiota- Interaktionen auf die Kanzerogenität in einem Mausmodell für Darmtumore untersucht. Keimfreie Mäuse wiesen eine insgesamt erhöhte Tumorlast auf. Eine kombinierte Transkriptomik- und Stabile-Isotope-Tracking-Analyse deckte eine erhöhte Fettsäureaufnahme und -Entsättigung als mögliche metabolische Faktoren der Tumorentstehung auf. Darüber hinaus konnten die Interaktionen zwischen Cholesterin und der Darmmikrobiota die durch eine fettreiche Diät ausgelöste Tumorigenese umkehren. In Abwesenheit von Cholesterin stachen die Zelloberflächenproteine Selektin E und P als Top-Kandidaten mit erhöhter Expression hervor. Zusätzlich wurden Sequenzierungsanalysen von tumornahen Bakteriengemeinschaften durchgeführt und Spezies identifiziert, die direkt mit identifizierten Kandidatenproteine interagieren können.

Mit der vorliegenden Arbeit wurde eine Plattform zur Untersuchung der Wechselwirkungen zwischen dem Lipid Cholesterin und mikrobiellen Spezies im Darm geschaffen. Im speziellem wurden relevante Interaktionen für die Krankheiten Adipositas und Darmkrebs untersucht. Durch den umfassenden Einsatz von keimfreien Mausmodellen und Multi-Omics-Technologien wurden neue bakterielle Stoffwechselwege und Metaboliten idenfiziert, die eine Rolle in diesen Krankheitsbildern spielen können.

1. Introduction

1.1. Lipid absorption in health & disease

The absorption of dietary lipids plays a crucial role in the energy metabolism of the body. It has thus been thoroughly investigated with relevance to metabolic diseases, aiming on identifying targets for pharmacological interventions. Recent advances in biomedical research in this area have identified the involvement of bacterial species colonizing different body sites in metabolic health and disease, in this case particularly the gastrointestinal tract (Fan and Pedersen, 2021). These findings are based on observational and correlational data obtained in the past decades and thus mostly purely descriptive. In consequence, defining underlying mechanisms in a cause-effect manner is the aim of modern research in this field. As correlational studies have identified gut microbial signatures not only in metabolic diseases but also for several types of cancer, the relevance is even more emphasized on. Here, studies have already identified gut microbiota dependent mechanisms in the disease pathologies, mainly in the field of colorectal cancer, with therapeutic potential (Wong and Yu, 2023). Yet, there are still big unknowns, especially when it comes to the connection of obesity and colorectal cancer, which is increasingly relevant (Cani and Jordan, 2018; Keum and Giovannucci, 2019) Elucidating further mechanisms in gut microbiome-host interactions is thus of utterly importance. Particularly, this calls for studies investigating not only gut microbiome-host interactions in either metabolic diseases or colorectal cancer, but in a combined and targeted manner. Thus, the present study aims on deciphering molecular gut microbiome-host interactions, which pose a combined relevance in obesity and colorectal cancer. As target lipid species in this context cholesterol was chosen, which has numerous implications in both disease pathologies (Huang, Song and Xu, 2020) and additionally interacts with the gut microbiota.

Generally, the most important site for the molecular processes facilitating lipid absorption is the small intestine, especially its upper parts. Major proportions of the lipids derived from ingesting foods found in a human body are fatty acids in the form of triglycerides and cholesterol (Baynes, 2014). Overconsumption of energy rich foods, which consist mainly of lipids and carbohydrates, is the main driver of obesity development in the western world. Obesity and excess lipid intake are further connected with diseases like cardiovascular diseases (CVD), type 2 diabetes (T2D), non-alcoholic fatty liver disease (NAFLD) and several types of cancers, among them colorectal cancer (CRC; Haslam and James, 2005).

1.1.1. Molecular regulation of intestinal lipid absorption

Before investigating the role of the gut microbiome in lipid absorption physiological processes in this field have to be defined. The digestion and absorption of fatty acids is a complex process involving numerous steps and rate-determining enzymes. Fatty acids are present in the diet mainly in the form of triglycerides (TG). Upon entering the stomach digestion starts by the breakdown of TGs through gastric lipase (most important in infants) and pancreatic lipase (most important in adults, Hamosh *et al.*, 1981). TGs are broken down into diglycerides (DG), monoglycerides (MG), free fatty acids (FFA) and glyceride. When entering the small intestine, dietary lipids are further emulsified by bile acids, which additionally increase the activity of the pancreatic lipase. The resulting micelles are then transported to the enterocytes where the actual absorption process takes place. Major transporters responsible for the uptake into enterocytes are cluster of differentiation 36 (CD36) and, to a lower degree, fatty acid transport protein 4 (FATP4; Ko *et al.*, 2020). Both of them, however, are suggested to play a minor role in intestinal lipid absorption, as experiments in mice propose (Drover *et al.*, 2005; Shim *et al.*, 2009). Instead, passive diffusion is the primary way of FAs entering the enterocyte. In the cell, FAs and MAGs are re-esterified by the respective actions of MGATs and DGATs in the ER. The resulting TGs can either be stored in lipid droplets or designated for secretion via chylomicrons. Chylomicrons are complexes consisting of TGs, cholesterol, lipoproteins and phospholipids. Biosynthesis and maturation of chylomicrons is multi-step process including addition of the lipoprotein Apolipoprotein B48 (ApoB48) and other Apolipoproteins. Upon maturation, chylomicrons enter the system by delivery into lymphatic vessels, enter the blood stream at the thoracic duct, and are transported to other organs, e.g. the liver or adipose tissue (Wit *et al.*, 2022).

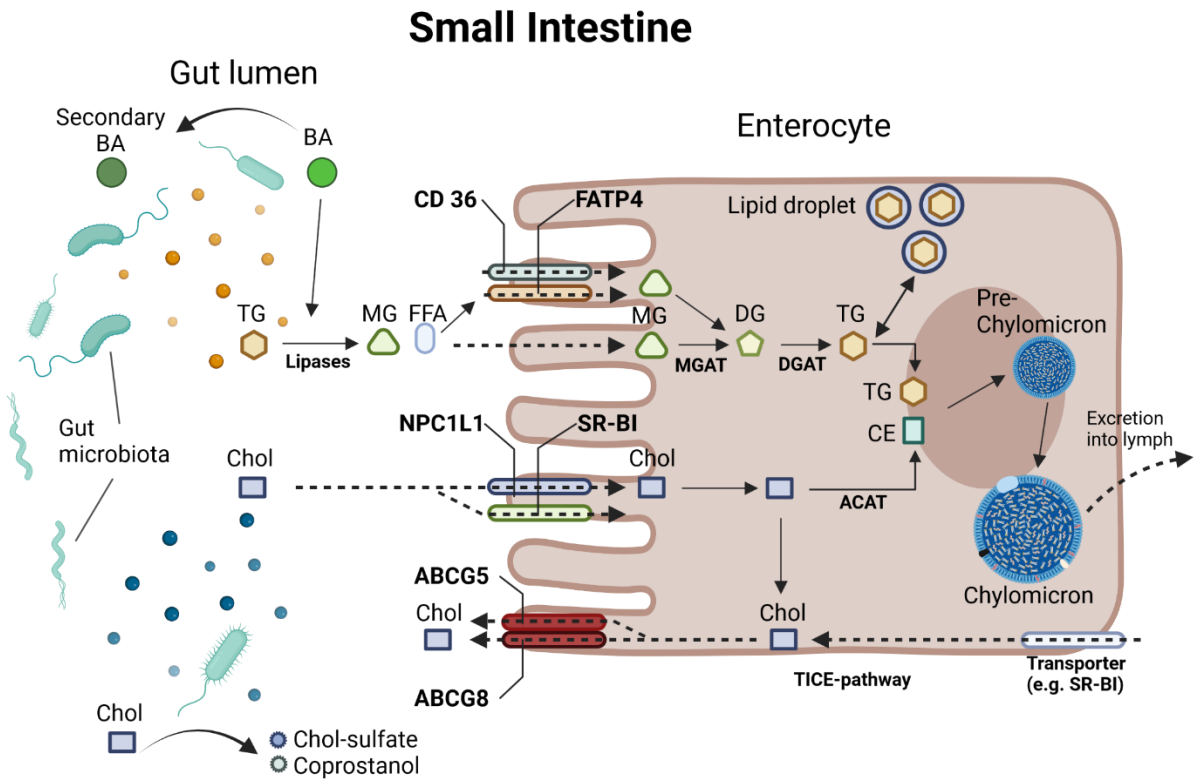

Figure 1: Summary of intestinal fatty acid and cholesterol absorption

Dietary lipids are predominantly absorbed in the upper regions of the small intestine. After breakdown through lipase activity and emulsification with bile acids, FAs and Chol are absorbed either by transporter activity or, in case of FAs, by passive diffusion. In the cell, FAs and Chol are re-esterified by their respective enzyme cascade and incorporated into chylomicrons, which are subsequently excreted into the lymphatic system. In the case of cholesterol, also excretion from the system into the gut lumen can take place, a process referred to as TICE. Small intestinal gut microbiota can influence these processes e.g. by the conversion of primary into secondary bile acids or by converting cholesterol into cholesterol-sulfate or coprostanol. BA, bile acid; TG, triglyceride; DG, diglyceride; MG, monoglyceride; chol, cholesterol; CD36, cluster of differentiation 36; FATP4, fatty acid transport protein 4; NPC11L, Niemann Pick 1C Like 1; SR-BI, Scavenger Receptor class B type 1; ABCG5, ATP-Binding cassette subfamily G member 5; ABCG8 ATP-Binding cassette subfamily G member 8; MGAT, monoacylglycerol acyltransferases;DGAT diacylglycerol acyltransferases; ACAT acyl-CoA:cholesterol acyltransferases.

Cholesterol is predominantly present in the diet in the raw form or esterified with a fatty acid. Thus, digestion of cholesterol starts as well by the breakdown through lipase activity. It is then further incorporated into micelles and transported to the enterocytes. The most important intestinal segments for the uptake of cholesterol are the Duodenum and the proximal Jejunum (Wang, 2003). Uptake of cholesterol into the enterocytes is facilitated by Niemann Pick C1 Like1 (NPC1L1) and accounts for about 70% of intestinal cholesterol absorption in mice (Jia, Betters and Yu, 2011). Another transporter implicated in cholesterol uptake into enterocytes is the Scavenger Receptor class B type 1 (SR-BI), yet its importance is more controversial (Mardones *et al.*, 2001). In the enterocyte, absorbed free cholesterol

is esterified by the action of acyl-CoA:cholesterol acyltransferases (ACAT) and incorporated into chylomicrons as one of their core elements (Dawson and Rudel, 1999). In contrast to the luminal absorption of cholesterol, enterocytes are also capable of releasing cholesterol into the gut lumen, a process referred to as transintestinal cholesterol efflux (TICE). This systemic removal is facilitated by the transporters ATP-binding cassette subfamily G member 5 and 8 (ABG5 and ABCG8), which form a heterodimer. TICE is a well-accepted essential pathway of cholesterol clearance in mice and humans (Jakulj *et al.*, 2016).

1.2.The (small) intestinal gut microbiome

The term “microbiome” refers to the sum of all microbes, including bacteria, viruses and fungi, their genes and gene products that are found in the mammalian body. Initially found to be negligibly connected to the described molecular machinery of intestinal lipid absorption recent studies proved these interactions to be directly relevant (Martinez-Guryn *et al.*, 2018). Whereas basically all body sites are colonized, the by far highest numbers and diversity can be found in the digestive system (Lloyd-Price *et al.*, 2017). In the gut, a concentration gradient is present along the intestinal system. The Duodenum contains a comparable low number of microbes of 10^7 per gram wet weight, which increases along the Jejunum to an amount of 10^{11}per gram wet weight in the Ileum. The highest number can be found in the colon, with numbers ranging up to 10^{14} microbes per gram wet weight (Sender, Fuchs and Milo, 2016). Due to this high number and its accessibility by taking stool samples most studies investigating host-microbiome crosstalk have focused on the large intestinal microbiome, which is thus well characterized (Kastl *et al.*, 2020).

Studies investigating the small intestinal microbiota remained scarce for a longer period, which is mainly owed to the more difficult accessibility. Given the fact that the small intestine is the main site of nutrient uptake and contains the largest mucosal surfaces with gut receptors, immune cells and nerve cells increasing research focus is placed on microbiota-host interactions here (Willem M de Vos *et al.*, 2022). This is especially important with relevance to lipid metabolism, which is also mainly facilitated here.

1.2.1. Microbiome in Obesity

The global numbers of overweight and obesity are rising, with about 1.9 billion adults and 380 children million affected respectively according to the WHO (*Obesity and overweight*, 2023). Connected with the resulting rising comorbidities, this generates a large burden for the health systems, especially in low-income countries. Changes in the gut microbiome

have been elucidated extensively in the last decade, discovering a multitude of microbiome dependent variations with relevance to obesity and its comorbidities (Carmody and Bisanz, 2023).

The concept of gut microbiota being involved in energy and nutrient harvest from the gut first evolved in the early 2000s (Bäckhed *et al.*, 2004) .It was then reported for the first time in 2007 that germ free mice are resistant to diet induced obesity (DIO) when fed a western type high-fat diet (HFD, Bäckhed *et al.*, 2007). Following this discovery, numerous further studies have been conducted to identify the underlying mechanism of this phenotype. The quality and composition of the diet was recognized to be a pivotal factor (Fleissner *et al.*, 2010). In further experiments the dietary fat source could be identified as a driving factor for this resistance with potential implications of dietary cholesterol (Kübeck *et al.*, 2016). Particularly, the authors fed diets with different primary fat sources, containing either animal-based lard or plant based palm oil. Only the lard-based diet was capable of inducing the DIO resistant phenotype in the GF mice and no resistance was detectable in conventional mice. Analysis of metabolites and gene expression yielded differences in cholesterol derived metabolites and the expression of cholesterol related hepatic genes Cyp7a1 and Nr1h4 (Kübeck *et al.*, 2016).

Whereas this pointed toward a clear resistance to diet-induced obesity in GF mice recent studies failed to reproduce these results, with GF mice showing the same induction of obesity as conventional (Conv) mice (Moretti *et al.*, 2021). Additionally, human trials investigating the efficacy of microbial interventions on obesity generally failed to achieve a reduction in body weight. However treatments showed potential towards improved lipid and glucose metabolism (Depommier *et al.*, 2019). Resulting from these findings the field now focuses more on deciphering specific microbiota dependent mechanisms with relevance to obesity and its comorbidities.

1.2.2. Interactions of gut microbiota and lipids

As this finding draws a clear correlation in obesity, the gut microbiome and intestinal and systemic lipid metabolism there is a growing interest in comprehending this intricate connection. Focus is thus placed on the molecular machinery connecting diet, microbiota, and their role in regulating lipid absorption, metabolism, and energy balance in the host. Various microbial signatures and metabolic pathways can influence these processes through numerous mechanisms. The impact of the gut microbiota on host lipid metabolism and overall lipid composition can be directly observed in different areas such as the plasma,

liver, and different segments of the intestines (Kindt *et al.*, 2018; Liebisch *et al.*, 2021). Feeding mice a HFD leads to specific changes in the microbiota of the Jejunum, resulting in a distinct HFD-associated microbial signature. When this signature is transferred to germ-free mice, it enhances lipid uptake not only on a HFD but also on a regular low-fat diet, indicating that the small intestinal microbiota can affect lipid absorption independently of the diet (Martinez-Guryn *et al.*, 2018). This effect is likely due to altered metabolic pathways associated with changes in microbiota signatures, which can persist even without continuous HFD feeding. Another study describes how bacterial metabolites like L-lactate or acetate directly influence the lipid metabolism of enterocytes by inhibiting the secretion of chylomicrons through various mechanisms (Araújo *et al.*, 2020). Additionally, short-chain fatty acids produced by bacterial fermentation of dietary fiber enter the bloodstream and serve as building blocks for the synthesis of long-chain fatty acids in the liver (Kindt *et al.*, 2018). Certain bacterial taxa, such as Lactobacillaceae, metabolize dietary polyunsaturated fatty acids (PUFA) as a defense mechanism against antimicrobial toxins. In mice fed a HFD supplemented with the omega-6 PUFA linoleic acid, the introduction of specific bacterial strains capable of producing a metabolite called 10-hydroxy-cis-12-octadecenoic acid (HYA) improved diet-induced obesity, adipose tissue inflammation, and glucose tolerance (Miyamoto *et al.*, 2019). HYA stimulated the secretion of glucagon-like peptide 1 (GLP1) from enteroendocrine cells and enhanced intestinal peristalsis through the prostaglandin 3 receptor (EP3), resulting in reduced intestinal lipid absorption. Mono-association of germ-free mice with HYA-producing bacterial strains confirmed the beneficial impact of these microbes (Miyamoto *et al.*, 2019).

In comparison to studies investigating the gut microbial influence on nutrient absorption, investigation of microbiome-cholesterol interactions are more uncommon. A long known and major bacterial mechanism of cholesterol turnover is the conversion of cholesterol to coprostanol (Juste and Gérard, 2021). Bacteria harboring pathways for this conversion are capable of reducing systemic host cholesterol levels, which is strongly associated with a reduced risk of CVD (Kenny *et al.*, 2020). Besides these well-known pathways, gut bacteria are further able to modulate cholesterol itself. A combined mass spectrometry and sequencing approach yielded the bacterial transformation of cholesterol to cholesterol sulfate in mice and humans (Le *et al.*, 2022). Cholesterol sulfate was further identified to be able to reduce inflammatory response in the gut and alleviate ulcerative colitis (Xu *et al.*, 2022).

These findings present the rather new concepts in gut microbiome- lipid interactions that have been established after coming from correlational studies. In the case of the lipid

cholesterol, interactions have been described as, yet mechanistic outcomes with relevance to disease pathologies are scarcer, which emphasizes on the need for further studies.

1.3. Colorectal cancer

In synopsis of the present work so far the influence of gut microbiome interactions with lipid species can be regarded as factor in obesity development. Another disease, where the interplay of lipid species and the gut microbiome play an emerging and that is further directly connected to obesity colorectal cancer (CRC). CRC ranks among most common cancers globally. In numbers, it accounts for the third most new cancer cases as well as for the third most cancer related deaths in humans (Siegel, Miller and Jemal, 2019). In the last decades the global diagnosed cases of CRC showed an increasing trend, which are estimated to hit 2.2 million cases, with 1.1 million deaths by 2030 (Arnold *et al.*, 2017). Rises in these numbers are especially seen in middle and low-income countries, which can be attributed to the adoption of "western" lifestyles in these countries. This lifestyle is defined by the intake of poor diets and alcohol, smoking reduced level of physical activity and ultimately the development of obesity (Keum and Giovannucci, 2019).

Next to the commonly known connection between obesity and metabolic diseases, excess body fat and body weight are further considered major risk factors for several types of cancer, among them CRC. Estimates range that obesity accounts for up to 20 % of all cancer related deaths (Calle *et al.*, 2003; Calle and Kaaks, 2004). These findings are mostly based on epidemiological studies based on body mass index (BMI) or waist circumference, which are rather blunt measures to capture the complex biology in this interplay. The cancer promoting character of an obese state is mainly attributed to a chronic level of inflammation of the adipose tissue (Quail and Dannenberg, 2019). Other factors involved are the direct influence of a high fat intake, which is often connected with an obese state, or a gut microbial dysbiosis (O'Keefe, 2016). Entangling the direct contribution of these two connected risk factors and obesity alone is subject to current research. Especially in the case of CRC investigating this interplay and establishing a mechanistic relationship is of utterly importance due to the direct exposure to fat and the gut microbiota in the intestine.

1.3.1. Risk factors for colorectal cancer – the gut microbiome

It is estimated that about 65 % to 88 % of CRC cases happen spontaneously and not resulting from genetic disposition (Lichtenstein *et al.*, 2000). Identification of potentially modifiable risk factors is thus considered a promising approach. The intestinal gut

microbiome is known to be involved in colorectal tumorigenesis since the 1960 and its role in intestinal carcinogenesis has received a lot of attention in the last decade (Laqueur, McDaniel and Matsumoto, 1967; Wong and Yu, 2019). Compared to obesity more mechanistic findings linked to disease pathologies have already been identified. Some of the bacterial taxa, where accumulating evidence exists are *Fusobacterium nucleatum*, *Escherichia coli* and *Bacteroides fragilis*.

F. nucleatum was one of the first bacterial species of the gut microbiome, which was identified to be involved in colorectal tumorigenesis. Correlational studies identified its presence in patients to be correlated with patient outcome and shorter survival in CRC patients (Flanagan *et al.*, 2014; Mima *et al.*, 2016). Mechanistically, *F. nucleatum* is proposed to promote immune evasion and an anti-inflammatory tumor microenvironment (Tilg *et al.*, 2018). Mucosa-associated *E. coli* has also been identified with an increased abundance in CRC tissue and association with tumor stage and prognosis (Bonnet *et al.*, 2014). This has been attributed to the *E. coli* produced colibactin, which causes DNA damage. In a similar manner *B. fragilis* is connected to CRC, which is proposed to cause inflammation-related tumorigenesis by secretion of the BFT toxin (Tilg *et al.*, 2018).

In addition to the directly defined actions of the above-mentioned bacterial species, the gut microbiota harbors more general mechanisms with relevance to intestinal carcinogenesis. One of the key areas is the microbial metabolism of dietary components. Several metabolites produced in this processed have been identified to be either pro- or anti-tumorigenic. Pathways producing detrimental metabolites include the products of bacterial protein fermentation, the production of hydrogen sulphide and secondary bile acids. Bacterial protein fermentation of aromatic amino acids N-nitroso compounds, which act pro-tumorigenic and cause mutations via DNA-alkylation (Gill and Rowland, 2002). Another pro-tumorigenic bacterial metabolite is hydrogen sulphide, which is produced from diet-derived sulfate and damages the colonocyte barrier (Marquet *et al.*, 2009). *Desulfovibrio spp.* is well known for this metabolic process. Special attention also goes to the bacterial conversion of primary to secondary bile acids (BAs). BAs exhibit strong antimicrobial actions, and thus modify composition of the gut microbiota. Microbial conversion of bile acids starts in the small intestine and is then extensively performed in the large intestine. The resulting secondary BAs are more hydrophobic than primary BAs, which boosts their ability to generate pro-tumorigenic ROS and RNS (Louis, Hold and Flint, 2014).

In contrast to these carcinogenic mechanisms, also tumor suppressive mechanisms of the gut microbiota have been identified. The most famous is the fermentation of dietary non-

digestible carbohydrates like dietary fibre and resistant starch to short chain fatty acids (SCFAs). Upon bacterial fermentation, SCFAs are quickly absorbed by colonocytes and further metabolized. Especially butyrate has been identified to act anti-inflammatory by inhibiting histone deacetylation and thus downregulate pro-inflammatory cytokines (Chang *et al.*, 2014). Further anti-inflammatory actions have been identified by modulating colonic regulatory T-cell responses (Furusawa *et al.*, 2013). Other tumor suppressive actions of gut microbiota comprise the biotransformation of phytochemicals, although mechanisms here are less defined and require further evaluation (Cani and Jordan, 2018).

The capability of the gut microbiota to act either pro or anti tumorigenic is also reflected in experimental settings using germ free mouse models, which are considered as gold standard in microbiome research. Results from these studies deliver conflicting results, with some yielding either increased or decreased tumorigenesis in microbial absence (Leystra and Clapper, 2019). Deciphering the interplay of specific components and classes with the gut microbiota thus poses promising new insights.

1.3.2. Aberrant lipid metabolism in colorectal cancer

A central aspect of identifying CRC relevant mechanisms in the interplay of the gut microbiome and lipid species is defining the pathological lipid metabolism. Generally, cancers show an extensive need for energy to fuel cell growth and proliferation, which results in a wide range of metabolic perturbations to adapt to those needs. The most famous is probably the Warburg effect, which identifies anaerobic glucose metabolism even in the presence of oxygen in tumor tissue (Warburg, 1956). Another key feature of cancer metabolism is the enhanced dependence on lipids and in particular fatty acids, which are obtained by intracellular synthesis or cellular uptake (Snaebjornsson, Janaki-Raman and Schulze, 2020). Because of this characteristic feature of reshaping lipid metabolism, cancer shows changes in the lipid profiles found in tumors across various organs such as the liver, lung, and the colon (Vriens *et al.*, 2019; Ecker *et al.*, 2021). The complexity of cancer related alterations in FA metabolism has been demonstrated in a recent study. Vriens et al showed that cancer cells where capable of bypassing SCD-dependent desaturation by an unusual desaturation pathway and thus producing the FA sapienate (Vriens *et al.*, 2019). SCD-dependent desaturation is generally considered the only synthesis pathway of MUFAs and essential for tumor growth and progression (Snaebjornsson, Janaki-Raman and Schulze, 2020). Such metabolic reprogramming of lipids extends to the surrounding tumor microenvironment, affecting also surrounding tissue. In CRC, it has been demonstrated that cancer-associated fibroblasts derived from malignant tissue exhibit an increase in FAs and

phospholipid accumulation while experiencing reduced breakdown, which influences the migration of cancer cells (Gong *et al.*, 2020).

The balance between de novo synthesis and uptake of lipids is directly influenced by the presence of various lipid species in the surrounding extracellular environment. This availability is not only affected by the lipid composition of the diet but is also impacted by the heterogeneity present in the tumor microenvironment (Röhrig and Schulze, 2016). In contrast to other cancers, CRC has the unique feature of lipids being present directly in the gut lumen. Next to obesity, intake of FA rich diets has been identified as a risk factor for CRC development (Steck and Murphy, 2020). This increased intake results in higher luminal availability of FAs, which in turn also alters present gut microbiota. A recent study investigating FA induced tumorigenesis and its dependence on gut microbiota in preclinical models identified HFD-induced changes in gut microbial metabolism as driver of aggravated tumorigenesis. HFD feeding in microbial deficiency resulted in no altered tumorigenesis compared to controls (Yang *et al.*, 2022).

Besides FAs, also cholesterol and aberrations cholesterol metabolism are regarded as essential to cancer development and growth. Cholesterol is a major sterol component of cell membranes and cholesterol-derived metabolites have intricate functions in both facilitating cancer progression and suppressing immune responses (Huang, Song and Xu, 2020). Cholesterol further shapes the tumor microenvironment, yet in the case of CRC, exogenous and dietary cholesterol have to be separated. Luminal cholesterol can either shape the TME directly or after its conversion to cholesterol metabolites by gut microbial action. Increased intake of dietary cholesterol is generally regarded as a risk factor for CRC. It has to be mentioned though that intake of dietary cholesterol is usually connected with other risk factors, which makes separation difficult (Hu *et al.*, 2012). Deciphering differing effects of endogenous and dietary cholesterol on tumor-related lipid metabolism with respect to gut microbiota can thus bring new insights into the specific role of luminal lipids in CRC.

1.4. Objectives

The overall aim of the present study was to elucidate the role of dietary cholesterol and gut microbiome-cholesterol interactions with relevance to obesity and CRC. Two murine disease models were thus introduced and comprehensively compared in germ free and conventional experimental settings.

The identification of mechanisms in the complex interplay of gut microbiome and lipid species interactions requires defined and targeted approaches. As a first objective of this work, the initial finding that germ free mice are resistant to diet induced obesity (Kübeck *et al.*, 2016) was reproduced. To refine the findings a purified diet supplemented with cholesterol was used. By employing a dose-response experiment in two microbiome deficient mouse model a solid backbone was established to specifically study disease relevant interactions in response to cholesterol

Following this, the second aim of this study was then to investigate gut microbiome-cholesterol interactions that are implicated in the resistance to obesity. Special focus was placed on two parts: First, differences in energy balance and cholesterol homeostasis parameters and secondly changes in gut microbial functional profiles. Even though clear results were obtained for obesity parameters changes in relevant metabolic processes were conflicting. Nevertheless, an interesting functional gut microbiota profile with potential implications in obesity was identified here.

The third aim of the present study was subsequently to identify cholesterol and gut-microbiome cholesterol interactions with relevance to colorectal cancer. The Apc^{1638N} mouse model for intestinal tumorigenesis was thus included in germ free and conventional settings. Cholesterol was thought to influence the intestinal tumorigenesis either alone or in interaction with the gut microbiota. Interestingly, the gut microbiota was clearly required to influence tumorigenesis here. A downstream multi-omics analysis revealed a complex interplay of cancer dependent adhesion-molecules and gut microbial action as underlying mechanism.

2. Material & Methods

2.1. Animal experiments

For the studies male C57Bl6/N (SPF), C57Bl6NJ (GF) and male as well as female Apc1638N were selected. Germ free mice were initially supposed to be Bl6/N, however SNP analysis of 39 strain specific SNPs yielded 5/39 Bl6/J specific SNPs and are therefore referred to as Bl6/NJ. Conventional Apc mice breeding pairs were derived from GF mice to preclude genetic differences. All animal experiments were conducted in either the SPF-I, SPF-II or Gnotobiology facility of the Technical University of Munich, School of Life Sciences Weihenstephan. Mice were bred in house and group housed at 22 ± 1 °C and 12 h/12 h light – dark cycles at ~ 55% humidity with *ad libitum* access to water and food prior and during the experiments. Before the experimental phase, all mice were fed a standard chow diet (Ssniff, V1124-300). Conventional (Conv) and antibiotics treated(AbX) animals were housed in individually ventilated cages (Greenline IVC, Tecniplast, 501 cm²), GF mice were housed in an open cage system (M2: 360 cm²; M3: 540 cm², Harlan) placed in a plastic film isolator (Harlan). Sterility inside the isolator was controlled regularly by aerobic and anaerobic cultivation in the Core Facility Microbiome of the ZIEL Institute for Food & Health as well as Gram staining of fecal smears and 16S rRNA gene targeted qPCR. No contaminations were detected during the experiments. In all facilities hygiene monitoring according to FELASA guidelines was performed quarterly to confirm the absence of pathogens. All experiments and procedures were approved by the local authorities in charge (Regierung von Oberbayern, approval number ROB 55.2-2532.Vet_02-19-193) according to national law.

2.1.1. Diets

All research diets were supplied by Ssnif Spezialdiäten GmbH (Soest, Germany). Until the start of the experiment at the age of 8 weeks mice received an autoclaved standard chow diet (V1124-000). Diets were then switched to a chemically defined CD until the age of 12 week followed by the respective experimental diet. In all diets the fibre component was modified using Inulin (2.5%) and oat fibre (2.5%) to account for the influence this component has on the intestinal microbiome (Morrison *et al.*, 2020). Sterilization of the specialized diets was performed by radiation at 50 kGy independent of the facility. Cholesterol was supplemented as raw substance (purity >95%; 97-103% total sterols). Table xy displays a detailed summary of the dietary composition.

Table 1: Composition of experimental mouse diets. Only one cholesterol-supplemented diet is shown exemplary, the others used differ just in the amount of the cholesterol component.

Ingredients [%]	**Control diet**	**PHFD + 0.00**	**PHFD + 0.05**
Product No.	*S5745-E906*	*S5745-E920*	*S5745-E924*
Casein	24.0	24.0	24.0
L-Cystine	0.2	0.2	0.2
Corn Starch	47.8	27.8	27.748
Maltodextrin	5.6	5.6	5.6
Sucrose	5.0	5.0	5.0
Inulin	2.5	2.5	2.5
Oat fiber	2.5	2.5	2.5
Vitamin premix	1.2	1.2	1.2
Mineral Premix	6.0	6.0	6.0
Choline Cl	0.2	0.2	0.2
Cholesterol. < 96 %	-	-	0.052
Palm oil	-	20.0	20.0
Soybean oil	5.0	5.0	5.0
Proximate contents			
Crude Protein	21.1	21.1	21.1
Crude fat	5.1	25.1	25.1
Crude fiber[1,2]	4.8	4.8	4.8
NDF[1,2]	2.3	2.3	2.3
Soluble fiber[1,2]	2.1	2.1	2.1
Total dietary fiber[1,2]	4.5	4.5	4.5
Crude ash	5.4	5.4	5.4
Starch	45.9	26.7	26.7
Dextrin	5.5	5.5	5.5
Sugar	6.2	6.2	6.2
Energy (Atwater)	15.4	19.7	19.7
Protein	23	18	18
Fat	13	48	48
Carbohydrates	64	34	34

1) *Calculated with 94% crude fiber, 90 % total dietary fiber and 85% soluble fiber*

2) *Calculated with 94% crude fiber, 90 % total dietary fiber and 85% soluble fiber*

3) *Physiological fuel value*

2.1.2. Antibiotic treatment

Antibiotic treatment started at an adult age of 12 weeks to prevent growth related implications and lasted until the end of the feeding trial at 20 weeks. Because of the rather long treatment period of 8 weeks the antibiotic cocktail was limited to two substances. Both Neomycin and Vancomycin are poorly absorbed in the GIT, further limiting the impact on the host (Zhang *et al.*, 2014). Neomycin (1g/l, bela-pharm, Vechta, Germany) and Vancomycin (0.5g/l, Eberth Arzneimittel, Ursensollen, Germany) were freshly dissolved in the *ad libitum* available drinking water. Water bottles were covered with tin foil to avoid photodegradation and changed 2 times a week. Drinking behavior of the mice was screened regularly to avoid dehydration and no complications were detected during the experiments.

2.1.3. Mouse model for intestinal tumorigenesis

To analyze the influence of high-fat diets on the development and progression of colorectal cancer, mice of the Apc^{1638N} model were used. These mice harbor a knockout mutation in the tumor suppressor gene Apc, with the allele Apc^{1638N} (international nomenclature: Apc^{tm1Rak}; first described: Fodde *et al.*, 1994). The allele Apc^{1638N} is lethal in the early embryonic stage in homozygous status, therefore only heterozygous animals are used for breeding and experiments. A mutation in this gene is considered the first step in the development of the vast majority of all sporadic, i.e. non-hereditary, colorectal carcinomas in humans, as well as in the hereditary FAP syndrome (Kinzler and Vogelstein, 1996; The Cancer Genome Atlas Network, 2012). In the mouse model, the phenotype results in the formation of intestinal polyps in nearly 100% of the mice. Several polyps (3-5 adenomas, or adenocarcinomas) develop per animal in the small intestine and less frequently in the large intestine, the appearance of which is associated with anemia, weight loss, and splenomegaly. Obstruction of intestinal passage has never been observed, nor have metastases to other organs. Tumors form after a latency period of ~ 6 months, before that only microadenomas (< 1 mm) are detectable, making this model a suitable choice for steady interventions such as feeding experiments (Zeineldin and Neufeld, 2013).

2.1.4. Genotyping

Mice were genotyped at an age of 3-4 weeks using earpieces obtained during tagging. Tissues were lysed in tail-buffer (10 mM TRIS, 50 mM KCl, 0.45 % Nonidet P40, 0.45 % Tween-20, 10 % gelatin in H_2O at pH 8.3 % with 0.2 mg/ml Proteinase K) for at least 4h at

65°C and constant shaking followed by inaction of Proteinase K at 95°C for 10 min. The resulting DNA – containing mix was analyzed using the PCR setup shown in table 2.

Table 2: PCR Setup for Genotyping of Apc^{1638N} mice

Component	Reaction Volume [µl]
2x MyTaq Mix (Bioline)	10
Nuclease-free water	7
Forward primer (10 µM)	1
Reverse Primer (10 µM)	1
DNA mix	1
Total	20

Step	Temperature [°C]	Time [s]	Cycles
Initiation	94	60	1
Denaturation	94	20	30
Annealing	58	20	30
Extension	68	20	30
Final extension	68	60	1
Cooling	10	pause	∞

Primer no.	Position	Sequence
2604	APC Gene - Forward	CAGCCATGCCAACAAAGT
2605	APC Gene - Reverse	GGAAAAGTTTATAGGTGTCCCTTCT
2606	Neomycin cassette - Reverse	GCCAGCTCATTCCTCCACTC

All used primers were synthesized by Eurofins Genomics, Ebersberg, Germany.

2.1.5. Sampling

Mice were asphyxiated using CO_2 und subsequently blood and organs were collected, shock frozen using liquid nitrogen and stored at -80 °C until further analysis. To investigate the role of different intestinal segments the intestinal tract was subdivided into different segments. For the WT mice small intestinal segments were defined as Duodenum (proximal 8cm) – Jejunum (middle region) – Ileum (distal 8 cm) (Fig. 2 A).

Apc^{1638N} smile intestinal segments were defined as Periampulary Region (0.5 cm proximal) – Duodenum (proximal 1/3) – Jejunum (middle 1/3) – Ileum (distal 1/3). For the assessment

of tumor burden the whole GIT was removed and directly transferred to an ice- cooled glass plate. Intestinal segments were separated, cut longitudinal and transferred to filter paper (Biorad Laboratories, Hercules, California, USA). Tumor size was assessed by calculating the product of the long diameter and the short diameter measured with a transparent laboratory ruler. An exemplary picture of a duodenal section with tumors marked is shown in Figure 2 B.

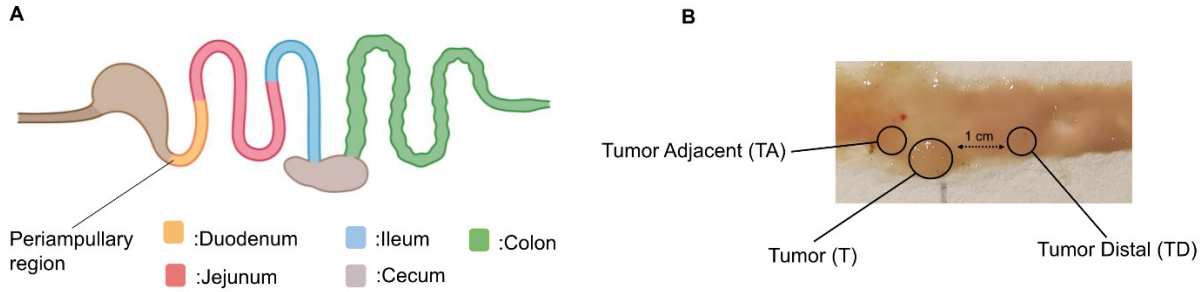

Figure 2: Intestinal segment definition

*Due to the lack of physiological partitioning, the small intestinal segments (**A**) have to be defined as described in the text for the different experiments. For the scoring of the tumoral burden and sampling of tumor tissue segments (**B**) were fixed on filter paper on a cooled glass plate, measured, and then collected separately. Samples were defined as Tumor (T), Tumor Adjacent (TA) directly next to the Tumor sample and Tumor Distal (TD) as distal of the tumor sample.*

2.2. Metabolic Phenotyping

2.2.1. Bomb calorimetry

Bomb calorimetry was used to determine energy content of food and feces and thus calculate energy intake and fecal excretion. Measurements were performed after at least one week of dietary adaption, at an age of 13-14 weeks. Cage contents of group-housed mice were collected after 3-5 days and dried for 24-48h. For the separation of dietary residuals, embedding, and feces, a multi sieve shaker (VWR, Darmstadt, Germany) with a respective sieve system (5 mm – 1 mm,) was used. Feces were dried at 55°C for 5 -7 days, homogenized using a TissueLyser (Retsch) and pelletized using an in house built pelleting press. 1g pellets were applied to the bomb calorimeter (Parr 6400, Parr instruments, Moline, Illinois, USA) and burned at a high-pressure oxygen atmosphere of 30 bar. In the case of limited material available a combustion aid (Benzoic Acid, Parr instruments, Moline, Illinois, USA) was added. Dietary energy content was determined by burning 1g of diet collected from feeding racks to preserve the feeding state.

Energy intake was calculated as the amount of diet consumed multiplied with dietary energy content and normalized to 24h and mouse number per cage. Fecal energy content values were normalized to 1g and mouse number per cage. Germ free and AbX mice have a liquid, diarrhea like fecal texture (Clavel *et al.*, 2016) making comprehensive collection and separation of feces impossible, therefore no assimilation efficiency values have been calculated.

2.3. Next Generation Sequencing

2.3.1. 16S rRNA Sequencing

Intestinal scrapings were obtained by carefully scraping pinned section with a sterilized microscope slide and then collected together with cecal contents and immediately snap frozen in liquid nitrogen and stored at -80 °C. DNA isolation, library preparation and sequencing were performed at the ZIEL – Core Facility Microbiome of the Technical University of Munich according to published protocols (Reitmeier *et al.*, 2020). Briefly DNA was isolated using a MaxWell® DNA isolation kit (Promega GmbH, Walldorf, Germany). Primers targeting the bacterial V3-V4 region of the 16S rRNA gene including a forward and reverse Illumina specific overhang and a barcode were used. PCR cycles in the second PCR were increased by 10 to 25 for scrapings due to the lower microbial density. Sequencing was then performed on an Illumina MiSeq® device.

Obtained sequencing files were demultiplexed and analyzed using the IMNGS2 platform, which is based on the UPARSE approach for sequence quality check, chimera filtering and cluster formation (Lagkouvardos *et al.*, 2016; https://www.imngs2.org/). Analysis was performed using standard values for barcode mismatches, trimming, expected errors and abundance cutoff. Downstream analysis of the IMNGS platform output files were performed using the NAMCO platform (Dietrich *et al.*, 2022). In brief, obtained abundances have been normalized to minimum sampling depth and quality of obtained sequences was assessed using rarefaction curves (McMurdie and Holmes, 2014). Alpha Diversity is displayed as Richness and Simpson effective (Jost, 2007), beta diversity based on Bray-Curtis dissimilarity and PCoA (Gower, 1966) and Heatmap clustering based on Phyloseq (McMurdie and Holmes, 2013) using the detrended correspondence analysis (DCA) method . Functional predictions of bacterial pathways was performed with PICRUST2 (Douglas *et al.*, 2020) and investigated using the centered log ratio function of the aldex2 R-package with 256 Monte Carlo simulations. For the identification and classification of bacterial enzymes and pathways the Biocyc meta collection was used (Karp *et al.*, 2019).

Assignment of species to specific zOTUs was performed with EZBioCloud (Yoon *et al.*, 2017).

2.3.2. Full length RNA Sequencing

Full length RNA sequencing was performed at the NGS core facility in cooperation with Dr. Christine Wurmser (Liesel-Beckmann-Str. 1, TUM School of Life Sciences, Technical University of Munich, 85354-Freising, Germany). RNA was isolated from the tumors and respective control tissue using an adapted version of the `single-step method´(Chomzynski, 1987). Briefly, tissue was transferred to 800 µl TRIsure™ (BIO-38033, Bioline) and lysed mechanically by ULTRA-TURRAX® (IKA®-Werke, Staufen). After centrifugation (12.000 g for 15 min at 4°C) the upper aqueous phase was transferred to a kit column and the isolation was proceeded according to the manufacturers protocol (SV Total RNA Isolation System, Promega, Walldorf). RNA concentration as well 260/280 and 260/230 control ratios were determined using a spectrophotometer (Nanodrop-1000).

Purity and integrity of purified RNA was evaluated on a 2100 Bioanalyzer system (Agilent, Waldbronn). RNA Integrity Number (RIN) of the RNA samples ranged between 6.3 and 9.5 with a mean at 8.3, representing good RNA quality for intestinal tissue samples since these are known to degrade fast (Heumüller-Klug, 2015). 500 ng of total RNA was used for the library preparation according to the manufacturers protocol (TruSeq® Stranded mRNA Library Prep, 20020594, Illumina GmbH, Berlin). The sequencing reaction of the prepared library was run on a NovaSeq 6000 sequencing system using a SP 100 flow cell in 101 single read modus by IMGM Laboratories, Martinsried, Germany. Signals were processed using the NVCS and Real Time Analysis v3.4.4. software packages and the bcl2fastq v2.19.1.403 software, applying the *FastQ only* processing pipeline.

Obtained FastQ files were first quality controlled using FastQC/MultiQC (Versions 0.11.9 and 1.14 respectively). The first base of every sequencing run was removed due to bad quality using Cutadapt v. 4.2 (Martin, 2011). Quality control after cutting using the above mentioned pipeline yielded Phred Scores >30, which can be considered as high quality and therefore qualify for further processing. Sequence Alignment was then performed using the HISAT2 algorithm v. 2.2.1 (Kim *et al.*, 2019) and the most recent version of the Mouse Genome Assembly GRCm39. Alignments were quality controlled using SAMtools 1.13. Reads aligned ranged from 17.4 to 32.2 million representing the sequencing depth with >97.5 % sequences aligned per sample. A count matrix was then generated using featureCounts v.2.0.1 (Liao, Smyth and Shi, 2014) and the Mouse Genome Assembly

GRCm39. Because of limited local computing resources some of these algorithms were run on the Galaxy Europe Platform v 22.05 (The Galaxy Community *et al.*, 2022). The obtained count matrix was normalized using DESeq2 v. 1.34 (Love, Huber and Anders, 2014) and corrected for unwanted alteration in library preparation using ruvseq v. 1.26 (Risso *et al.*, 2014). DESeq2 was further used to analyze the differential gene expression of the obtained files. Gene Set Enrichment Analysis (GSEA) of the obtained DESeq2 – normalized count matrices was then performed using GSEA v. 4.3.2. and pathways were assigned by the MDB mouse-ortholog hallmark gene set collection v2022.1 (Liberzon *et al.*, 2015).

2.4. Mass Spectrometry

2.4.1. Fatty Acids

Stable isotope labelled fatty acids were synthesized by CDN Isotopes, Pointe-Claire, Canada. Shortly, for the preparation of the stable isotope labelled lipid gavages, 10 µmol FA 16:0[D5] (hexadecanoic acid-15,15,16,16,16-d5) and 3.33 µmol TG (16:0[D31])3 (glyceryl tri(hexadecanoate-d31)) (both from CDN isotopes) were weighed into separate glass tubes for each gavage. 100 µL of isooctane:isopropanol 3:1 (v:v) were added to both glass tubes. The tube containing FA 16:0[D5] was sonicated at 37 °C until the FA was completely dissolved, and all liquid was transferred to the second tube containing the incompletely dissolved TG (16:0[D31])3. The tube now containing both lipids was sonicated at 37 °C until the TG (16:0[D31])3 had dissolved. Per gavage, 200 µL of the prepared solution was aliquoted into 1.5 mL tubes and evaporated to dryness using a vacuum concentrator (Jouan RC 10.10). To each tube 100 µL of olive oil (Rewe Beste Wahl) was added and the gavages were stored at 4 °C until use. Prior to gavaging, the labels were sonicated at 37 °C for 30 min and checked for any precipitated label lipids. The workflow of the experiment is described in Figure 3.

For FA quantification in the different intestinal section, the mass of tumors and healthy tissue was determined in non – thawing conditions. 2-30 mg of frozen samples were aliquoted into 2 mL screw-capped tubes (Sarstedt). The tubes were prefilled with 0.7 g ceramic beads (1.4 mm diameter, Bertin Technologies) and cold tissue extraction solution (MeOH:ddH2O 1:1, 1% SDS) was added to a final concentration of 0.05 mg/µL. Samples were homogenized using a FastPrep-24 homogenizer (MP Biomedicals) with the following settings: 1 × 30 s, 6 m/s. For the quantification in plasma, whole blood was obtained by cardiac puncture and plasma was obtained using EDTA- coated tubes (Sarstedt, Sarsted) according to the manufacturer's protocol.

Figure 3: Workflow of the lipid uptake experiments

For the intestinal uptake experiments of fatty acids mice were fasted for 2 hours and then the label dissolved in olive oil was gavaged. After 60 minutes mice were killed and blood and tissue was sampled.

GC-MS analysis was performed as previously described (Ecker *et al.*, 2012). Briefly, 20 µL of the intestinal tissue extraction solutions (= 1 mg tissue equivalent) or 10 µl of plasma were used for the fatty acid derivatization. Acetyl chloride and methanol treatments were used to generate fatty acid methyl esters (FAMEs), which were extracted with hexane. The analysis of the total FA content was performed using a Shimadzu 2010 GC-MS system. FAMEs were separated from SGE using helium as a carrier gas on a BPX70 column (10 m length, 0.10 mm diameter, 0.20 µm layer thickness). The oven temperature was set to 50°C and increased at 40°C/min to 155°C, 6°C/min to 210°C and finally 15°C/min to 250°C. To detect specific fragments of saturated and unsaturated FAs (saturated, m/z 74; monounsaturated, m/z 55; di-unsaturated, m/z 67; polyunsaturated, m/z 79), the FA species and their positional and cis/trans isomers were characterized in scan mode and quantified by single ion monitoring. Isotope-tagged FA species were quantified by single ion monitoring of their respective molecular ions using the calibration curves of the untagged species. Non-naturally occurring C21:0 iso was used as an internal standard.

Obtained measurement have been processed analyzed and quantified using the integrated pipeline in Lab Solutions Software package (Shimadzu, Duisburg, Germany). Amounts of measured FAs were normalized to the sample weight or volume applied and given in nmol/g wet weight or nmol/10 µl respectively. Downstream analysis was then performed using the Metaboanalyst platform v. 5.0 (Pang *et al.*, 2021).For visualization purposes data was scaled using range scaling.

2.4.2. Bile Acids

Gall bladder content (=bile) was acquired by direct puncture of the gall balder with a cannula (30.5 g). 1 µl of bile was then dissolved in 99 µl of methylated DHCA and 20 µl of bile acid standard prior to measurement.For the cecal content approximately 20 mg were weighed into 2 mL bead-beater tubes (FastPrep-Tubes, Matrix D, MP Biomedicals Germany GmbH,

Eschwege). As an internal standard for recovery losses, 1 mL of methanol-based dehydrocholic acid extraction solvent (c=1.3 µmol/L) was added. Samples were extracted using a FastPep-24TM 5G bead beater (MP Biomedicals Germany GmbH, Eschwege, Germany) with a CoolPrepTM (MP Biomedicals Germany, dry ice cooled) for 3 times 20 seconds each at a speed of 6 m/sec followed by a 30 second pause.

Measurement of bile acids has been performed as previously described (Reiter *et al.*, 2021). Briefly, a QTRAP 5500 triple quadrupole mass spectrometer (Sciex, Darmstadt, Germany) coupled to an ExionLC AD ultra-high performance liquid chromatography system (Sciex, Darmstadt, Germany) was used for targeted bile acid measurements. Bile acids were detected and quantified using a multiple reaction monitoring (MRM) method. An electrospray ion voltage of -4500 V and the following ion source parameters were used: curtain gas (35 psi), temperature (450 °C), gas 1 (55 psi), gas 2 (65 psi) and injection potential (-10 V). The MS parameters and LC conditions were optimised with commercially available standards of endogenous bile acids and deuterated bile acids for the simultaneous quantification of a selection of 34 analytes. For the separation of the analytes, a 100 × 2.1 mm, 100 Å, 1.7 µm, Kinetex C18 column (Phenomenex, Aschaffenburg, Germany) was used. The chromatographic separation was performed at a constant flow rate of 0.4 mL/min. The mobile phase consisted of water (eluent A) and acetonitrile/water (95/5, v/v, eluent B), both containing 5 mM ammonium acetate and 0.1% formic acid. The following program has been used for elution (Table 3).

The injection volume for all samples was 1 µL. The column oven temperature was set at 40 °C and the autosampler was maintained at 15 °C. Data acquisition and instrument control were carried out using Analyst 1.7 software (Sciex, Darmstadt, Germany).

Obtained measurement data are given either in µM (bile) or in µM per gram wet weight. For missing values, a mean imputation has been performed when at least 50% of the samples per group presented with confirmed and quality controlled measurements. Statistical evaluation and visualization has been performed using the Metaboanalyst platform v. 5.0 (Pang *et al.*, 2021).

Table 3: Elution protocol of the HPLC.

Time [min]	Eluent B [%]
2	25
3.5	27
5.5	43
Hold - 1	43
8.5	58
hold - 3	58
17.5	65
18	80
19	100
Hold - 1	100
20.5 - 25	Stop - Equilibration

2.5.Statistics

Statistical analysis was performed using GraphPad Prism version 9.5.1 (GraphPad Software, San Diego, California) for all non-omics data. For two group comparisons unpaired and parametrical t-tests with Welch's correction were applied, for three or more groups ANOVA followed by Tukey's post hoc test was used if not specified otherwise. To analyze microbiota data non-parametric Mann-Whitney U (two groups) and Kruskal-Wallis tests (>two groups) were applied. Differences in Beta Diversity were assessed using PERMANOVA.

All statistical tests in multivariate datasets (16S Sequencing, full length RNA-Sequencing, fatty acids and bile acids) are corrected for multiple testing using FDR (False Discovery Rate) based on the Benjamini-Hochberg Method (Benjamini and Hochberg, 1995). For data presentation volcano plots have been created using the VolcanoseR App (Goedhart and Luijsterburg, 2020) and heatmaps using the morpheus app (https://software.broadinstitute.org/morpheus/).

Data are presented as means + SD if not specified otherwise. The only exception are graphs of body mass development (total and delta), where mean + SEM is shown. Bar charts further indicate every single measurement as one individual point. Violin and Boxplots central bands indicate the median, lower and upper part of the box the respective 25 and 75 percentiles and the whiskers connect data points outside these quartiles. Outliers are indicated as separate points. Violin plots additionally contain a probability based kernel

density plot. Statistically significant results are indicated with asterisks: * = $p < 0.05$. ** = $p < 0.01$, *** = $p < 0.001$, **** = $p < 0.0001$.

3. Results

3.1. Resistance to diet induced obesity in microbiome deficient models is dependent on the cholesterol dosage

The resistance to diet-induced obesity (DIO) in germ free (GF) mice is an often described phenotype (Bäckhed *et al.*, 2007; Rabot *et al.*, 2010), yet approaches to identify a mechanism responsible for this observation failed so far. The lack of consistency in reproducing this phenotype proves that this is a more complex interplay than initially found. One very promising approach showed that the phenotype is dependent on the dietary fat source with strong hints towards an involvement of dietary cholesterol (Kübeck *et al.*, 2016). Only a cholesterol containing, lard based diet, was able to induce the resistance.

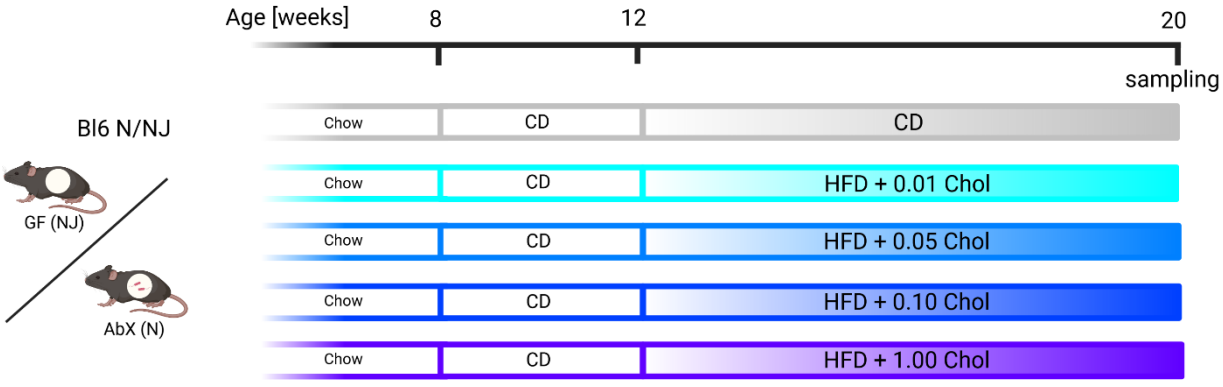

Figure 4: Setup of the cholesterol dose dependency study

Starting week 8 mice were fed a control diet (CD), at week 12 the respective high-fat diet (HFD) or a CD were fed until week 20. GF mice were kept in an isolator, antibiotics-treated (AbX) in regular cages with the treatment starting at week 12. Diets contained purified supplemented cholesterol and are available ad libitum.

To test the hypothesis if dietary cholesterol, which was present only in the lard-based diet, is the driving factor for the phenotypic resistance to DIO, the following feeding setup was chosen (Fig. 4). Instead of using cholesterol-containing lard, cholesterol was supplemented to a cholesterol free palm oil high-fat diet (PHFD). Cholesterol was supplemented in a range of 0.01 % to 1.00 % which is in consonance with human nutrition (Xu, McClure and Appel, 2018). Concentrations have been chosen higher compared to the initial finding (the lard based diet contained about 0.011 % cholesterol) due to the counteracting properties of plant sterols on cholesterol uptake, which are present only in the PHFD (Brauner *et al.*, 2012).

Figure 4 depicts an overview of the setup chosen to scrutinize the role of dietary cholesterol in microbiome deficient models in a dose dependent manner.

3.1.1. Antibiotic treatment efficiently induces microbiome deficiency

Germ free (GF) mice are referred to as gold standard in microbiome research harboring no microbes at all and are thus an optimal control for conventional (Conv) mice. Concomitant with this advantage there are also some drawbacks in this model, like physiological changes and an underdeveloped immune system (Kennedy, King and Baldridge, 2018). To overcome these difficulties and directly identify cholesterol – gut microbiota interactions as phenotypic drivers conventional mice treated with antibiotics served as a second microbiome deficient model.

Even though it is impossible to completely eradicate all bacteria in the GIT using an antibiotic cocktail, the crucial reduction of bacterial diversity results in a disturbed microbial ecosystem. The effectivity of the treatment was evaluated by 16S sequencing of cecal content at the end of the study. In comparison to the cecal content of untreated mice a dramatic reduction in Alpha Diversity was achieved indicated by the differences in Simpson index and Richness (Fig. 5 A). This was independent of dietary fat and cholesterol content (Fig. 5 C). The reduction in bacterial diversity is further demonstrated by a significant drop in the abundance of a vast majority of bacterial sequences in the cecum (Fig. 5 B). Looking at what bacterial genera are detectable remarkably AbX mice are predominantly inhabited by *Akkermansia* and *Escherichia – Shigella*, accounting for approximately 98% of all detectable bacterial sequences (Fig. 5 D). In line with the other metrics, Conv mice show a broad variety of gut bacterial genera, indicating that antibiotic resistances as a result of the long treatment period are negligible. Following antibiotic treatment, physiological changes can occur as well, comparable to those detected in germ free animals (Bayer *et al.*, 2019). One of the hallmarks of these changes is the enlarged cecum, which also is clearly present and comparable to those of germ free mice (Fig. 5 E). Consequently, the antibiotic treatment of Conv mice established a validated and qualified model of microbial deficiency.

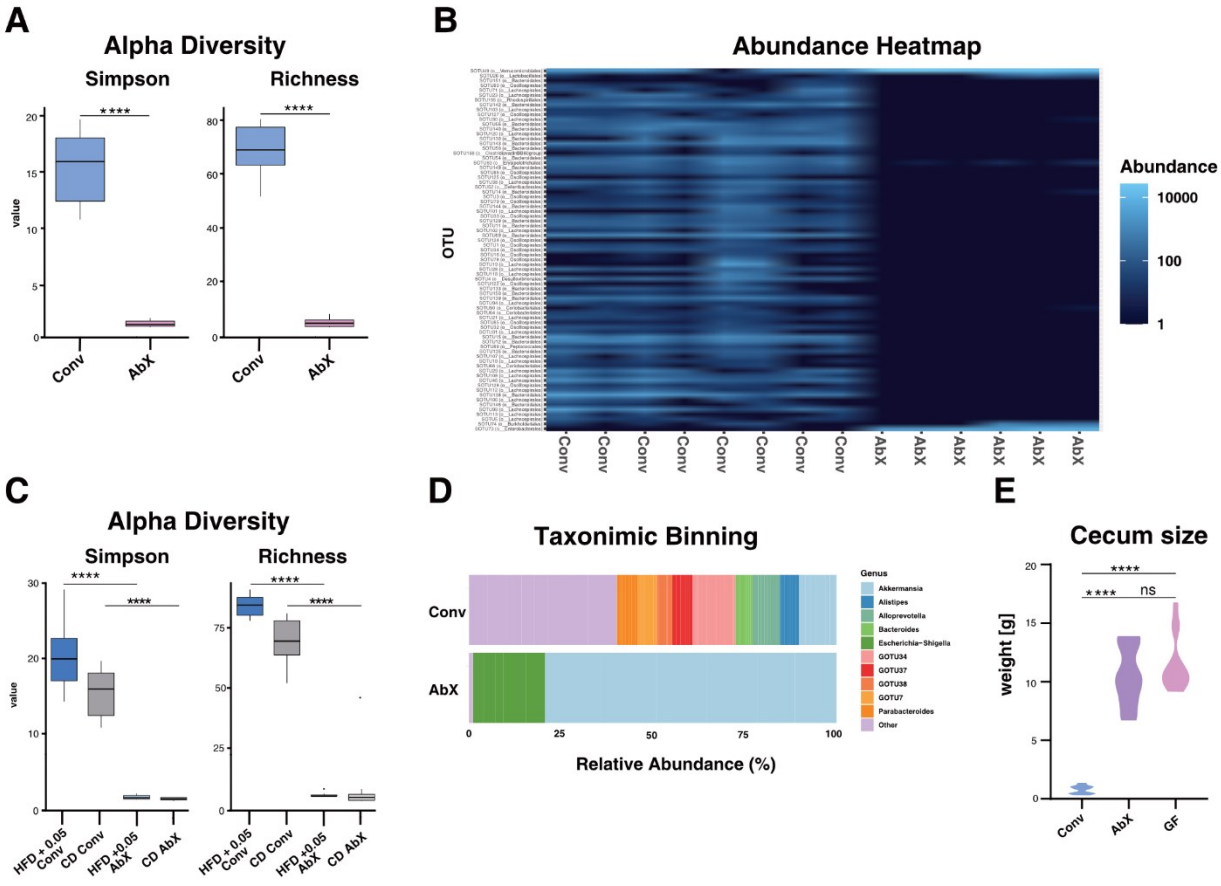

Figure 5: Efficacy of the antibiotic treatment.

(A) *Differences in the bacterial Alpha Diversity shown by effective Simpson index and Richness (CD only, n=6-8).* ***(B)*** *Abundance of bacterial sequences on OTU/Species level based on unsupervised Bray-Curtis distance* ***(C)*** *Differences in Alpha Diversity indicated by effective Simpson index and Richness in a diet comparison showing CD and one exemplary HFD (n= 6-8).* ***(D)*** *Taxonomic binning on Genus level based on the relative bacterial abundance.* ***(E)*** *Cecal weight of Conv, AbX and GF mice determined by weighing. Violin and Boxplots central bands indicate the median, lower and upper part of the box the respective 25 and 75 percentiles and the whiskers connect data points outside these quartiles. Outliers are indicated as separate points. Violin plots additionally contain a probability based kernel density plot. GF and AbX animals were 20w old, Conv 24w. Statistically significant results are indicated with asterisks: * = p < 0.05. ** = p < 0.01, *** = p < 0.001, **** = p < 0.0001.*

3.1.2. Resistance to obesity depends on the cholesterol dosage

The resistance to DIO was previously shown to be induced by dietary cholesterol (Kübeck *et al.*, 2016), however how the supplementation of cholesterol to the PHFD influences the onset of DIO remains elusive so far. In order to experimentally determine which concentration is most effective in inducing this resistance, it is necessary to take into account not only body mass, but also body composition and, in particular, fat mass. Starting with the GF mice total weight development was indeed dependent on the cholesterol dosage (Fig. 6 A), which was further supported when normalized for the starting weight

(Fig. 6 B). Here, the lowest cholesterol concentration of 0.01 % resulted in the highest weight gain and body mass. Further, body composition determined by NMR showed the highest level of fat mass induced by the lowest cholesterol concentration. The lowest amount of body fat was detected at a dose of 0.05 % (Fig. 6 C). Nevertheless, it has to be taken into account that NMR body composition measurement tend to be incorrect in GF mice due to the enlarged cecum (Krisko *et al.*, 2020). Thus, looking at the size of two major fat depots iWAT and eWAT might give a more comprehensive insight into the accumulation of body fat. The weight of iWAT is significantly decreased at 0.05 % cholesterol with a similar trend in eWAT when normalized to body mass (Fig. 6 D; Kleinert *et al.*, 2018). Taken together these data indicate a clear dose dependency in the induction of resistance to DIO, with the least degree of obesity at a cholesterol concentration of 0.05%.

When including the AbX treatment as a second model of microbial deficiency, a reduced final body mass and weight gain compared to GF mice was detected. Interestingly, the HFD fails to induce a higher body mass and weight gain in this model. The CD fed mice show a higher weight increase especially in the first weeks of the feeding study (Fig. 6 A and B). A potential reason for this phenotype is the antibiotic-induced cecal growth, which accounts for several grams (Fig. 5 E) and is known to be reduced when fed a HFD (Riedl *et al.*, 2021). Whereas body composition indicates no dietary difference, possibly biased by the physiological changes (Fig. 6 G), corrected fat depots iWAT and eWAT show no induction of DIO in CD fed mice. In the HFD fed mice, a strong trend hints towards reduced obesity induction at a cholesterol concentration of 0.05 % in the iWAT, with a similar, though weakened, picture in the eWAT (Fig. 6 H). The antibiotic treatment generally disturbs weight gain as a primary predictor of DIO. Fat depot size however still indicates a HFD induced phenotype and supports the previous finding in the GF mice with the strongest resistance to DIO induced by 0.05 % cholesterol.

Besides obesity, further parameters have to be taken into account to deepen the understanding of the cholesterol-induced resistance to DIO. To assess which side of the energy balance equation is influenced by dietary cholesterol bomb calorimetry was performed. GF mice fed the 0.01 % cholesterol diet displayed a significantly lower energy intake and a lower fecal energy content (Fig. 7 A and B). A similar trend was observed in the AbX treated mice in the energy intake but not in the fecal energy content (Fig. 7 C and D). Mice fed a 0.05 % cholesterol HFD showed a deficiency in the uptake of dietary energy, which is in line with the primary outcome in obesity parameters. Even though this energy deficit was counteracted by an increased dietary energy intake, cholesterol protected from development of DIO.

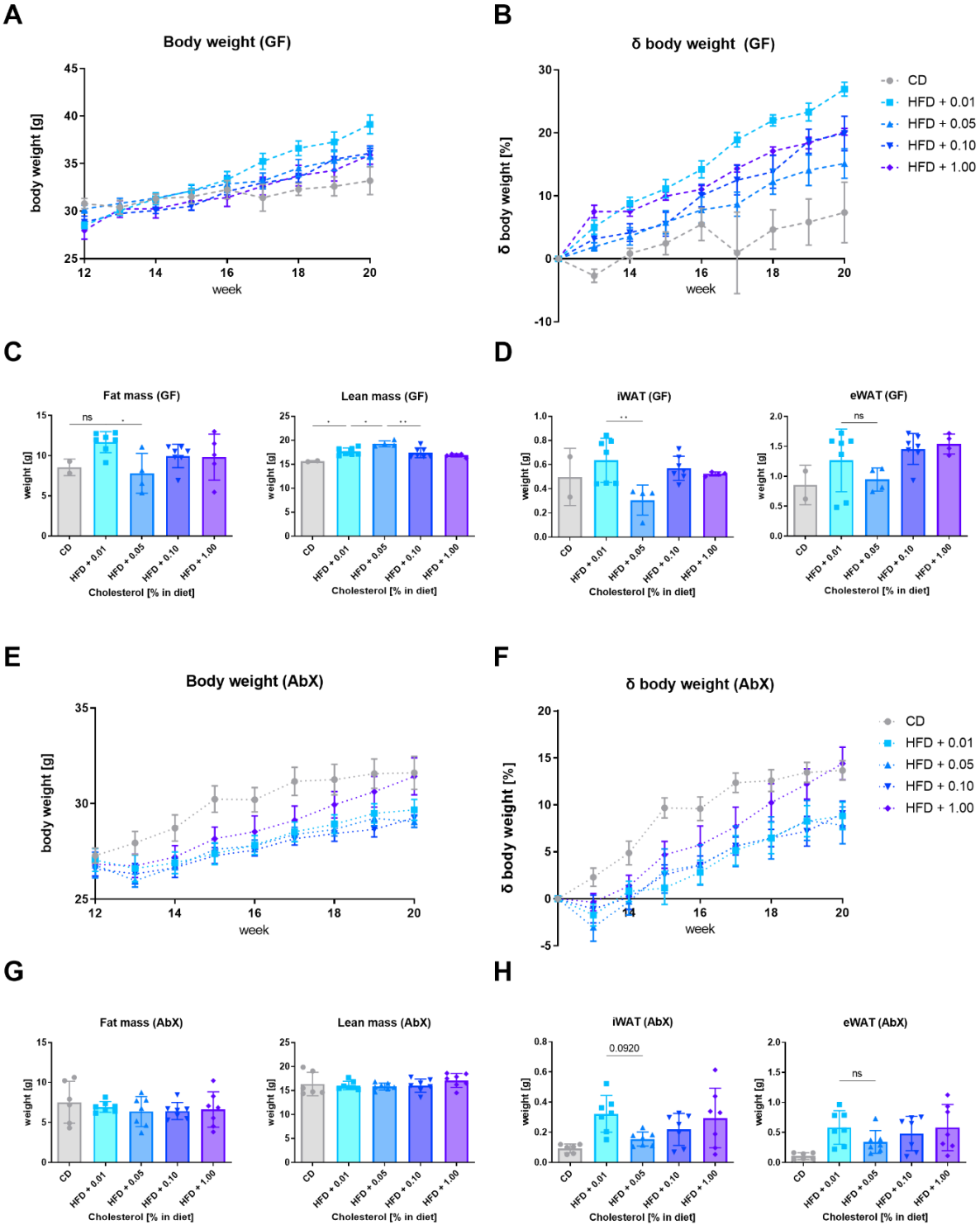

Figure 6: Cholesterol protects mice from DIO

*(**A**) Weight development of GF mice shown as total body mass. (**B**) Percentage changes in body mass normalized to differences in the starting weight at w12. (**C**)Total fat mass and lean mass determined by NMR at the end of the feeding trial, fasted overnight. (**D**) Major fat depots iWAT and eWAT mass, ANCOVA corrected with total body mass as cofactor. Total weight development (**E**) and w12 normalized percentage changes (**F**) of the AbX treated mice. NMR determined body composition (**G**) and body mass-ANCOVA corrected fat depots iWAT and eWAT (**H**).GF: n = 2 (CD), 4-7(HFD).AbX: n = 6-7. Statistically significant results are indicated with asterisks: * = p < 0.05. ** = p < 0.01, *** = p < 0.001, **** = p < 0.0001.*

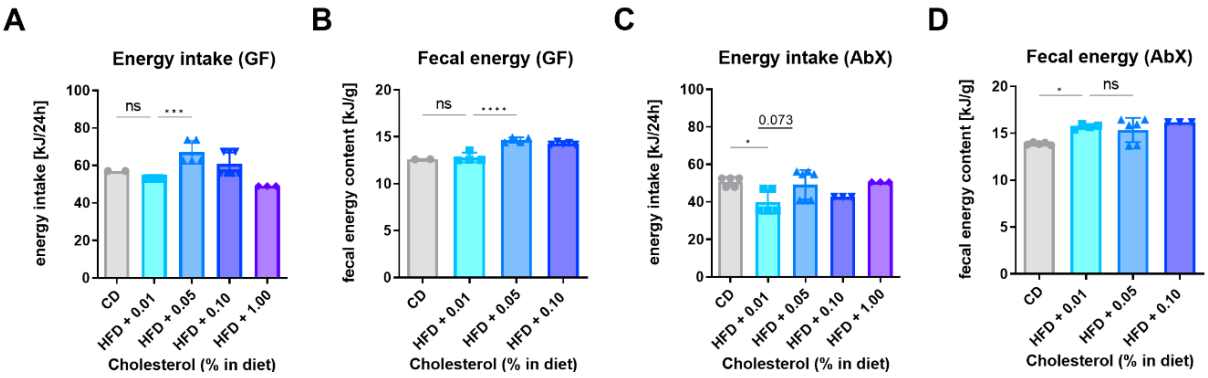

Figure 7: Altered energy intake and fecal excretion in response to cholesterol

*Daily energy intake of GF **(A)** and AbX **(C)** mice in week 13 of the feeding experiment from grouped cages calculated given as value per mice and fecal energy content of pooled fecal samples from GF (B) and AbX (D) mice. n numbers are indicated per dot and given per mouse (energy intake; n = 2-5) or per measurement (fecal energy; n = 3-6). Statistically significant results are highlighted with asterisks: * = p < 0.05. ** = p < 0.01, *** = p < 0.001, **** = p < 0.0001*

The changes in obesity development and energy balance parameters in these two microbiome deficient models deliver a comprehensive insight into the cholesterol dose dependent resistance to DIO. Compared to the initial finding of Kübeck et al., where a dose of 0.011 % induced a resistant phenotype, in this experiment a similar supplementation of 0.01 % was inefficient. A possible reason is the counteracting character of phytosterols in the HFD and their effect on cholesterol metabolism (Ostlund, 2004; Gylling and Simonen, 2015). Increasing the cholesterol concentration to 0.05 % proved to be most efficient in inducing the resistant phenotype, characterized by reduced measures of obesity and a deficiency in dietary energy uptake. In the following experiments, this concentration is thus used to establish a mechanistic model for the interaction of dietary cholesterol, the gut microbiota, obesity and intestinal cancer.

3.2.The role of gut-microbiota in cholesterol dependent resistance to DIO

Gut microbiota are considered a major factor in the pathophysiology of obesity and related metabolic disorders like cardiovascular diseases (CVD) and type II diabetes (T2D). Some of the described mechanisms with which the gut microbiota are capable of influencing host metabolism are the production of short-chain fatty acids (SCFAs, Dalile *et al.*, 2019), influencing intestinal permeability (Chakaroun, Massier and Kovacs, 2020) or the direct or indirect effects of bacterial metabolites on host metabolism (Canfora *et al.*, 2019). Dietary cholesterol has been identified to directly interact with gut microbiota (Le *et al.*, 2022), yet a mechanism how this interaction influences host metabolism with respect to obesity has not been established thus far.

To identify metabolic alteration in response to dietary cholesterol as well as related bacterial metabolism and establish a causal link between dietary cholesterol, gut microbial dependent metabolism shifts and obesity another feeding study was conducted. Cholesterol has been shown to induce resistance to DIO at a concentration of 0.05% most efficient in GF mice, thus this cholesterol concentration was compared to an identical diet without cholesterol supplementation (HFD +0.00). This study was performed in a GF and in a conventional setting, which enables the comparative analysis of the influence of dietary cholesterol in the presence or absence of the microbiome. Figure 8 shows the setup for the feeding study.

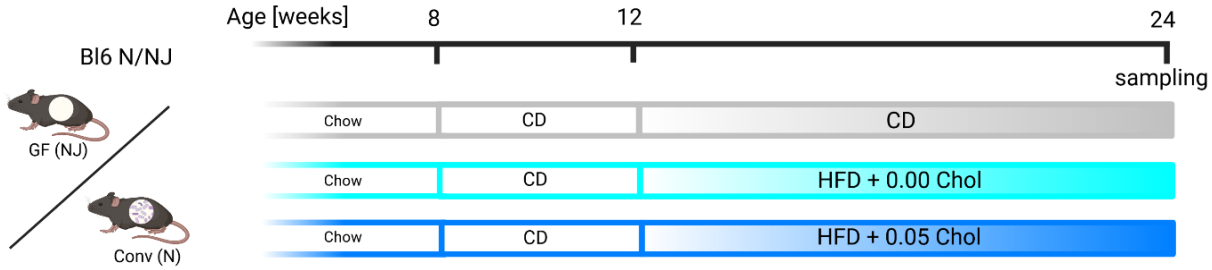

Figure 8: Setup of the comparative DIO feeding study

For the identification of cholesterol related changes in host metabolism with respect to the gut microbiota a feeding study comparing a HFD with or without cholesterol was performed. This study was equally performed in GF and Conv mice and the feeding time is prolonged to an age of 24 weeks, which delivers a more solid obesity phenotype in both models.

3.2.1. Cholesterol induced resistance to DIO is dependent on the gut microbiota

In order to investigate how dietary intervention with HFDs influences obesogenicity, the development of body mass and the accumulation of body fat were assessed. The role of cholesterol and cholesterol – gut microbiota interaction was investigated by comparing the effects of the cholesterol supplementation in the diets in GF and Conv mice.

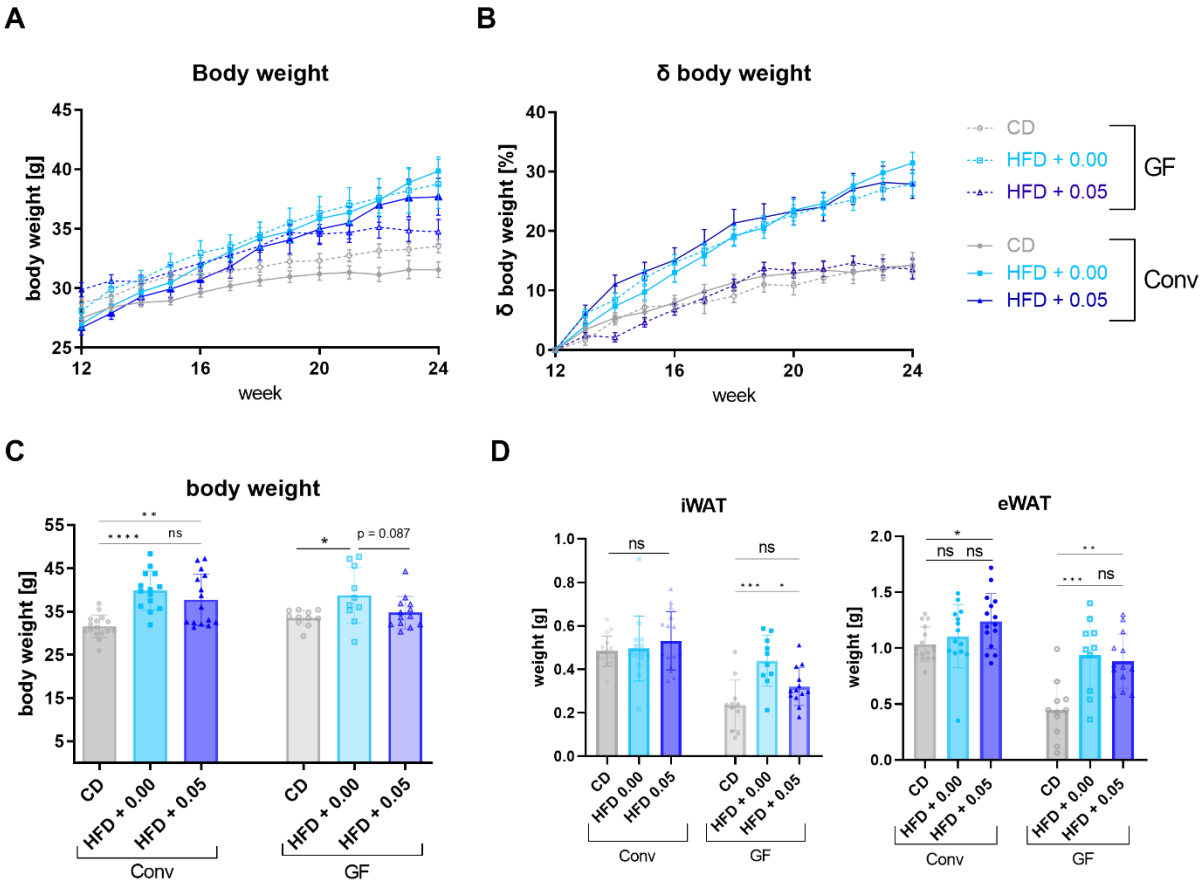

Figure 9: Cholesterol induced protection from DIO is microbiome dependent

Weight development and fat depots of GF and Conv mice in the feeding study. ***(A)*** *Total body mass of the mice in the feeding trial. n = 13-16* ***(B)*** *Body mass change in the timeline of the study normalized to the starting weight in w12 of the trial and given as percentage. n=13-16* ***(C)*** *Total body mass determined at the end of the study at week 24. n = 10-16* ***(D)*** *Weight of major fat depots iWAT and eWAT determined at sampling and ANCOVA corrected with total body mass as cofactor n =10-16. Statistically significant results are highlighted with asterisks: * = p < 0.05. ** = p < 0.01, *** = p < 0.001, **** = p < 0.0001*

General body mass assessment displayed an efficient induction of obesity by the HFDs in Conv mice (Fig. 9 A). In GF conditions, mice fed the HFD + 0.00 showed a similar rise in body mass compared to both Conv HFDs, however the cholesterol supplementation lead to a decreased accumulation of body mass. This phenotype was further emphasized when

being normalized to starting body mass (Fig. 9 B). The HFD + 0.05 failed to induce an obese phenotype and showed a rise in body mass similar to those of both CD fed groups. Thus, the cholesterol supplementation of the diet efficiently induced a microbiome dependent resistance to DIO.

Measurement of total body mass at the end of the feeding study presented a similar picture. However, the weight difference between the HFD + 0.00 and HFD + 0.05 failed to reach significance in both GF and Conv conditions (Fig. 9 C). In GF conditions, a trend towards a higher body mass in the HFD + 0.00 compared to the HFD + 0.05 was detected, which was absent in the Conv mice. Fat depots ANCOVA-corrected for total body mass further indicated reduced accumulation of fat mass in response to cholesterol in the GF mice, detectable in the iWAT but not in the eWAT. This phenotype was absent in Conv mice, where neither a HFD nor a cholesterol supplementation resulted in increased fat accumulation in the iWAT and only a cholesterol supplemented diet induced fat accumulation in the eWAT. Concluding, these data deliver an inconsistent picture, with some measures indicating a cholesterol dependent resistance to DIO in GF mice and some fail to reach significance in this aspect. It has to be noted however, that in the timeline of the feeding study, an increased number of mice fed the HFD + 0.00 with high body mass accumulation failed to finish the trial. Investigation of these dropouts yielded in increased number of cecal torsion, a known complication in GF mice (Djurickovic, Ediger and Hong, 1978). Accumulation in body mass increased the occurrence of such cecal torsions in GF mice, thus influencing the contradictory results in Figure 9.

In a next step, energy balance of the mice was assessed using bomb calorimetry to investigate differences in feeding behavior and assimilation efficiency. Contradictory to the previous findings of an increased energy intake in microbiome deficient models, mice fed the HFD + 0.05 had no increased energy intake in comparison to the HFD + 0.00, which was also microbiome independent. (Fig. 10 A). Fecal energy excretion was increased in the HFD + 0.05, which hints towards a decreased assimilation efficiency (Fig. 10 B). Interestingly this was present in both GF and Conv mice, however with an increased effect size in GF mice. This indicates a reduced assimilation of energy in the presence of dietary cholesterol, especially in GF conditions

To sum up the obesity phenotype indicates a cholesterol dependent resistance to DIO. Even though some of the data present conflicting results, weight development and accumulation of fat mass indicate a resistance to DIO when 0.05% cholesterol is supplemented to the, which affected GF but not Conv mice.

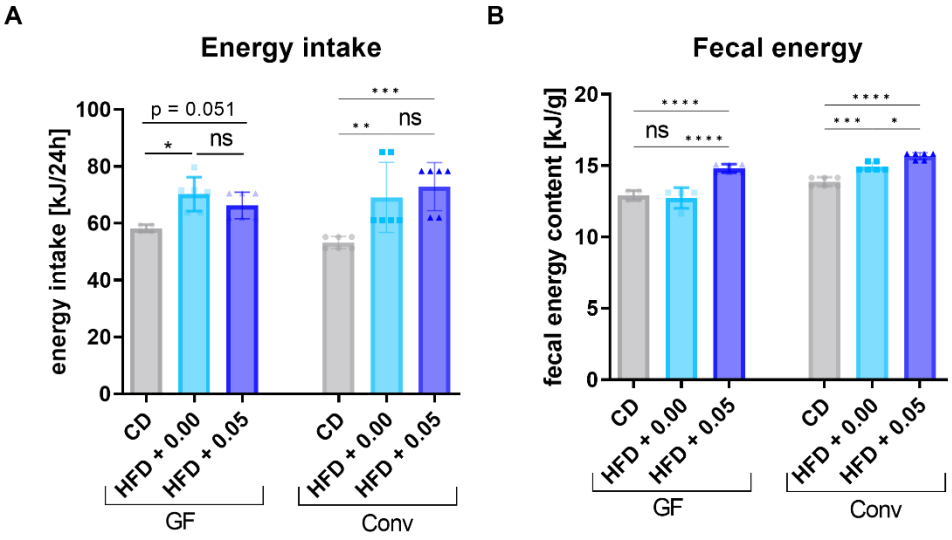

Figure 10: Energy intake and fecal energy in response to cholesterol

(A) *Energy and Intake and* ***(B)*** *Energy content of feces of GF and Conv mice normalized to 24h and gram feces respectively. All measurements were performed in week 13 of the feeding experiment, after at least 1 week of dietary adaption. n numbers are indicated per dot and given per mouse (energy intake; n = 4-6 per group) or per measurement (fecal energy; n = 4-6 per group). Statistically significant results are highlighted with asterisks: * = p < 0.05. ** = p < 0.01, *** = p < 0.001, **** = p < 0.0001*

3.2.2. Fatty acid uptake and plasma composition are unaffected by cholesterol

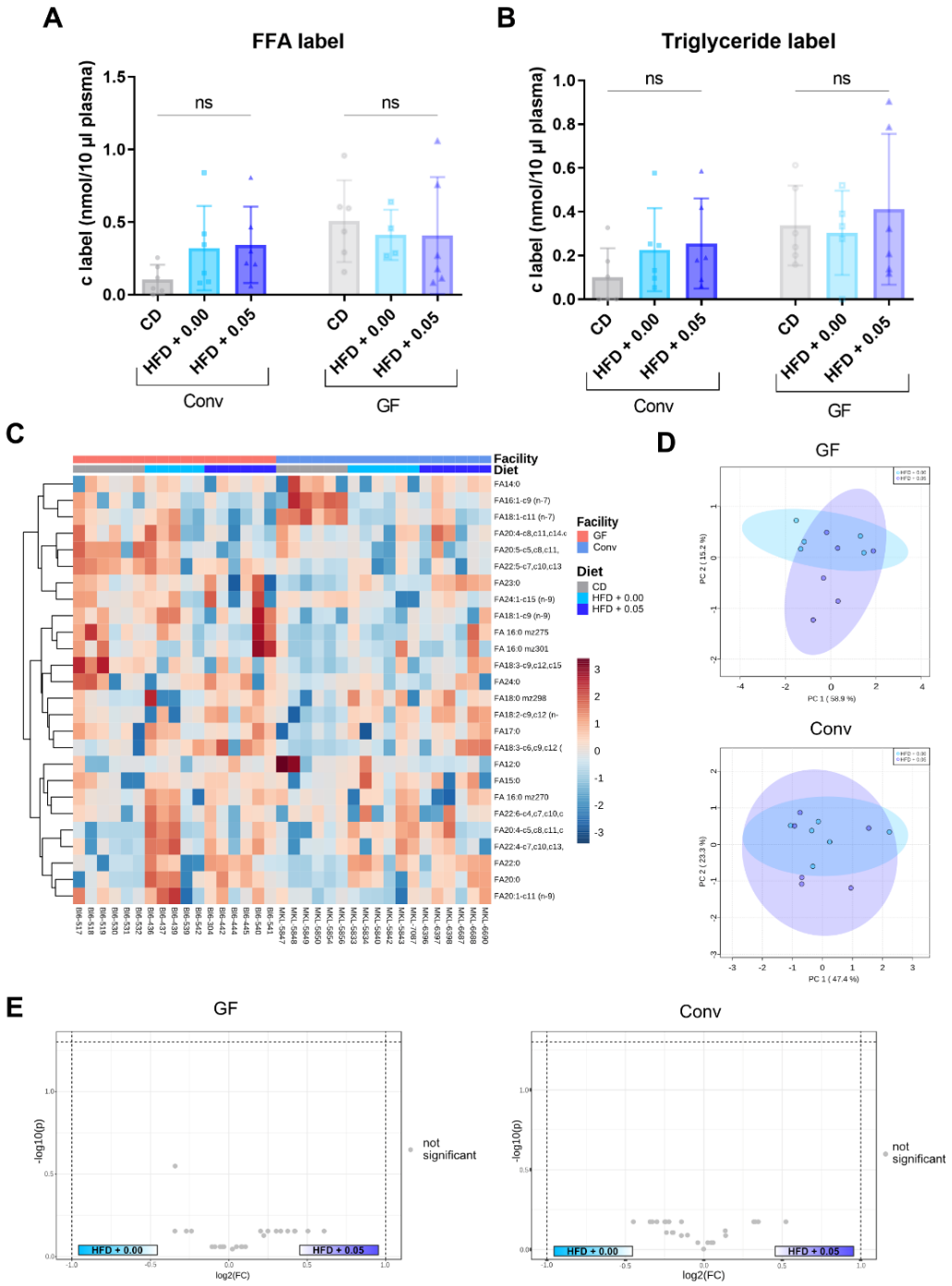

Figure 11: Uptake of fatty acids and fatty acid composition in murine plasma

To track luminal fatty acid uptake into plasma, mice were gavaged with a lipid cocktail containing a stable isotope labelled free fatty acid (palmitate) and a stable isotope labelled tripalmitate and sacrificed after 1 h. ***(A)*** *Label concentration of the free fatty acid (FFA) label in the plasma.* ***(B)*** *Label concentration of the triglyceride label in the plasma.* ***(C)*** *Heatmap of all FAs measured and arranged using Euclidean distance for the FAs and no group clustering* ***(D)*** *Unsupervised Prinicipal Component Analysis (PCA) of fatty acid profiles comparing HFD + 0.00 and HFD + 0.05 of Conv and GF mice respectively.* ***(E)*** *Volcano plots comparing HFD 0.00 and HFD 0.05 with FDR corrected p <0.05 and log2FC > 2 considered significant. n = 4-6 mice per group for all panel parts.*

The intake of high amounts of fat in the diet is a main factor for the development of obesity. These dietary fats are absorbed in the upper parts of the small intestine with the Duodenum and Jejunum being the most important sites. Even though the bacterial mass in these intestinal sections is low compared to the large intestine, these bacteria are capable of influencing the absorption of luminal fatty acids (Martinez-Guryn *et al.*, 2018). Differential uptake of fats influenced cholesterol and cholesterol – microbiome interaction could thus pose a possible confounding factor in the development of obesity. To address this question a stable isotope labelling approach followed by GC-MS was applied.

Following gavage with a fat cocktail containing labelled FFAs and Triglycerides concentrations of these labels were assessed in the plasma of the mice after 1 hour. In Conv mice the label levels of the FFA and the Triglyceride label showed no detectable difference caused by the feeding regime, although a trend towards higher uptake in all HFD fed mice compared to CD feeding is visible (Fig. 11 A and B). In GF mice the uptake was not altered compared to the Conv mice and additionally no dietary difference was detected (Fig. 11 A and B). GC-MS based analysis also allows for the quantification of different FAs and thus create plasma FA profiles for the mice. The profiles of these mice showed no detectable differences when being clustered and deliver no separation neither by diet nor by microbial state (Fig. 11 C). In addition, the direct comparison of profiles of the HFD 0.00 and the HFD 0.05 to detect cholesterol specific effects showed no separation in GF and Conv mice (Fig. 11 D). This was further confirmed when scrutinizing for changes in specific FAs, where the statistical analysis of all measured metabolites yielded no difference in GF and Conv mice (Fig. 11 E).

Taken together the stable isotope labelling approach indicated no diet-induced difference in the luminal fatty uptake after a lipid load challenge. Despite higher energy content in the feces, neither dietary cholesterol nor the presence or absence of gut microbiota had a detectable influence. Analysis of plasma fatty acid profiles further displayed no detectable difference and underlined that an altered uptake of fatty acids cannot be identified as a proximate reason for the resistance to DIO.

3.2.3. The bile acid pool is altered in response to cholesterol

Bile acids are potent digestive surfactants, which promote the uptake of fats, other lipids and fat-soluble vitamins from the digestive tract into the system, by acting as emulsifiers. Additionally they have an established role as major regulator of metabolism, affecting triglyceride, cholesterol, glucose and energy homeostasis (Lefebvre *et al.*, 2009). Further,

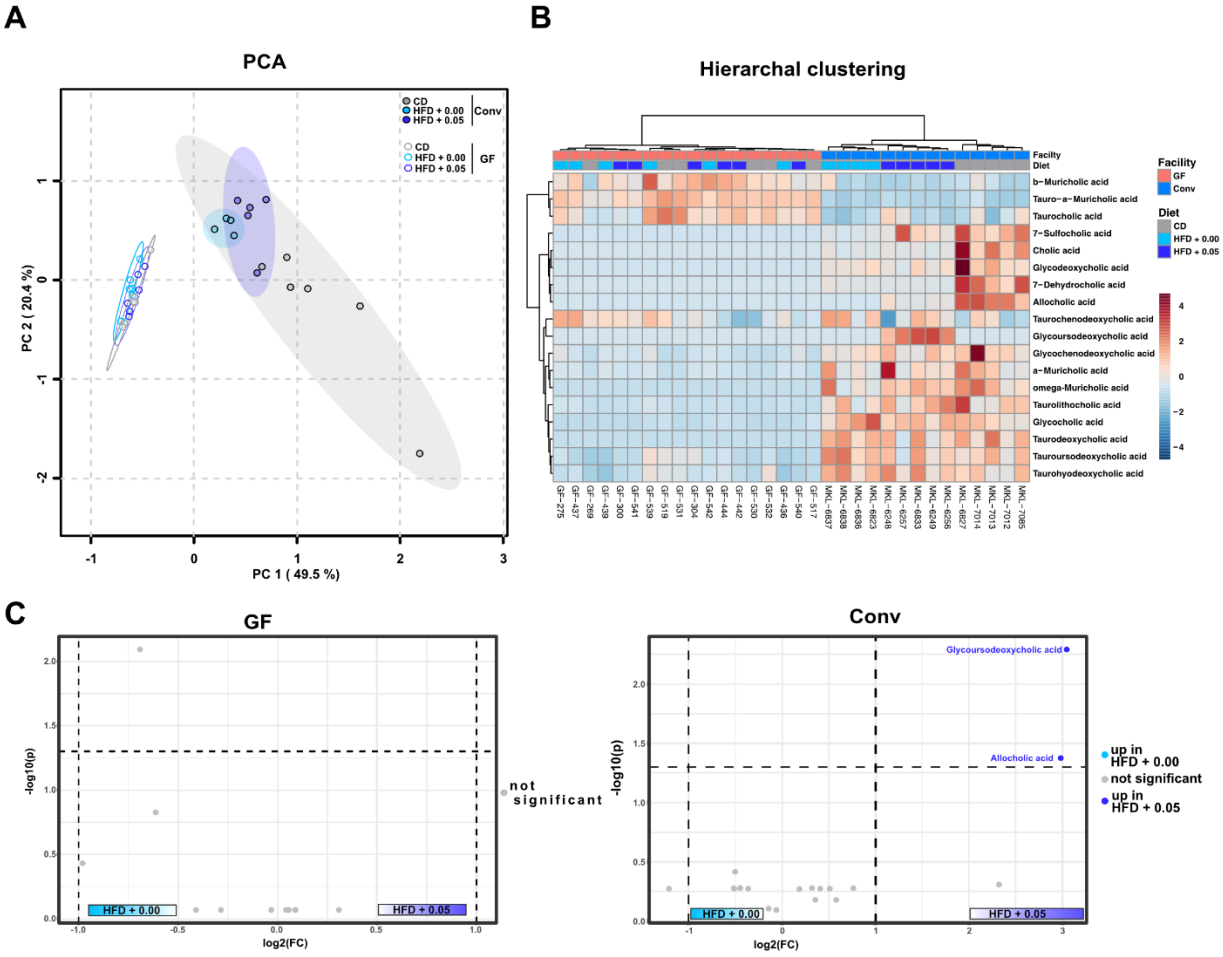

Figure 12: Composition of bile acids in the gall bladder

Bile was obtained by direct puncture of the gall bladder and composition has been determined using LC-MS. ***(A)*** *Unsupervised Principal Component Analysis (PCA) of GF and Conv mice shows higher variety of bile acids in Conv bile.* ***(B)*** *Unsupervised hierarchical clustering using Euclidean distance identifies distinct clustering according to diet in the Conv mice, which is absent in the GF mice.* ***(C)*** *Comparison of HFD 0.00 and HFD 0.05 in GF and Conv conditions using volcano plots present difference in response to cholesterol. FDR corrected p values <0.05 and FC of >2 are considered significant. Data are given in µM and n = 4-6 mice per group for all panel parts.*

they represent the primary pathway for systemic cholesterol catabolism and account for more than 50 % of daily cholesterol turnover (Staels and Fonseca, 2009). Bile acids are stored in the gall bladder, enter the intestine via the pancreatic duct, and are reabsorbed in the ileum to about 95% (Lefebvre *et al.*, 2009). The bile acid pools of GF and Conv mice differ in their composition due to the complete absence of secondary bile acids in GF mice.

To investigate how cholesterol-microbiota interactions affect the bile acid pool and consequently the host metabolism, bile acids were measured in the gall bladder and cecum of Conv and GF mice. Starting with the bile composition, unsupervised clustering yielded a distinct bile acid signature for GF mice, unaffected by the diet (Fig. 12 A). In Conv mice, the

situation differed with alterations in the signature according to the diet. Hierarchical clustering further revealed that each diet group had its distinct bile acid signature, whereas no dietary differences could be detected in GF mice. (Fig. 12 B). In consequence, the specific influence of cholesterol in presence or absence of the gut microbiota on the bile acid pool was investigated (Fig. 12 C).

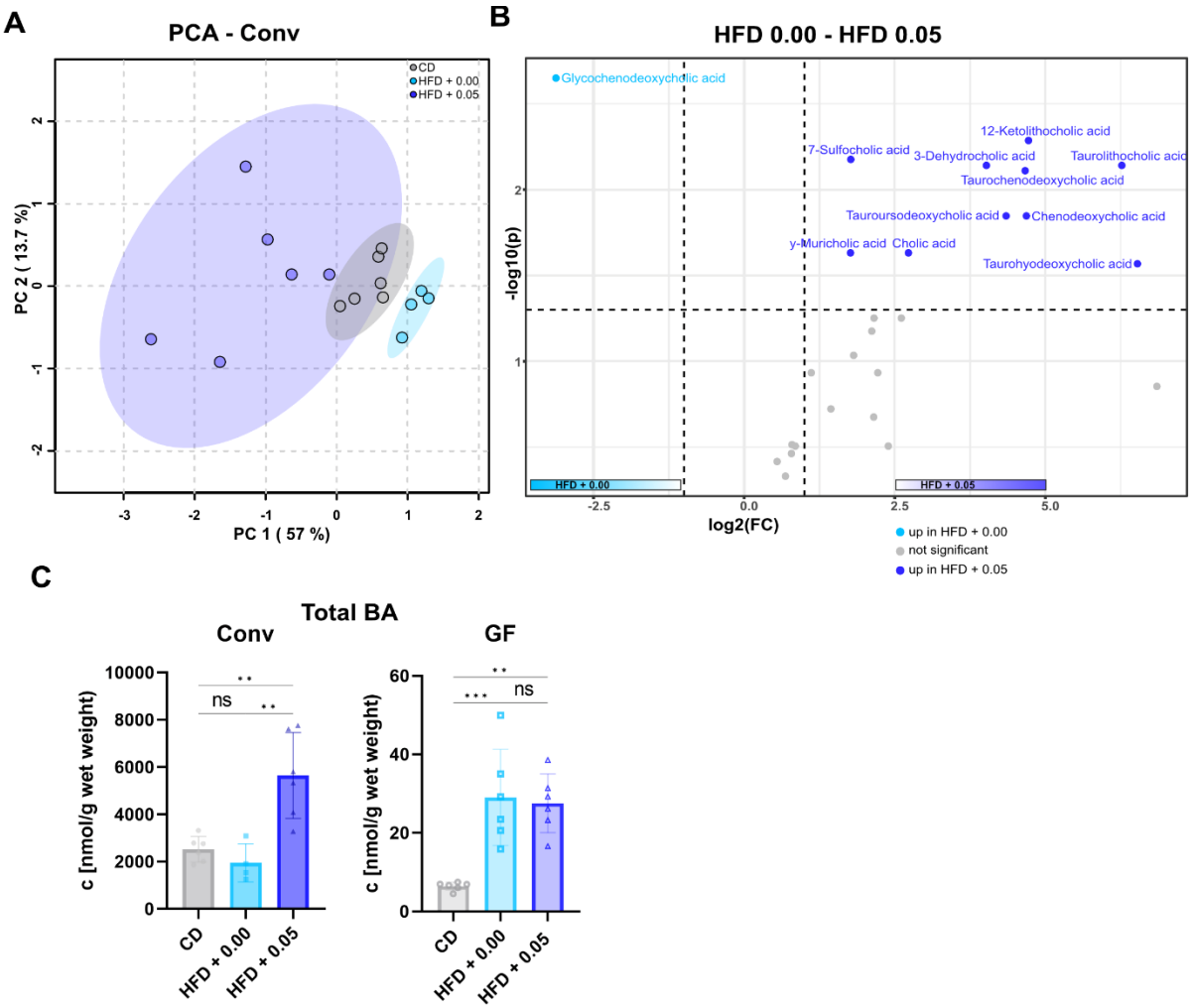

Figure 13: Quantification and composition of cecal bile acids

Bile acids were measured and quantified in cecal content of GF and Conv mice. ***(A)*** *Unsupervised Principal Component Analysis (PCA) of Conv mice bile acid pool.* ***(B)*** *Comparison of HFD 0.00 and HFD 0.05 in Conv conditions using volcano plots show cholesterol specific alterations. FDR corrected p values <0.05 and FC of >2 are considered significant* ***(C)*** *Analysis of total BA amounts in Conv and GF mice. Data are given in µmol/g wet weight and n = 4-6 mice per group for all panel parts. Statistically significant results are highlighted with asterisks: * = p < 0.05. ** = p < 0.01, *** = p < 0.001, **** = p < 0.0001*

In GF mice, no cholesterol-induced difference in the analyzed components was detected. Conv mice, in contrast, showed higher levels of *Glycoursodeoxycholic* acid and *Allocholic acid* in HFD + 0.05 fed mice. Even though these bile acids present rather small parts of the

general bile acid pool, these data underline the distinct bile acid signatures in the dietary groups. *Ursodeoxycholic acid* is further capable of boosting the conversion of cholesterol to bile acids (Nilsell *et al.*, 1983) These differences in bile acid species were only present in Conv mice, which identifies gut microbiota as possible drivers of dietary differences.

Where this analysis delivers information regarding the composition of the bile acid pool, the amount of bile acids excreted remains elusive. Following influx of bile into the small intestine and acting in lipid digestion, bile acids are reabsorbed in the Ileum to an amount of 95%. To address the question how dietary cholesterol influences excretion, bile acids were measured in cecal content of Conv and GF mice.

In Conv mice, cecal bile acids showed a distinct clustering according to the feeding regime, with a clear separation induced by cholesterol (Fig. 13 A). Analysis of single biliary components further identified several elevated bile acid species in response to cholesterol, indicating a general rise in bile acids, rather than that of specific species (Fig. 13 B). Investigation of the general amount of bile acids in the cecum identified a significant higher amount of bile acids in HFD + 0.05 fed Conv mice (Fig. 13 C), which is a strong indicator of increased cholesterol catabolism in this pathway. In GF mice, no cholesterol-induced effect was detectable. It has to be noted that the bile acid concentrations in GF ceca are low due to the cecal enlargement and thus several species were below detection limit. The measurement however clearly identified a HFD induced and cholesterol independent effect and thus delivered valid results.

In conclusion, gall bladder bile acids cluster according to diet and specifically in response to cholesterol in Conv but not GF mice, indicating a possible role of gut microbiota. Downstream differences in cecal bile acids further indicate microbial involvement, with elevated bile acids in response to cholesterol only detectable in Conv mice. These microbiota-induced differences very likely have an impact on the systemic metabolism and can thus be identified as candidates, which underlie the different effect of cholesterol on DIO in Conv and GF mice.

3.2.4. Gut microbiota are altered in response to cholesterol

Intestinal gut microbiota are known to be altered in metabolic disease and also specifically in response to feeding a HFD. Since the present study demonstrated, that development of DIO in response to a HFD is dependent on the gut microbiome in presence of dietary cholesterol, induced changes in gut microbial communities present an interesting target.

The cecum is the major habitat for gut microbes in the mouse, however also small intestinal microbes have been identified to contribute to systemic metabolism (Martinez-Guryn *et al.*, 2018). Thus, 16S Sequencing of small intestinal scrapings and cecal content has been performed.

Duodenal Alpha Diversity dropped in response to cholesterol, shown by significant lower bacterial Richness and Simpson Index (Fig. 14 A). This cholesterol dependent effect was further highlighted by changes in the Beta Diversity, where the microbial signature of the HFD + 0.05 group significantly differed from the CD and HFD (Fig. 14 C).

Interestingly in the Jejunum, the difference in Alpha Diversity was absent and a strong trend in both Richness and Simpson towards higher diversity induced by cholesterol was evident (Fig. 14 D). Beta Diversity further presented a significant separation by cholesterol in this segment (Fig. 14 F).

In contrast the Ileum depicted a reduced Alpha diversity in response to cholesterol in both metrics (Fig. 14 G), which also significantly differed from the other dietary groups indicated by Beta Diversity (Fig. 14 I).

To sum up, these metrics of bacterial diversity indicated specific effects of dietary cholesterol in the small intestinal microbiota. In all of the segments analyzed, a significant distinct signature can be attributed to cholesterol. Interestingly the features of these signatures are specific to the respective segment with significantly lower Alpha Diversity in the Duodenum and Ileum and a trend towards the opposite in the Jejunum. In addition, Taxonomic Binning on family level showed no consistent change in specific taxa across all segment, concluding that dietary cholesterol had a segment specific effect on the small intestinal microbiome.

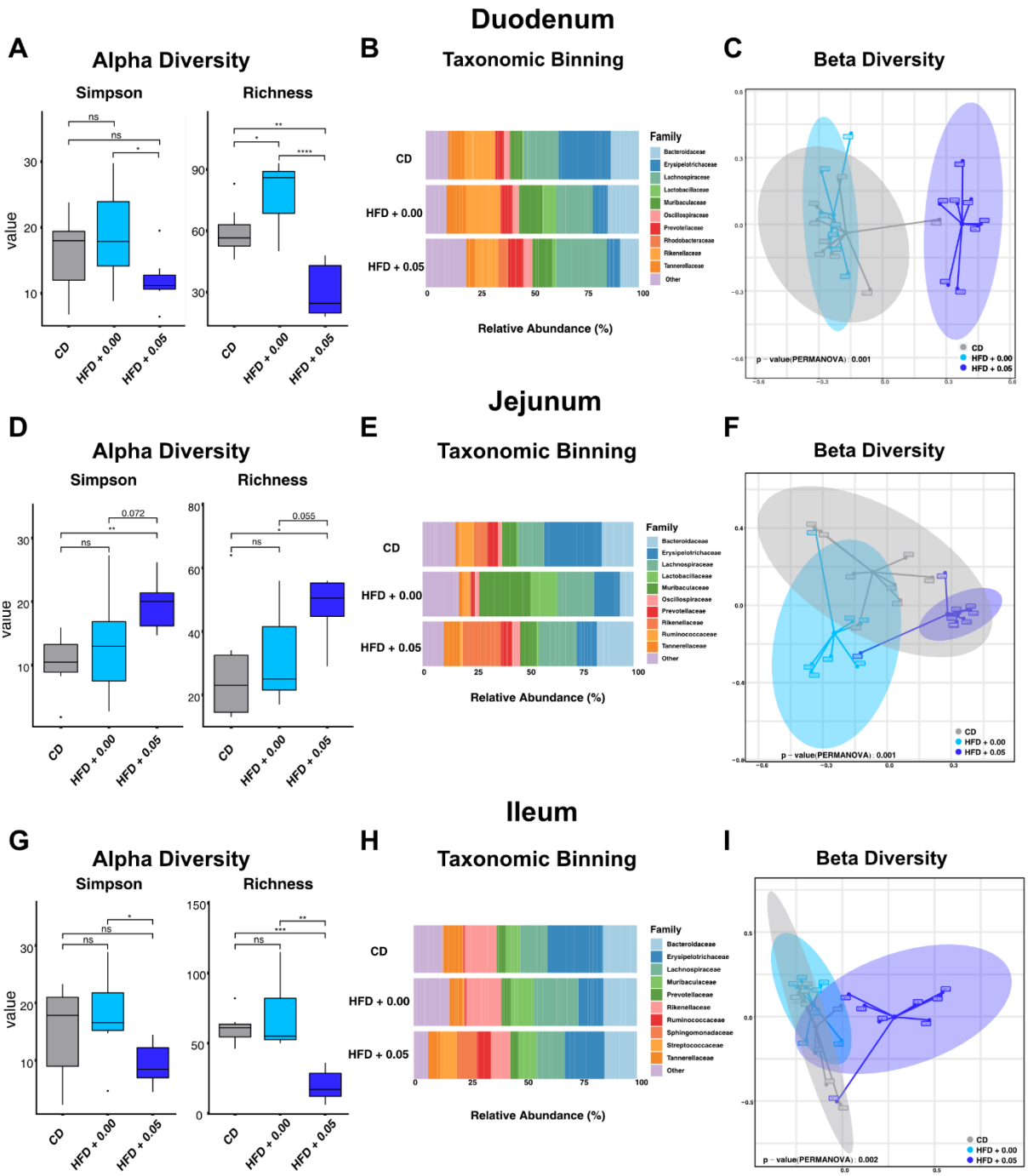
Duodenum
A
Alpha Diversity
Simpson
Richness
value
CD
HFD + 0.00
HFD + 0.05
B
Taxonomic Binning
Family
Relative Abundance (%)
C
Beta Diversity
p − value(PERMANOVA): 0.001
Jejunum
D
Alpha Diversity
Simpson
Richness
E
Taxonomic Binning
Family
Relative Abundance (%)
F
Beta Diversity
p − value(PERMANOVA): 0.001
Ileum
G
Alpha Diversity
Simpson
Richness
H
Taxonomic Binning
Family
Relative Abundance (%)
I
Beta Diversity
p − value(PERMANOVA): 0.002

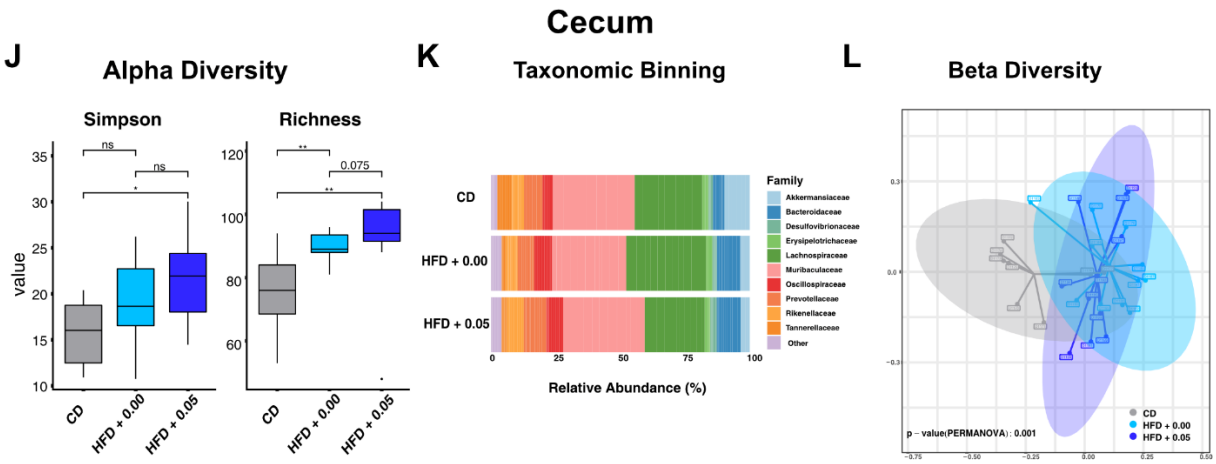

Figure 14: Gut microbial shifts in murine intestinal sections

Sequencing of the bacterial V3/V4 16S region derived from mucosal scrapings of the intestinal sections Duodenum Jejunum and Ileum as well as cecal content. ***(A, D, G and J)*** *Bacterial Alpha Diversity of the respective intestinal segment presented by the metrics Richness and effective Simpson Index.* ***(B, E, H and K)*** *Taxonomic Binning on Family level based on the relative bacterial abundance in the dietary groups and respective segments.* ***(C, F, I and L)*** *Principle Coordinate Analysis (PCoA) based on Bray-Curtis distance showing dissimilarities in Beta Diversity across the samples on OUT/Species level. Differences between the samples have been investigated using PERMANOVA-testing across all groups. n = 7-8 for the intestinal scraping (Duodenum, Jejunum and Ileum) and 8-11 for the cecal content. Boxplots central bands indicate the median, lower and upper part of the box the respective 25 and 75 percentiles and the whiskers connect data points outside these quartiles. Outliers are indicated as separate points. Statistically significant results are indicated with asterisks: * = p < 0.05. ** = p < 0.01, *** = p < 0.001, **** = p < 0.0001.*

Downstream of the small intestine the microbial signature of the cecum yet presented another situation, where no significant effect of cholesterol was detected. Beta Diversity indicated a significant difference in the signatures of the two HFDs to the CD but no cholesterol specific effect and Taxonomic Binning further only indicates minor differences in bacterial composition. This highlights the segment specific effect of cholesterol on the gut microbiota with a multitude of possible metabolic implications. These implications and their interplays widens the impact of the cholesterol – gut microbiome interactions and emphasizes on their role in the development of DIO.

3.2.5. Ileal gut microbiome signature links dietary cholesterol with metabolic diseases

Recent research has already identified gut microbial changes in metabolic disease by mainly identifying relevant bacterial taxa based on correlations. The underlying mechanism often remains elusive due to either technical limitations or lack of knowledge in the complex interplay of the microbial ecosystem. To discover mechanistic changes in the cholesterol

induced changes and establish a causal link in cholesterol – gut microbiome interactions and the development of obesity PICRUSt2 (Phylogenetic Investigation of Communities by Reconstruction of Unobserved States, Douglas *et al.*, 2020) based analysis has been performed.

Murine bacterial diversity and density increases along the gastrointestinal tract reaching highest levels in the cecum. When investigating cecal gut microbial functional profiles no significant differences induced by cholesterol were detected (data not shown). Consequently small intestinal bacterial pathways were investigated, which matter especially due to the metabolic activity of the small intestine. Whereas no significant changes in pathways were detected in the Jejunum (not shown), functional bacterial profiles in the Ileum presented with significant changes in response to cholesterol.

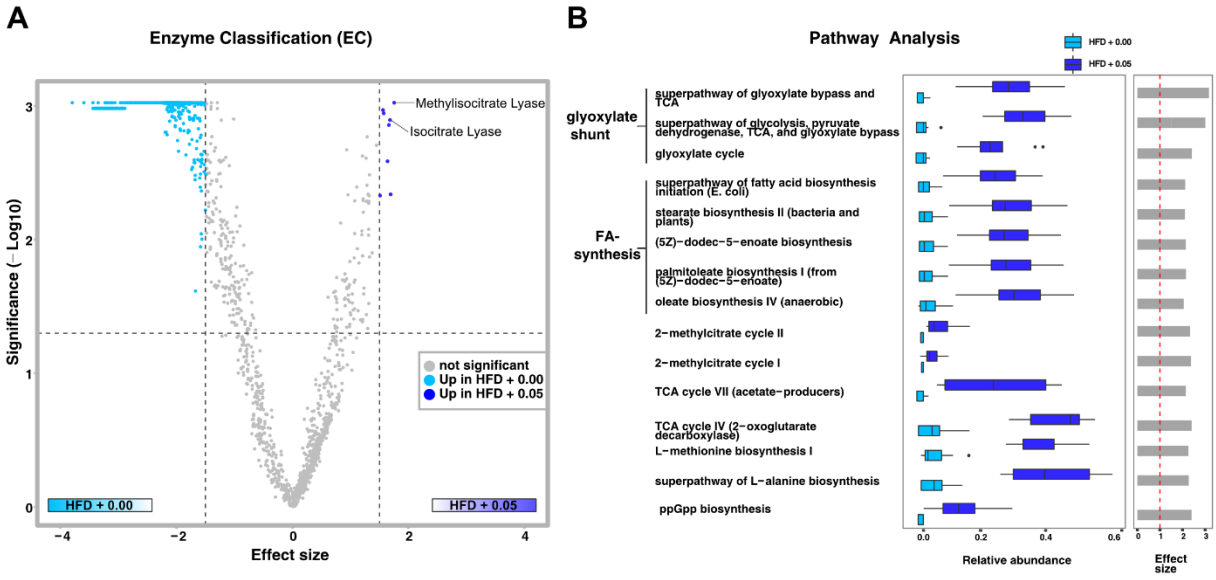

Figure 15: Functional changes in ileal bacterial pathways

PICRUSt2 was used to assign metagenomics functions to the 16S based microbial analysis of the Ileum. ***(A)*** *Volcano plot showing a 2-group comparison of the HFD + 0.00 and the HFD + 0.05 with all differential regulated enzymes based on enzyme classification (EC) number. $p < 0.05$ and is significant, data are BH corrected for multiple testing* ***(B)*** *Pathway analysis displaying all significant increased bacterial pathways in the ileal section of the HFD + 0.05 compared to the HFD + 0.00. P values < 0.05 are considered significant and data are corrected for multiple testing using the BH method.. n = 7 for all groups and panels. Data are normalized by copy numbers and analysis was performed with the ALDEx2 R-package on the NAMCO-platform. Enzymes and pathways were assigned to bacteria using the Metacyc database(Karp, 2002).*

Alpha Diversity in the Ileum is significantly increased in the absence of cholesterol. When inspecting differences in enzymes as a response to this reduction Methylisocitrate Lyase and Isocitrate Lyase are significantly enriched (Fig. 15 A). These enzymes represent key regulators of a metabolic adaption in bacteria called the glyoxylate shunt and are required for the survival on fatty acids as energy source (Eoh and Rhee, 2014). In addition, at functional levels, pathways resembling bacterial fatty acid synthesis and subsequent glyoxylate bypass were most enriched in response to cholesterol (Fig.15 B). A special programming in gut microbial metabolism towards a glyoxylate bypass has been associated with metabolic disorders like obesity, T2D and atherosclerosis (Proffitt *et al.*, 2022) and more specifically with the accumulation of visceral fat (Beaumont *et al.*, 2016).

In conclusion, a metabolic adaption of gut microbiota towards increased fatty acid synthesis and the glyoxylate bypass can be detected in the Ileum. Although direct consequences for the host metabolism remain elusive, these cholesterol induced adaptions link gut microbiota with metabolic diseases. Especially the described increased accumulation of visceral fat (Beaumont *et al.*, 2016) establishes a connection between DIO and gut microbiota-cholesterol interactions and identifies an underlying mechanism for the resistance to DIO in the HFD+0.05 GF mice.

3.3. Bacteria - cholesterol interaction suppresses intestinal tumorigenesis by altering gut microbial metabolites

Tumors of the GIT are one of the most commonly diagnosed cancers accounting for the third most fatalities among cancers (Siegel, Miller and Jemal, 2019). As major risk factors, both obesity in general and excess dietary fat intake in specific, play an important role in the development of this malignancy (Keum and Giovannucci, 2019). Besides excess dietary fat intake, one shared feature of obesity and colorectal cancer is a dysbiosis of the intestinal microbiome. The mechanistic reasons behind this relationship are so far largely unknown. Specifically, the key question is the ´cause or causation´ problem. Is the microbial dysbiosis one of the drivers or the result of carcinogenesis? Another factor associated with a higher risk of colorectal cancer is dietary cholesterol (Hu *et al.*, 2012). A shift in the intestinal microbiome is also considered a possible reason (Zhang *et al.*, 2021). The ability of cholesterol - gut microbiota interactions to influence HFD induced obesity has already been shown in this study and combines a complex interplay of the above-mentioned risk factors. Thus, investigating this interplay with respect to intestinal tumorigenesis can widen our understanding and deliver new insight into the ´cause or causation' question.

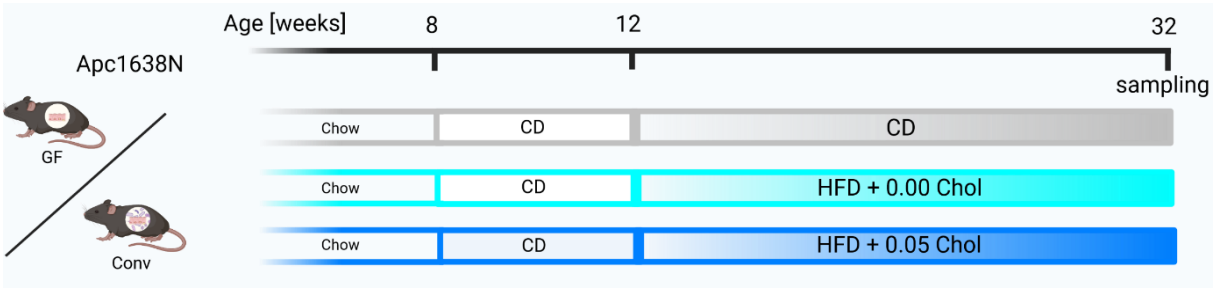

Figure 16: Setup of the Apc^{1638N} intervention study.

To minimize genetic differences breedings of Conv mice were established from GF colonies by transferring breeding pairs from the isolator to the Conv facility. In comparison to the previous feeding studies, the setup was prolonged to a final age of 32 weeks due to the latency period. This results in a solid and comparable tumor phenotype.

The use of transgenic mouse models to study tumorigenesis related interactions is well established (Lampreht Tratar, Horvat and Cemazar, 2018). Such a system can mimic cholesterol – dietary fat – gut microbiota interplay in a controlled setting. The Apc^{1638N} model is a suitable transgenic model for feeding studies due to the latency period, which enables studying of long-term effects. The setup for the feeding study was adapted accordingly (Fig. 16) and delivers a comprehensive way to study the effect of dietary cholesterol and fat crosstalk with the gut microbiota on intestinal tumorigenesis.

3.3.1. Cholesterol – gut microbiota interactions ameliorate HFD induced tumorigenesis

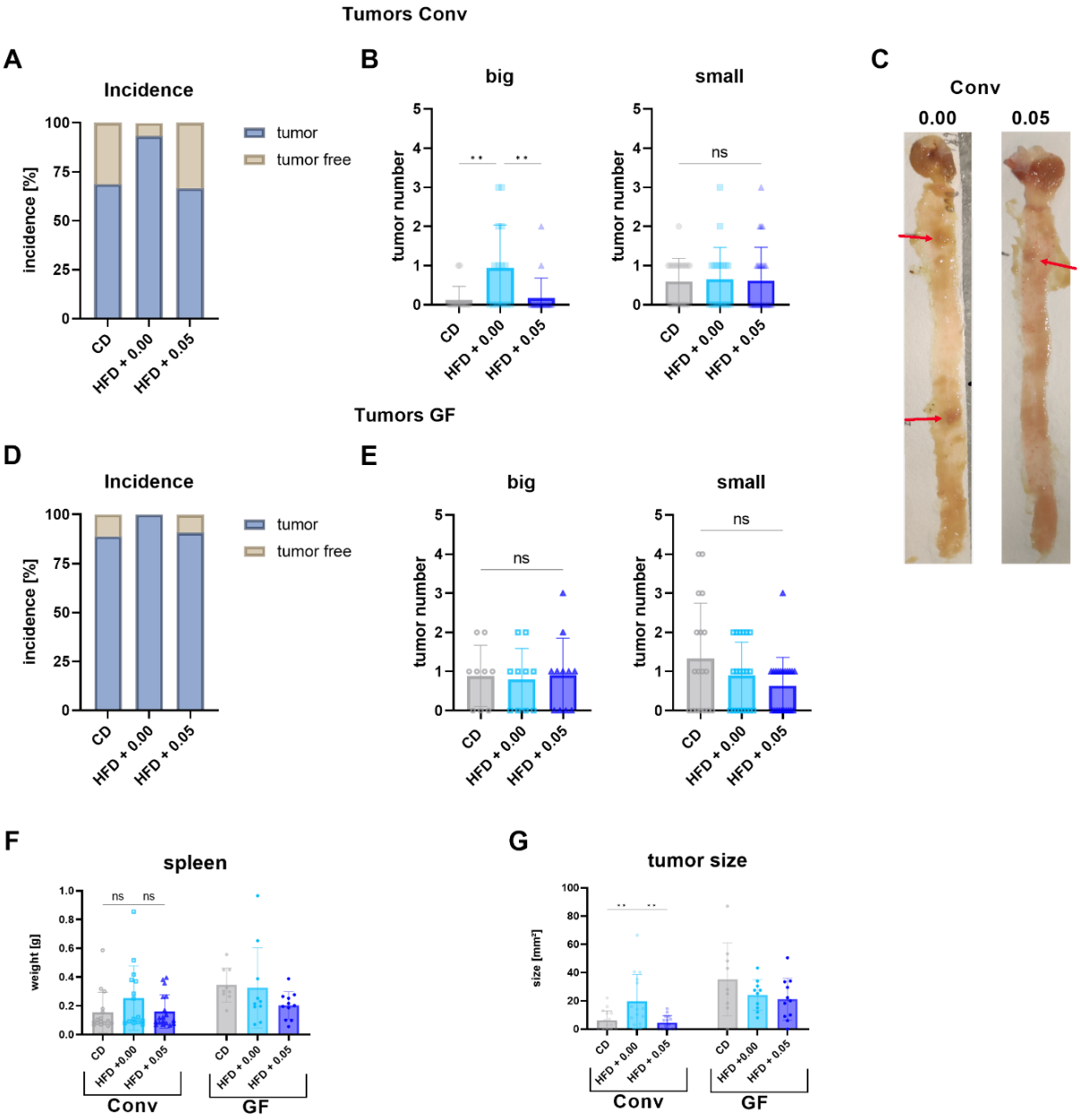

Figure 17: HFD and cholesterol influence intestinal tumorigenesis.

*(**A and D**) Tumor incidence defined as percentage of mice presenting with a tumor phenotype for Conv and GF mice. (**B and E**) Tumors were separated into small (<10 mm²) and big (>10 mm²) and total numbers of either small or big per animal were evaluated. (**C**) Representative pictures of tumor bearing intestinal sections with tumors indicated in red. (**F**) Spleen size of the mice determined by weighing. (**G**) Tumor size determined by cumulative tumor surface per animal Outliers have been removed using the ROUT method with default Q (G only). n (GF) = 9 – 11 per group; n (Conv) = 15 – 18 per group. Statistically significant results are highlighted with asterisks: * = p < 0.05. ** = p < 0.01, *** = p < 0.001, **** = p < 0.0001*

To investigate the HFD induced tumorigenesis in absence or presence of either the gut microbiota or cholesterol the tumor burden was evaluated at the end of the feeding study. Conv mice showed an increased incidence of lesions when fed a HFD + 0.00 compared to the CD, which is in line with previous studies (Yang *et al.*, 2022). Remarkably, this effect was ameliorated when cholesterol was supplemented to the diet. Mice fed the HFD + 0.05 showed an incidence of ~ 70% similar to the CD (Fig. 17 A). Intestinal tumor formation presented no difference when inspecting small tumors but presence of big tumors was significantly higher in HFD + 0.00 fed mice, again with cholesterol reversing the phenotype (Fig. 17 B).

Comparing these results to GF mice, no dietary effect was detectable in either incidence, small tumors or big tumors (Fig. 17 D and E). Another phenotypical feature of this mouse model is splenomegaly, which increases with a proceeding tumor burden (Fodde *et al.*, 1994). While the spleen size is not altered, (Fig 17 F) cumulative tumor size is increased only in the HFD + 0.00 group in Conv mice but not in GF mice (Fig. 17 G). In line with literature, these findings identified a HFD induced increased tumor phenotype only in the presence of gut microbiota (Yang *et al.*, 2022). Interestingly, supplementation of cholesterol to the HFD completely reversed this phenotype and showed a tumor burden comparable to that in CD fed mice.

Across these data, GF mice showed no diet dependent alterations in tumorigenesis. However compared to the Conv mice overall tumor burden was elevated. By evaluating only CD fed mice and thereby avoiding a potential dietary effect, tumor number and size was consistently increased in GF mice (Fig. 18 A). Additionally, an increase in spleen size was detectable (Fig. 18 B). There are conflicting reports whether GF mice exhibit an increased or decreased tumor phenotype in comparison to Conv counterparts. (Leystra and Clapper, 2019). In the present study, the overall tumor burden was clearly elevated in microbial absence.

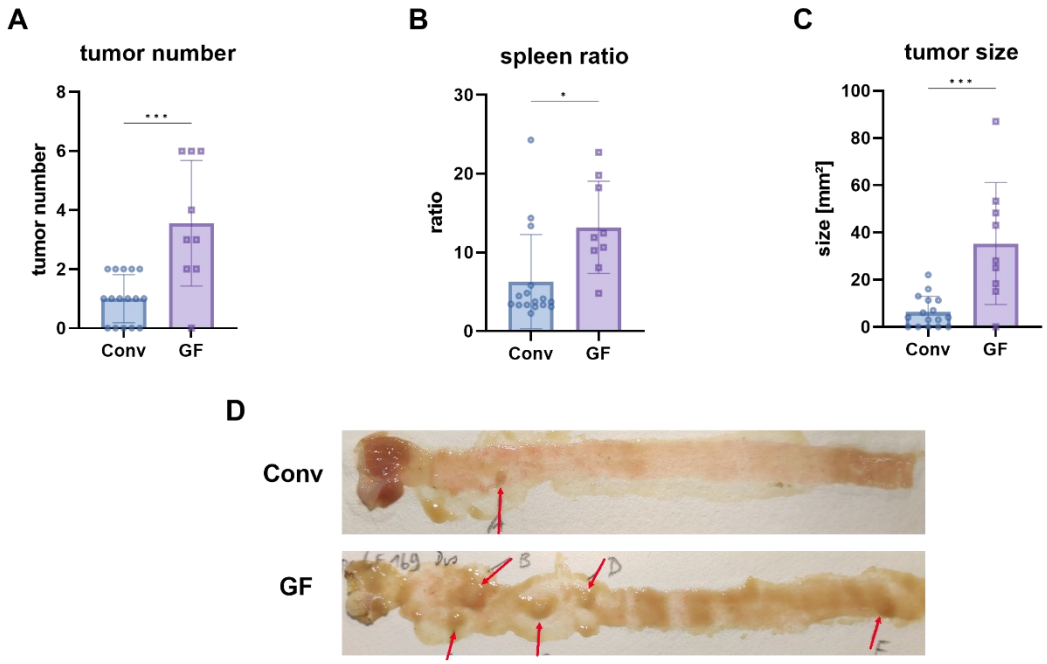

Figure 18: GF mice exhibit an advanced tumor phenotype

(A) *Total numbers of tumors was increased in CD fed GF mice independent of the size.* ***(B)*** *Because of the absence of dietary differences the spleen to body mass ratio can be calculated as a phenotypical identifier.* ***(C)*** *Tumor size determined by cumulative tumor surface per mice.* ***(D)*** *Representative picture of tumor bearing intestinal sections with tumors indicated in red. n(GF) = 9; n(Conv) = 16. Statistically significant results are highlighted with asterisks: * = p < 0.05. ** = p < 0.01, *** = p < 0.001, **** = p < 0.0001*

3.3.2. HFD rather than obesity induces a tumor phenotype

Since both, obesity and excess dietary fat intake are major risk factors for intestinal tumorigenesis, induction of obesity by the different HFDs in the murine tumor model was evaluated. Total body mass and body mass change (Fig. 19 A) showed an increased induction of DIO as a consequence of HFD feeding only in Conv mice. Under GF conditions, both HFDs failed to induce a higher body mass than the CD. This was independent of cholesterol supplementation. GF mice are known to have an enlarged cecum, which also depends on the type of diet fed. Thus, correcting the final body mass for the cecum resulted in a significant though dampened induction of DIO in GF mice (Fig. 19 B). The fat depots, split by gender displayed no dietary induction of obesity in GF mice at all, with no differences in iWAT and eWAT/pgWAT under GF conditions, but in Conv mice. Overall, GF mice of this model were resistant to DIO independent of the diet and the dietary cholesterol concentration, which is in conflict with the obese phenotype observed in WT mice. Given the fact that this mouse model has a heterozygous deletion of the APC- Gene, which is part of the WNT/β-catenin pathway that is involved in tissue growth (Steinhart and Angers, 2018), this is a potential confounder.

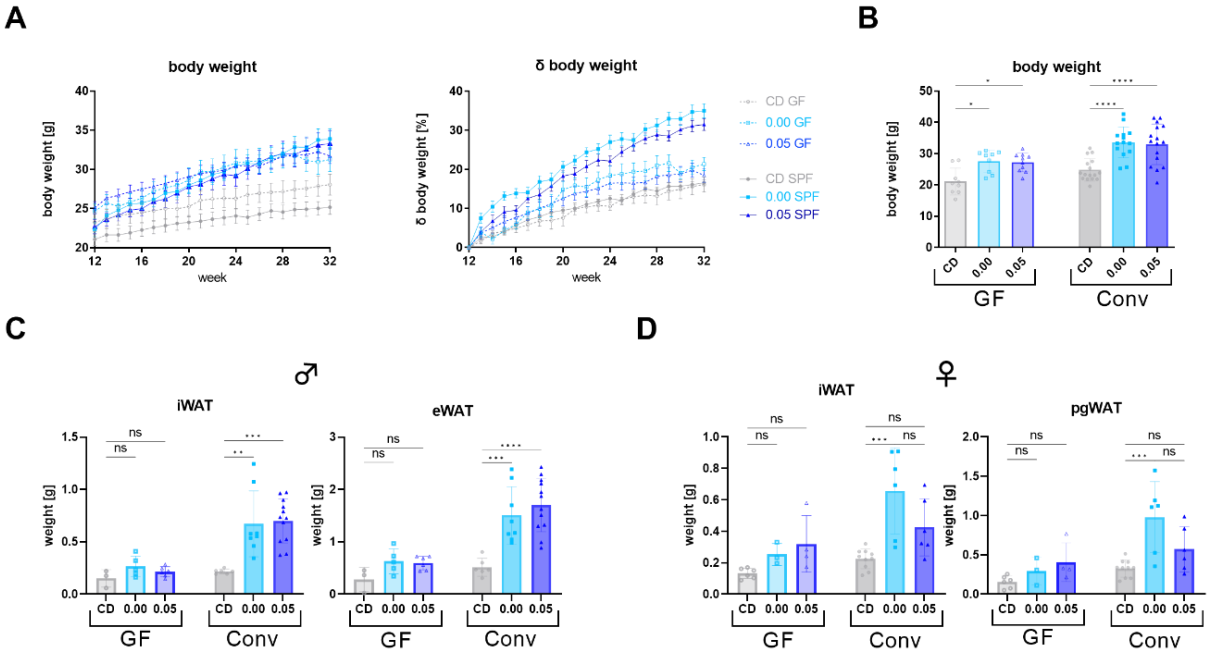

Figure 19: DIO in Apc^{1638N} mice depends on the gut microbiota and not cholesterol

*(**A**) Weight development of Apc^{1638N} mice shown as total and percentage normalized to the start at week 12. **(B)** Body mass at the end of the study normalized for physiological changes by removing the weight of the cecum **(C)** Total weight of the major fat depots iWAT and eWAT determined by weighing in male mice. **(D)** Weighed fat depots for female mice, separated from the male values due to sex biased physiology. n(GF) = 9 – 11; n(Conv) = 15 – 18 for A and B; n(GF) = 3 – 6; n(Conv) = 6 – 12 for C; n(GF) = 3 – 6; n(Conv) = 6 – 10 for D; all per group. Statistically significant results are highlighted with asterisks: * = p < 0.05. ** = p < 0.01, *** = p < 0.001, **** = p < 0.0001*

Altogether, these findings failed to identify a relationship between tumor incidence and obesity in this model, indicating that rather HFD induced excess dietary fat intake than accumulation of body fat boosted tumor formation.

3.3.3. Gene expression profiles of tumors are defined by the gut microbiota

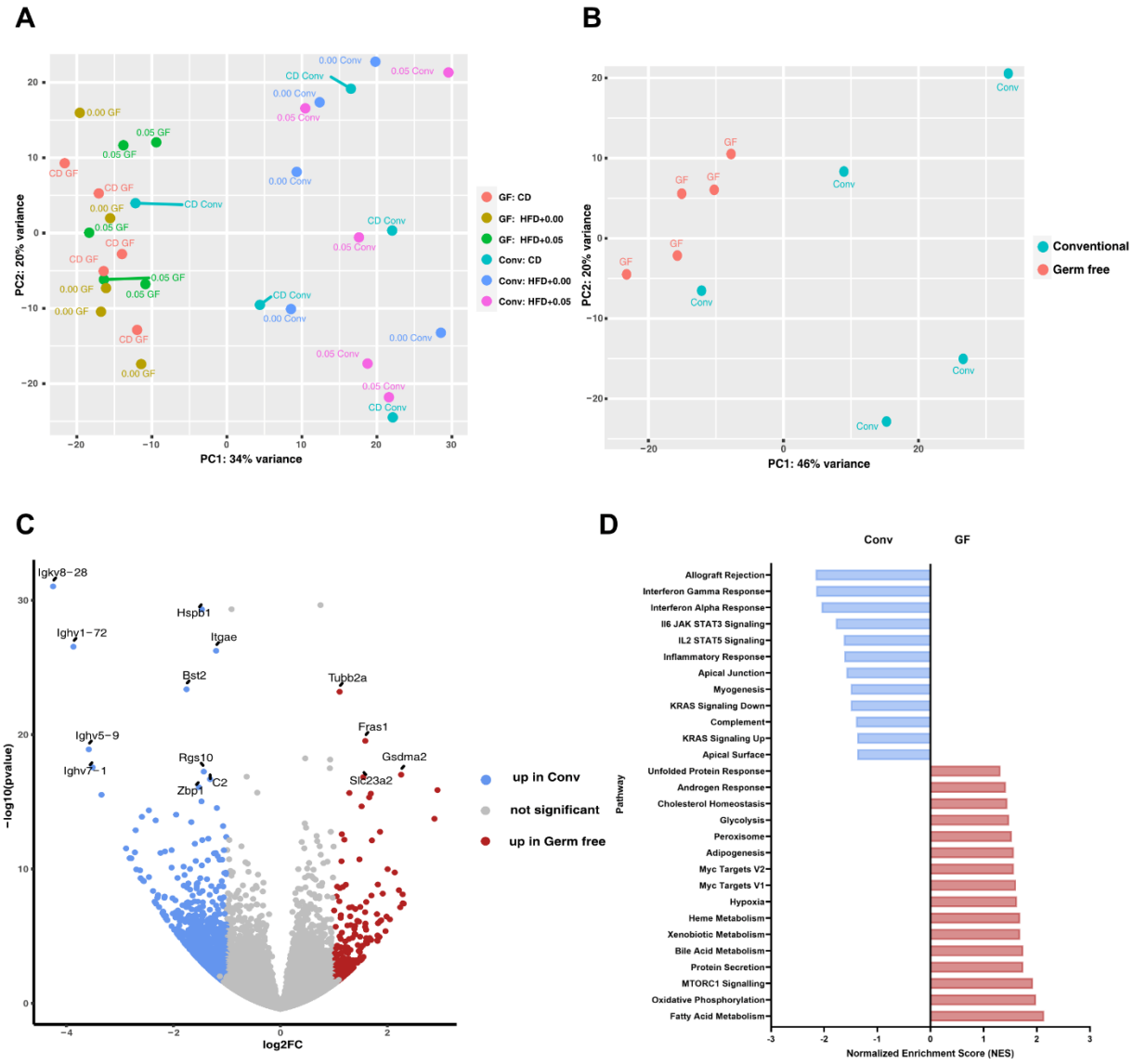

Figure 20: Gene expression profiles of Conv and GF tumors

*Full length RNA sequencing of intestinal lesions. A total of 40 841 transcripts were detected across the samples **(A)** Unsupervised principal component analysis of all six dietary and microbial groups reveals a microbial signature defined by PC1 and no dietary pattern. **(B)** Unsupervised PCA of CD fed tumors only identifies differences caused by microbial presence/absence. Conv tumors present with a higher variance in gene expression than GF lesions. PCAs in A and B have been created using DESeq2. **(C)** Significantly different regulated genes in CD fed mice. In the volcano plot genes with a FDR corrected p value of <0.05 and a fold change of >2 have been considered significant. Created using the galaxy `Volcano plot` tool version 0.0.5. **(D)** Gene Set Enrichment Analysis (GSEA) on normalized gene expression of the tumors derived from CD fed animals. Pathways were assigned on the MDB mouse-ortholog hallmark gene set collection v2022.1 using GSEA version 4.3.2 and all FDR corrected pathways at a significance level of 0.05 are shown. n = 5 for each group, all data are normalized using ruvseq and corrected for multiple testing using FDR.*

Omics approaches are frameworks that deliver insight into cellular signaling and can help in defining cancer pathophysiology. To get a better understanding of the molecular processes triggered by the different microbial conditions, dietary fat and cholesterol and their interplays, full length RNA sequencing of tumor tissue was performed.

Analysis of differential gene expression revealed a distinct difference in the signatures of the lesions. The main driver for these differences is the microbial state, indicated by separation across the principal component 1 (PC1) in the principal component analysis (Fig. 20 A). In both conditions, no clear dietary effect and thus clustering can be detected. This indicates that the influence of the diets and diet – microbiota interactions induce specific changes in gene expression of the tumors rather than modifying the general genetic programming. Germ free tumors were more homogenous in their gene expression compared to the conventional ones. This clearly demonstrates the importance of investigating the interplay between dietary components and the gut microbiota in tumor development.

So far, six groups defined by microbial status and diet fed were analyzed, which gives a first hint on the global gene expression profiles. To direct the analysis towards alterations in response to specifically the microbial influence, only CD fed mice were considered further. Concomitant with the previous findings Conv tumors displayed a higher variability in gene expression than their germ free counterparts (Fig. 20 B) . Following the observed differences in the PCA, especially in PC1 differential gene expression revealed several differentially regulated genetic targets (Fig. 20 C). Among the top overexpressed genes upregulated in Conv tumors several immunoglobulins were detected. There are numerous implications of B-cell dependent immunity in tumorigenesis, which possibly contributes functionally to the observed differences in tumorigenesis (Sharonov *et al.*, 2020).

Information on differential expression of genes can be integrated into functional profiles using databases. In order to retrieve a functional profile of the differential regulated genes and better understand the underlying biological processes Gene Set Enrichment Analysis (GSEA) was carried out (Fig. 20 D). Starting with the functional pathways upregulated in the tumors derived from conventional mice several pathways related to immune responses were enriched most. Responses to both, Interferon type I (alpha) and type II (gamma) signaling were overrepresented. The downstream targets of these major regulators of antitumor immunity, the JAK/STAT pathways were enriched consequently. Interferon gamma is considered as cytostatic, antiproliferative and pro-apoptotic and can thus inhibit tumor growth. (Castro *et al.*, 2018; Jorgovanovic *et al.*, 2020). Type I interferons are able to

influence tumor progression in a similar way. Their role, however, is more conflicting (Parker, Rautela and Hertzog, 2016; Cheon *et al.*, 2023).

Contrary to the increased activity of the immune system in Conv tumors, tumors derived from germ free mice were metabolically more active according to their genetic signature. Fatty Acid Metabolism and Oxidative Phosphorylation were the top two enriched pathways in GF tumors, indicating a higher turnover of fatty acids and subsequent mitochondrial energy production. Both fatty acids and the mitochondrial ATP production, are essential for tumor growth and progression (Porporato *et al.*, 2018; Koundouros and Poulogiannis, 2020; Sica *et al.*, 2020). Another interesting aspect is the increased Hypoxia in these lesions, which leads to an altered metabolism with higher dependency on fatty acids (Röhrig and Schulze, 2016). Also, activation of the mTOR pathway contributes to cell proliferation and is essential for tumor growth (Zou *et al.*, 2020).

To sum up the findings from the gene expression studies, tumors derived from conventional and germ free mice differ in the activity of their immune system and metabolism. Conventional derived tumors show higher activity of immune related processes and elevated Interferon signaling. In contrast, germ free mice derived tumors mice are characterized by a modified energy metabolism with a shift towards fatty acid utilization. Higher metabolic activity boosts tumor growth and progression and can thus be identified as a driver for the increased tumorigenesis observed in GF mice derived tumors.

3.3.4. Microbial state but not diet facilitates fatty acid uptake and composition in tumors and healthy tissue

Cancers are known to modify their metabolism to meet the energy requirements for continuous growth. Hypoxic conditions, which are often encountered in cancer due to extensive growth, lead to a higher dependency on extracellular fatty acids (Koundouros and Poulogiannis, 2020). In the special case of intestinal tumors, fatty acids are either available from the system or directly in the gut lumen, and it remains elusive if luminal or systemic fatty acids deliver nutrients required for growth.

To address this question, a stable isotope labelling approach with subsequent GC-MS analysis was implemented. Mice were gavaged with a fat cocktail containing stable isotope labelled free fatty acids (FFAs) and triglycerides dissolved in olive oil. In the process of digestion, enzymes like gastric and pancreatic lipase break down dietary triglycerides into monoacylglycerids (MAGs), free fatty acids (FFAs) and the glycerol backbone. Thus,

differences in both these labels account for the ingestion of fatty acids. The uptake in healthy and diseased tissue was evaluated after 1 hour and yielded significantly lower uptake of luminal fatty acids into tumors compared to controls independently of the gut microbiota (Fig. 21 A and B). Healthy tissue directly adjacent to the tumor as well as distal (1 cm downstream of the tumor) tissue took up significantly more fatty acids, which was evident in both labels. Both these control tissues displayed no detectable difference in their label concentrations, indicating that the reduced uptake into the lesions is tumor specific. This showed that the tumor tissue itself has limited luminal fatty acid uptake capacities and consequently that tumors rather fulfill their energy needs by systemic uptake than from the lumen.

Across these data, GF tissues consistently showed a higher uptake of luminal fatty acids in both labels. Comparing fused data of both labels in GF and Conv tissues, all GF tissues revealed a higher uptake with respect to their disease state (Fig. 21 C). Higher lipid uptake into these tissues was in line with increased activity of fat related metabolism detected in GF lesions.

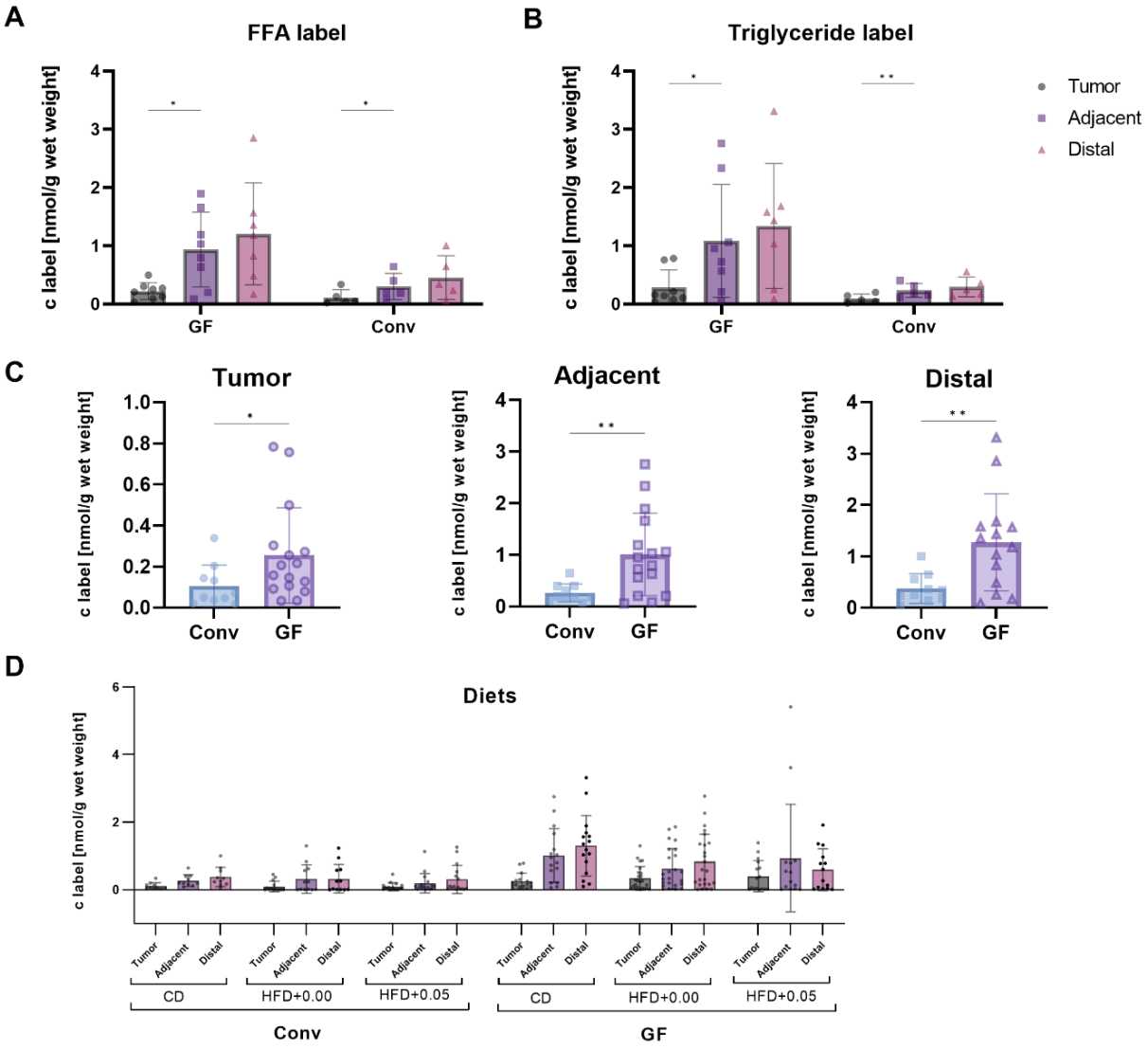

Figure 21: Luminal fat uptake is reduced in tumors and Conv tissue.

Mice were gavaged with a lipid cocktail containing a stable-isotope labelled free fatty acid (Palmitate) and a stable-isotope labelled Tripalmitate and sacrificed after 1 hour to follow lipid uptake into tumors and healthy control tissues. Tumor Adjacent tissue was sampled directly next to the tumor, Tumor Distal 1 cm downstream. ***(A)*** *The uptake of the free fatty acid label from the gut lumen into tumor tissue is reduced in GF and Conv mice.* ***(B)*** *Uptake of the Triglyceride label is similarly reduced in tumor tissue indicating that the delivery has no physiological impact; n= 5-8 per group for A and B and multiple paired t-tests using the Holm-Sidak method were applied.* ***(C)*** *Fused data of both labels comparing the FA uptake in CD fed GF and Conv mice show that the uptake is increased in GF tissue independently of the tissue; n=10-16 per group.* ***(D)*** *Comparison of fused label uptake indicate no dietary influence on FA uptake into tumors on neither Conv nor GF conditions; n =10-24. Statistically significant results are highlighted with asterisks: * = p < 0.05. ** = p < 0.01, *** = p < 0.001, **** = p < 0.0001.*

Another aspect to be considered is the influence of the used diets and diet related shifts in the gut microbiota. HFD induced changes in the intestinal microbiota are suggested to increase the lipid uptake capacities in the intestine (Martinez-Guryn *et al.*, 2018). A dietary effect however was not detectable in this study. Neither GF nor Conv tissue showed diet dependent differences in fatty acid uptake independent of the disease state of the tissue (Fig. 21 D). Fatty acid uptake can thus be excluded as a driver for diet-induced differences in tumorigenesis, however can be identified to play a pivotal role in the elevated tumor phenotype in GF mice.

To further elucidate the consequence of an altered lipid metabolism and higher luminal fatty acid uptake in GF tumors, the fatty acid composition of the tumors was investigated. Fatty acid signatures of GF and Conv tumors were analyzed using principal component analysis (PCA) and partial least squares – discriminant analysis (PLS-DA, Fig. 22 A and B). PCA is an unsupervised method for reducing dimensionality and identifying general patterns in the data. PLS-DA is a similar but supervised method, where the variance between predefined groups is maximized and thus differences can be identified. Analysis of distinct fatty acids further identified three significantly altered species, however no pattern could be identified (Fig. 22 C). Further profile visualization yielded clustering according to the microbial state (Fig. 22 D), yet high inter-individual variations were detected. Since these analyses yielded no specific pattern in single fatty acid profiles, general classes were analyzed next. Here, a strong trend towards higher total FA present in GF tumors was identified (Fig. 22 E).

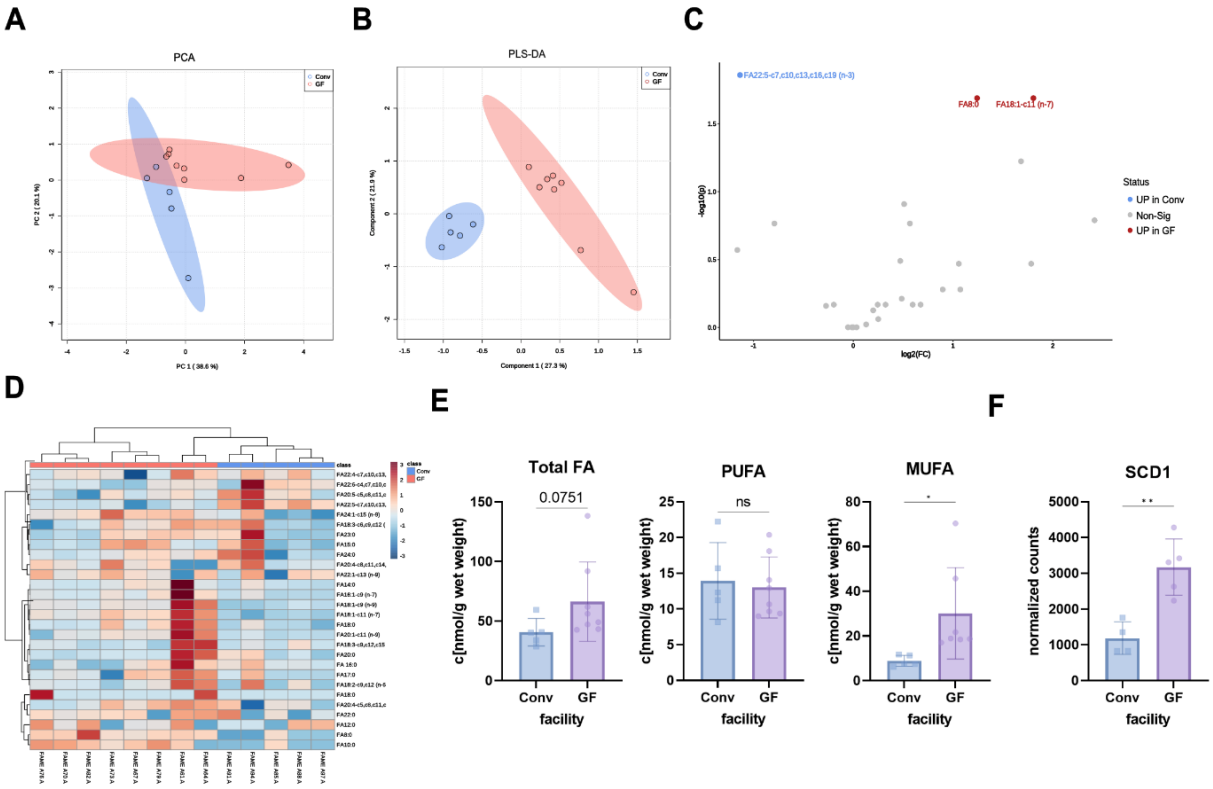

Figure 22: Fatty acid composition in GF and Conv derived tumors

Fatty acid profiles of CD fed murine tumors determined by GC-MS. ***(A)*** *Unsupervised Principal Component Analysis (PCA) of the fatty acid profiles.* ***(B)*** *Supervised Partial Least Squares-Discriminant Analysis (PLS-DA) maximizes differences in components between samples.* ***(C)*** *Volcano plot of FA profiles with significant metabolites marked. Metabolites with an FDR-corrected p value of <0.05 and fold change >2 are considered significant.* ***(D)*** *Heatmap of all FAs measured and arranged using unsupervised Euclidean clustering.* ***(E)*** *Total values of all FAs, PUFAs and MUFAs measured in the intestinal tumors.* ***(F)*** *Expression level of SCD1 determined in the RNA-sequencing experiment. n = 5-8 per group for A-E and n = 4-5 per group for F. Statistically significant results are highlighted with asterisks: * = p < 0.05. ** = p < 0.01, *** = p < 0.001, **** = p < 0.0001*

This is in agreement with the elevated uptake of fatty acids observed. Additionally PUFAs are reportedly altered in colorectal cancer (CRC) and play a role in progression of cancer (Coleman, Ecker and Haller, 2022), however are not influenced by gut microbes (Fig. 22 E). On the other hand, monounsaturated fatty acids (MUFAs) are significantly higher in GF tumors. Two polyunsaturated fatty acids (PUFAs) are essential and have to be consumed by the diet; MUFAs can be synthesized by desaturation of saturated fatty acids (SAFAs). The key enzymes of the desaturation from SAFAs to MUFAs is SCD1 with implications in CRC (Ran *et al.*, 2018) and both the concentrations of MUFAs and the expression of SCD1 were elevated in GF tumors.

Concluding, it can be proposed that the GF environment promotes uptake of luminal, saturated fatty acids into the tissue and that the tumors adapt their metabolic program

towards increased utilization of fatty acids. Whereas the tumors itself had a decreased luminal FA uptake independent of the microbial status, surrounding tissues had an increased uptake in GF mice compared to Conv mice. The altered tumor microenvironment with increased availability of fatty acids led to a surge in desaturation of fatty acids and thus fueled tumor growth in this model of intestinal tumors.

3.3.5. Cholesterol induces changes in gene expression of oncogenes and tumor suppressors

The analysis of gene expression and fat metabolism in Conv and GF intestinal tumors delivers information on how either presence or absence of the gut microbiota influences tumorigenesis. Another question though, which remains unanswered so far, is the influence of dietary cholesterol on the formation and progression of gastrointestinal cancer. The initial scoring of the tumor burden in the Apc^{1638N} yielded an advanced tumor phenotype induced by HFD feeding (Fig. 17 A-E). Adding 0.05 % cholesterol to this HFD reversed this phenotype and resembled a tumor burden similar to CD feeding. This phenotype was only present in Conv mice, absence of microbiota resulted neither in a HFD nor in a cholesterol dependent effect, thus indicating an involvement of gut microbiota.

In order to get a better understanding of the molecular mechanisms driving the cholesterol-induced reduced tumorigenesis, gene expression patterns of the intestinal lesions were analyzed using RNA sequencing. In the previous analysis of all diets and conditions, no diet-induced shift in gene expression pattern was detectable, irrespective of the microbial setting (Fig. 20 A). Additionally, when comparing the distinct features in gene expressions of Conv mice derived tumors in Venn diagrams, every diet showed its unique features (Fig 23 A). The overlaps of differentially expressed genes in comparisons to the other dietary conditions were low, indicating that the suppression of tumorigenesis from CD and cholesterol followed a specific genetic pattern. To assess the effect of the cholesterol supplementation comparison of the two HFDs was thus favorable. In line with the previous analysis, general gene expression patterns displayed no cholesterol specific signature in the PCA, with a wide variety in between each group (Fig. 23 B).

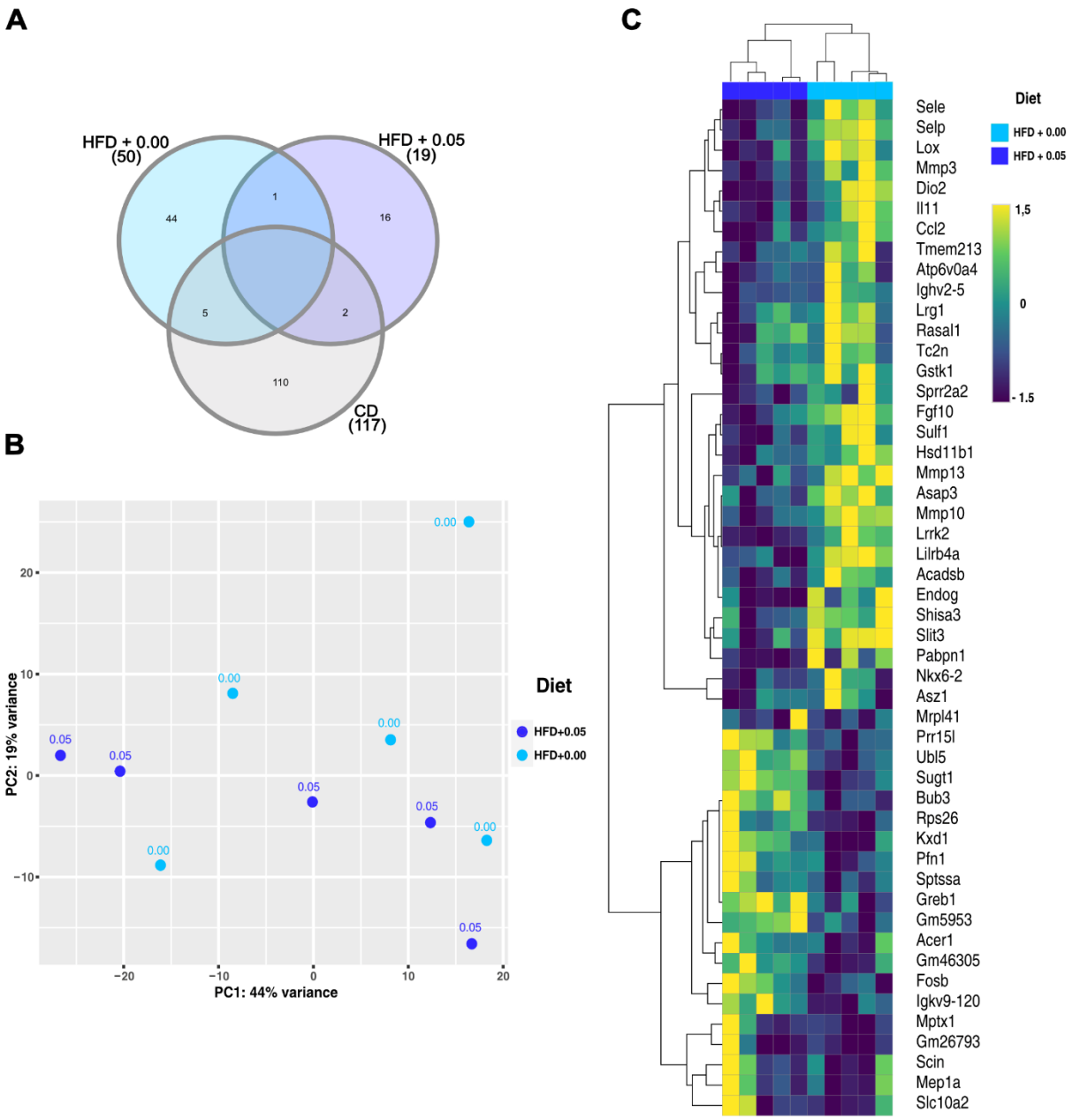

Figure 23: Shifts in gene expression profiles in response to cholesterol

Full length RNA-sequencing of Conv intestinal lesions. ***(A)*** *Venn diagram of significant different expressed genes. Each circle presents the differently expressed genes when compared to the other diets with shared features in between. This gives a first idea of the genetic variance with respect to the tumor phenotype and shows that the induced genes by HFD and/or cholesterol differ from the CD.* ***(B)*** *Unsupervised PCA of tumors derived from Conv mice fed the HFDs without or with 0.05% cholesterol. Transcriptional signatures do not cluster according to diet and show a wide variety in between each group, suggesting that there are rather distinct than global changes in gene expression. Created using DESeq2* ***(C)*** *Heatmap of all significant differential expressed genes (FDR corrected p <0.05) in HFD+0.00 and HFD+0.05 chol tumors. Data are VST-transformed (variance stability transformation) and centered around the mean, clustering of rows and columns is performed using Euclidean distance Created using Morpheus. n = 5 per group for all panel parts.*

This indicates that the expression of specific genes rather than the global genetic program is influenced and defines the tumor pathophysiology. Differential gene expression (DGE) yielded a total of 50 differential expressed transcripts presenting possible candidates for the tumor-suppressive action of cholesterol (Fig. 23 C).

Of the identified transcripts seven displayed a fold change of >2 (Fig. 24 A). Taking into account germ free tumoral expression as a negative control, all 7 of these candidates showed no alteration in microbial absence, confirming the relevance of gut microbiome and diet interactions for their expression (Fig. 24 B). Among these candidates, several have been reported to be implicated in tumorigenesis. Most striking is the increased expression of Selectin E (Sele) and Selectin P (Selp), which showed the two highest scores in significance and fold change (Fig. 24 A and B). The Selectins are a family of cell adhesion molecules, consisting of three members, Selectins L – P and E. Selectin L is expressed in leukocytes, E in endothelial cells and P in platelets and endothelial cells. Functionally, they comprise different functions of cell adhesions and are involved in cell recruitment and inflammation. During inflammation, Selectin P is expressed on endothelial cells first and followed by Selectin E upon demand, which is well reflected by the expression levels observed in this study. Their role in cancer progression and metastasis formation is also established (Borsig, 2018), making them the most promising candidates.

Other candidates, however, also deserve consideration. The role of matrix metalloproteinases (MMPs) in cancer is also well established. Their mechanism of action in tumor progression is promoting neovascularization and subsequent angiogenesis and Epithelial – Mesenchymal Transition (EMT, Quintero-Fabián *et al.*, 2019). MMP3 meets threshold limits for the fold change, however in sum three different MMPs (MMP3, MMP10, MMP13) are significantly higher expressed in the HFD + 0.00 group, underlining their role as possible candidates.

Further candidates involved in tumorigenesis among differential expressed transcripts are the Lysyl Oxidase (LOX) and Iodothyronine Deiodinase (DIO2). The LOX family consists of a group of extracellular copper-dependent enzymes that structure the extracellular matrix (ECM) and can promote tumor growth in CRC (Wang, Hsia and Shieh, 2016). DIO2 was reported to be involved in intestinal tumor growth of $Apc^{\delta 716}$ tumors, which also harbors a KO- of the Apc-gene (Kojima *et al.*, 2019) .

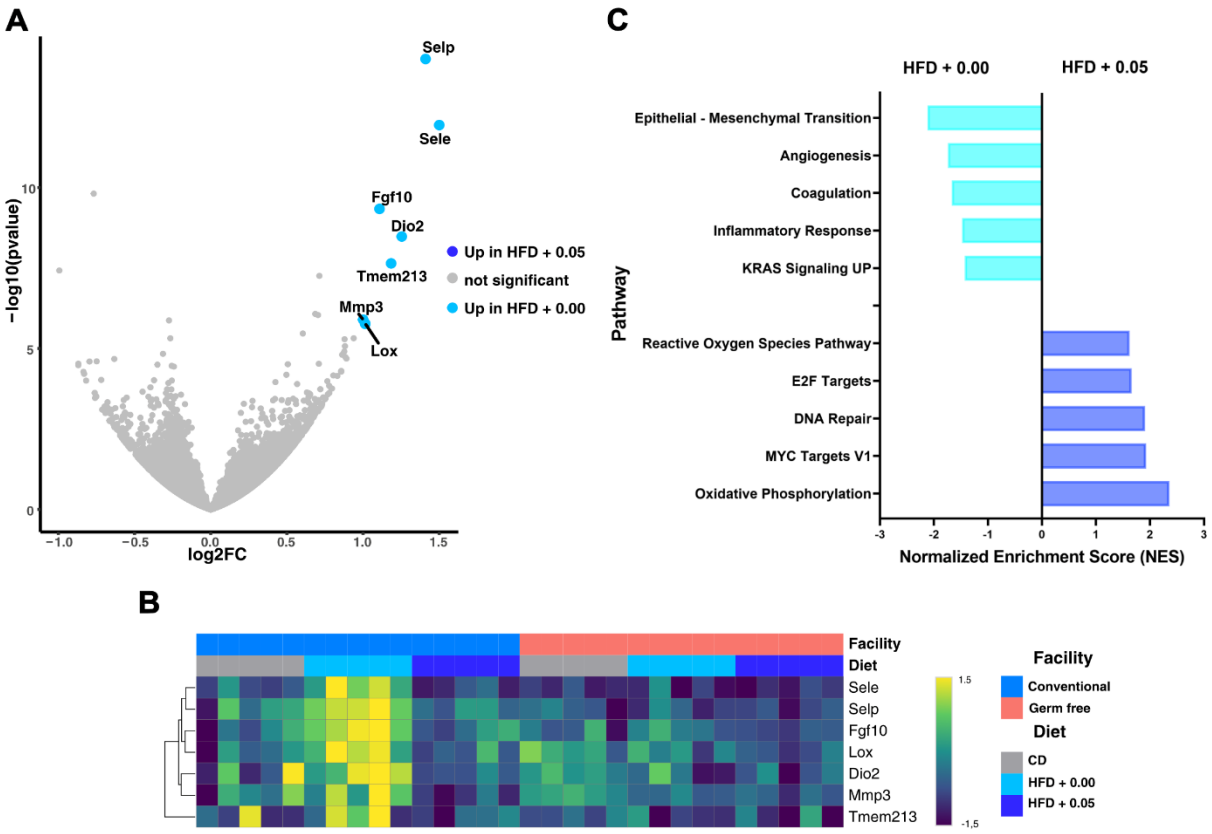

Figure 24: Candidate genes are implicated in tumorigenesis relevant pathways

Data analysis of the RNA-Sequencing was enhanced to identify the most promising candidates. ***(A)*** *Volcano plot of DGE in the HFD +/- cholesterol. No gene met the quality criteria to be significantly upregulated in the cholesterol group. Genes with a FDR corrected p value of <0.05 and a fold change of >2 are considered significant. Created using the galaxy `Volcano plot` tool version 0.0.5.* ***(B)*** *Heatmap with the identified candidates and expression data of all 6 groups indicates that changes in these markers are not induced in GF tumors. Data are VST-transformed (variance stability transformation) and centered around the mean, clustering of rows is performed using Euclidean distance. Created using Morpheus. (C) Gene Set Enrichment Analysis (GSEA) on normalized gene expression of tumors from Conv HFD fed mice. Pathways were assigned on the MDB mouse-ortholog hallmark gene set collection v2022.1 using GSEA version 4.3.2 and all FDR corrected pathways at a significance level of 0.05 are shown. n = 5 for all panel parts.*

In the next step, Gene Set Analysis (GSEA) delivers a more comprehensive view on how the cholesterol dependent induction of these candidates influenced functional changes in the tumors. Starting with the highest enriched pathway by the HFD + 0.00, the EMT, is a complex phenomenon involved in embryonic development and allows tumor becoming more malignant, increasing their invasiveness and metastatic activity (Ribatti, Tamma and Annese, 2020). Additionally, angiogenesis is required for tumor growth to deliver oxygen and nutrients necessary for extensive growth (Lugano, Ramachandran and Dimberg, 2020) as well as the coagulome, which is an essential part of the tumor microenvironment (TME, Galmiche *et al.*, 2022). The enrichment of a general inflammatory response as well as

signaling of KRAS – induced signaling, one of the most important oncogenes in colorectal cancer (Liao *et al.*, 2019), emphasizes on the advanced tumor phenotype present.

Investigation of pathways enriched in cholesterol feeding (HFD + 0.05) delivers a more inconsistent picture than the pro- tumor enriched pathways induced by the HFD + 0.00. On the one hand, potential pro- tumorigenic pathways like oxidative phosphorylation (Ashton *et al.*, 2018), or MYC – targets, a proto-oncogene, are enriched in response to cholesterol. Next, reactive oxygen species (ROS) are necessary at moderate levels for tumor proliferation, but can also trigger programmed cell death such as necroptosis and ferroptosis and can therefore be considered as either pro- or anti-tumorigenic. The same is true for E2F, a family of transcription factors regulating the cell cycle, which can act either as pro– or anti proliferating. On the other hand, the DNA repair pathway is enriched as well, which inhibits excessive proliferation and thus tumor growth. Concluding, in contrast to the oncogenic gene expression profile induced by the HFD + 0.00, the HFD + 0.05 induces enrichment of also anti-proliferative pathways in the tumors.

In order to establish a comprehensive connection between pathways and candidates, a comparative analysis of tumor promoting pathways in the HFD + 0.00 and differential expressed genes was established. The Selectins E and P are involved in a wide variety of cancer progression and growth as well as metastasis formation. Especially because of their concomitant role and the fact that both transcripts are enriched most in the HFD + 0.00 group underlined their importance. Selectin P is able to facilitate platelet adhesion at the site of the tumor and thus promoting growth by angiogenesis, one of the pathways by HFD + 0.00 feeding (Qi *et al.*, 2015). The adhesive platelets at the tumor site also induce activation of the coagulome contributing to tumor progression, which is a pathway induced by the HFD + 0.00 as well (Galmiche *et al.*, 2022). There are also numerous reports on the role of platelet adhesion in EMT, further representing an induced pathway in the absence of cholesterol (Wang *et al.*, 2022). Additionally there are reports on Selectin P to be involved in metastasis formation (Kim *et al.*, 1998). Even though studies on E-Selectin are scarcer, potentially due to the timeline of expression of P and E, there are also report on its involvement in metastasis formation (Kang *et al.*, 2016). Taken together, the upregulated expression of Selectins possibly explains the enriched pathways in the absence of cholesterol, which all contribute to tumor growth, progression and metastasis formation, as observed in the mice. The role of Selectin P in colorectal cancer was investigated in a recent study (Cariello *et al.*, 2021). By crossing a Selp -/- mouse with different mouse models for colorectal and intestinal tumors a cancer related phenotype with reduced tumor growth and

number was discovered, similar to this study. This confirms that Selectins alone are able to induce the observed alterations.

To conclude, tumors derived from mice either fed a no cholesterol diet (HFD + 0.00) or a diet with supplemented cholesterol (HFD + 0.05) differ in gene expression in a limited number of transcripts with Selectins E and P being top regulated. Pathway analysis yields a number of enriched pathways with pro- tumorigenic properties in the absence of cholesterol. The Selectins E and P connect these pathways by 1.) being able to induce them, and 2.) other studies showing the ability of Selectin P to induce a similar phenotype in the mouse model. Thus, the upregulation of Selectin E and P presents the most promising tumor promoting mechanism induced by HFD and repressed by cholesterol.

3.3.6. Cholesterol shifts gut microbiota in tumor bearing intestinal sections

Duodenum

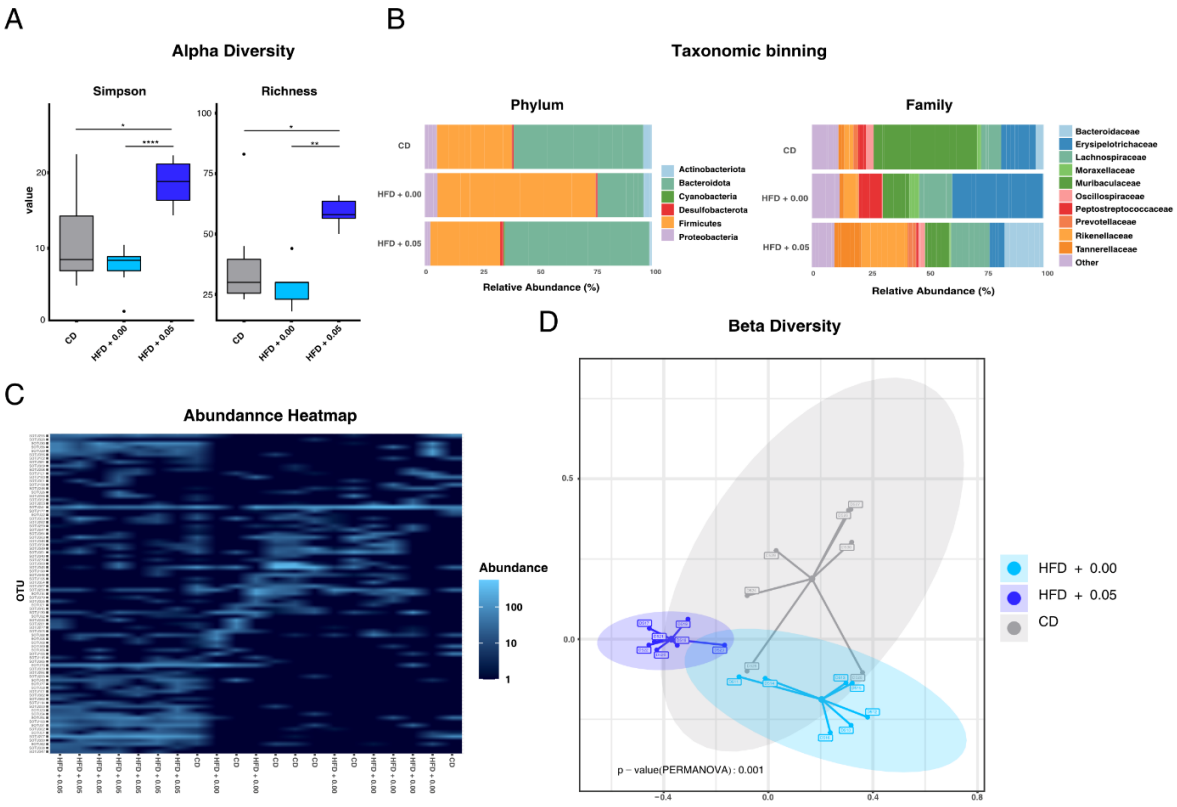

Jejunum

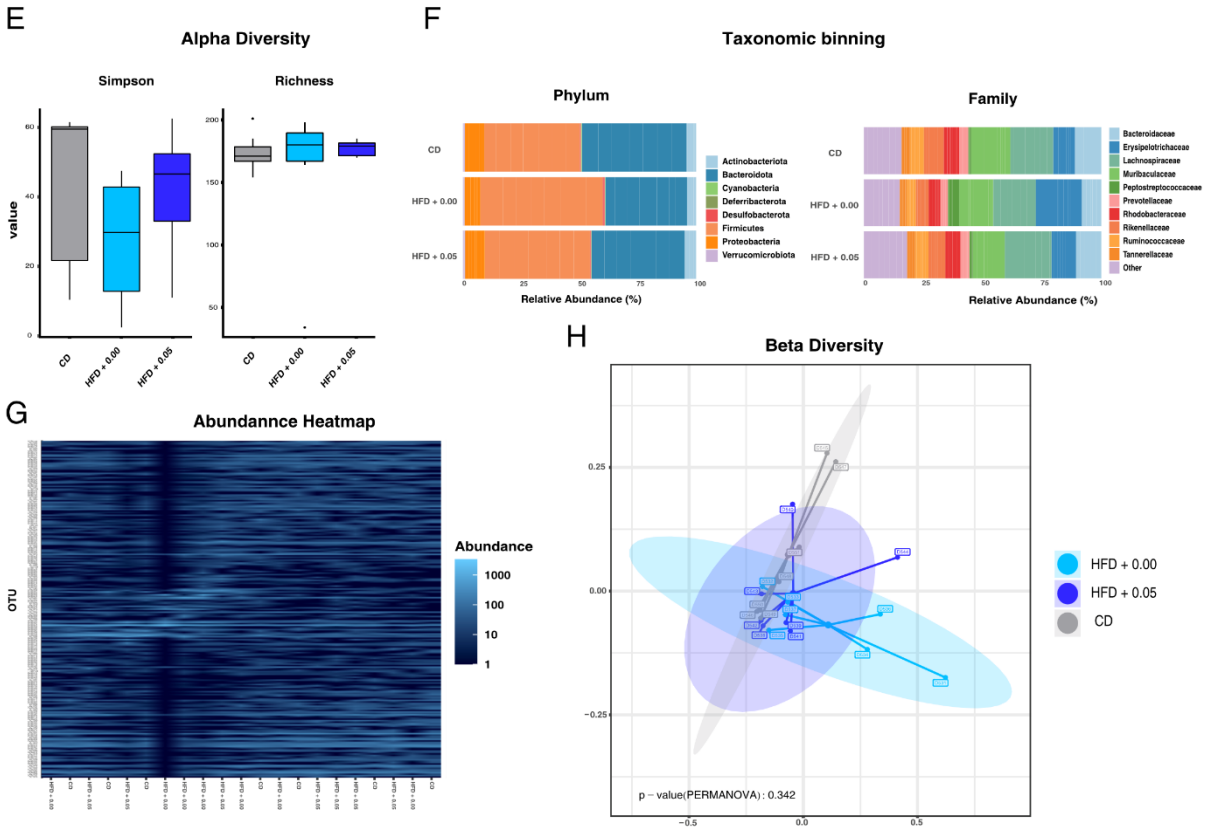

Figure 25: Bacterial signatures affected by HFD and cholesterol in gut sections

Sequencing of the bacterial V3/V4 16S region derived from mucosal scrapings of tumor bearing sections Duodenum and Jejunum. ***(A and E)*** *Bacterial Alpha Diversity presented by the metrics Richness and effective Simpson Index.* ***(B and F)*** *Taxonomic binning on Phylum and on Family level based on the relative bacterial abundance in the groups.* ***(C and G)*** *Abundance of bacterial sequences on OTU/Species level based on Bray-Curtis distance and clustered unsupervised.* ***(D and H)*** *Principle Coordinate Analysis (PCoA) based on Bray-Curtis distance showing dissimilarities in Beta Diversity across the samples. Differences between the samples have been investigated using PERMANOVA-testing across all groups. n = 7 for all groups and panels. Boxplots central bands indicate the median, lower and upper part of the box the respective 25 and 75 percentiles and the whiskers connect data points outside these quartiles. Outliers are indicated as separate points. Statistically significant results are indicated with asterisks: * = p < 0.05. ** = p < 0.01, *** = p < 0.001, **** = p < 0.0001.*

Since a cholesterol dependent altered tumor phenotype was only present in Conv mice and no alterations were detected in GF mice, investigation of gut microbial communities present an interesting target. To assess differences caused by dietary fat and cholesterol intestinal sections bearing tumors were analyzed. This enables the detection of communities in the direct proximity of the lesions and thus the most relevant changes concerning tumorigenesis. 16S sequencing yielded no difference in the Alpha Diversity of duodenal scrapings induced by HFD, however bacterial diversity was significantly increased by cholesterol visible in both Richness and effective Simpson index (Fig. 25 A).

Taxonomic Binning gave more insight into shifts at different stages. At the Phylum level the HFD + 0.00 showed a strong increase in the abundance of *Firmicutes* and a decrease in *Bacteroides* when compared to the CD (Fig. 25 B). Cholesterol supplementation abrogated this shift and manifested with a composition similar to the CD. At the Family level, the shifts were shown in more detail: While the HFD + 0.00 increased the abundance of *Erysipelotrichaceae* and *Peptostreptococcaceae* compared to the CD, the HFD + 0.05 showed a more distinct composition. Notably the increases in abundance of *Bacteroidaceae*, *Rikenellaceae* and *Tannerellaceae* were exclusively induced in the presence of cholesterol. Especially the increase in *Bacteroidaceae* is remarkable, since this family was only negligibly present in the HFD + 0.00 group (0.34 %). Unsupervised clustering additionally showed that this microbial signature is specific to the HFD + 0.05 (Fig. 25 C), which was further visible in the Beta Diversity (Fig. 25 D) and confirmed that signatures differ significantly in the mucus layer of the Duodenum.

The Jejunal situation differed from the clear shifts in the Duodenum. Alpha Diversity yielded no detectable difference in neither Richness nor Simpson Index (Fig. 25 E). Taxonomic Binning showed mild shifts induced by the HFD + 0.00 compared to the CD and reversed by the cholesterol in similar bacterial Phyla and Families as observed in the Duodenum (Fig. 25 F). Further analysis by unsupervised clustering also showed no distinct dietary clustering in the duodenum, induced neither by HFD nor by cholesterol (Fig. 25 G). Analysis of Beta Diversity confirmed this, indicating no detectable difference in the groups (Fig. 25 H). This further confirms the general findings that no diet-induced difference is detectable in the duodenum.

To sum up the findings from the 16S rRNA sequencing based analysis of the intestinal sections significant shifts can be detected in the Duodenum with no or only minor shifts in response to cholesterol in the Jejunum. This corresponds very well with the cholesterol uptake in the gut, which is mainly absorbed in the Duodenum and the proximal Jejunum (Wang, 2003). Additionally, most of the tumors in this mouse model occur in the Duodenum, where the cholesterol - dependent shifts are detected. This highlights the relevance of these shifts and establishes a connection between cholesterol and the altered tumor phenotype in the Conv mice.

3.3.7. Bacterial pathways and enzymes involved in Selectin binding are activated by cholesterol induced bacteria

Next generation 16S sequencing is a well-established tool to identify bacterial species and characterize bacterial signatures and their shifts in health and disease. In this case, distinct changes in the tumor adjacent bacteria were detected. In order to add a mechanistic analysis and identify distinct bacterial enzymes and pathways involved in the tumor – cholesterol phenotype PICRUSt2 (Phylogenetic Investigation of Communities by Reconstruction of Unobserved States, Douglas *et al.*, 2020) based analysis was performed.

Assignment of functional bacterial pathways yielded enrichment of several pathways in the HFD + 0.05 compared to the other two dietary conditions (Fig. 26 A). The fact that only pathways enriched in the HFD + 0.05 can be detected is due to the increased bacterial diversity, which has been discussed previously, and results in a higher variety of pathways and metabolic activity. Several of the pathways, which are significantly altered, have potential implications in the observed tumor phenotype. Pyridoxal 5´phosphate, the active form of vitamin B6, has a wide variety of functions affecting gene expression, metabolism and the immune system. Menaquinol-8 (MK8) is a long, bacterial derived, form of vitamin K2, which is required for blood coagulation. Several pathways related to MK8 are altered in response to diet (superpathway of menaquinol 8 biosynthesis II, 1, 4-dihydroxy-6-naphthoate biosynthesis I+II). The role of the length of the side chains of this vitamin is subject to further research and many variants have been found to harbor anti-cancer activity (Bus and Szterk, 2021).

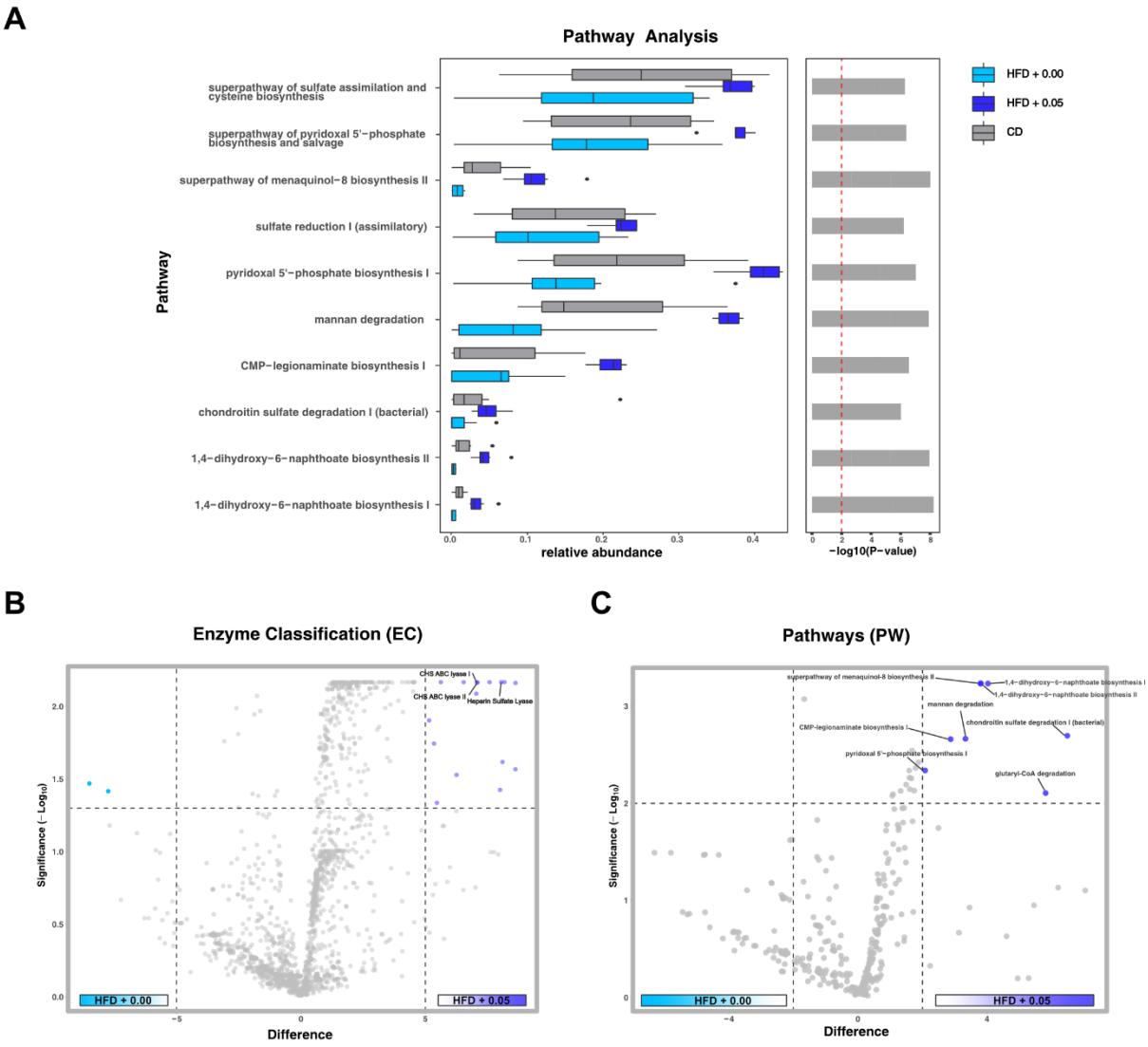

Figure 26: PICRUSt2 based analysis of bacterial enzymes and pathways

PICRUSt2 was used to assign metagenomics functions to the 16S based microbial analysis of the Duodenum. ***(A)*** *Pathway analysis displaying all significant different bacterial pathways in the duodenal section of the three different diet groups. P values < 0.1 are considered significant and data are corrected for multiple testing using the BH method.* ***(B)*** *Volcano plot showing a 2-group comparison of the HFD + 0.00 and the HFD + 0.05 with all differential regulated enzymes based on enzyme classification (EC) number. p < 0.05 is significant, data are BH corrected for multiple testing* ***(C)*** *Pathway analysis displayed as a volcano plot comparing differential pathways in the HFD + 0.00 group and the HFD + 0.05 group. Significant (p < 0.1) pathways are highlighted. n = 7 for all groups and panels. Data are normalized by copy numbers and analysis was performed with the ALDEx2 R-package on the NAMCO-platform. Enzymes and pathways were assigned to bacteria using the Metacyc database (Karp, 2002).*

These pathways were also among the highest regulated when comparing the two HFDs and thus showing the distinct effect of cholesterol (Fig. 26 C). Another interesting aspect was the alteration in mannan degradation, which is a precursor for the CMP-legionaminate biosynthesis I (Fig. 26 A and C). Legionaminate or legionaminic acid is a bacterial sialic acid analogue. Sialic acids are usually found on cell surfaces in all animal tissues with the

highest occurrence in the brain. Hypersialation is also a well-established hallmark of cancer cells in many different cancer types, which leads to cancer progression and metastasis (Dobie and Skropeta, 2021). Binding partner of sialic acids are all three Selectins P- E- and L, where P and E have been found to be upregulated in the absence of cholesterol. In consequence and with respect to the observed phenotype, the increased level of this bacterial analogue of sialic acid possibly influences Selectin dependent signaling and thus tumor progression and growth.

Across the detected significant candidates, several pathways with implications in sulfate metabolism are altered. Two of these pathways (sulfate reduction (assimilatory) I and the superpathway of sulfate assimilation and cysteine biosynthesis) can be regarded as assimilatory and suggest a direct benefit for bacteria. Interestingly a recent publication describes the interaction of dietary cholesterol and the gut microbiome to specifically include the conversion from cholesterol to cholesterol sulfate (Le *et al.*, 2022). The sulfate required for this process is delivered by endogenous sources. This conversion is dependent on *Bacteroides,* a bacterial genus, which is nearly exclusively found in the HFD + 0.05 in the present study (Fig. 26 B). Additionally the bacterial degradation of chondroitin sulfate is enriched in response to cholesterol and presents the pathway with the highest difference in the two HFD conditions (Fig. 26 A and C). On the enzyme level, the two enzymes responsible for the degradation of chondroitin, chondroitin sulfate ABC Endolyase and chondroitin ABC Exolyase are two of the most enriched bacterial enzymes in response to cholesterol (Fig. 26 B). Chondroitin sulfate is a naturally occurring sulfated glycosaminoglycan and important part of the extracellular matrix (ECM). In cancer cell surface chondroitin regulates cancer cell properties like proliferation and invasion (Nadanaka, Tamura and Kitagawa, 2022). Also, it is be able to promote tumor growth and metastasis in breast cancer by the interaction with Selectin P (Cooney *et al.*, 2011). The increased bacterial degradation of chondroitin sulfate might thus be a possible supplier of endogenous sulfate and the sulfuration of cholesterol. This degradation alters the tumor microenvironment and can thus be considered a possible contributor to the observed reduced tumorigenesis in response to cholesterol.

To sum up the bacterial signature in the duodenum induced by dietary cholesterol harbors pathways producing metabolites, which are involved in coagulation thus contribute to the cholesterol dependent reduced tumorigenesis in HFD feeding. Further, bacterial pathways producing the xenobiotic binding partners of Selectins, bacterial sialic acid analogues, are enriched in response to cholesterol. Concomitant, chondroitin, which is a further binding partner of Selectins, is degraded by gut bacteria induced by cholesterol feeding. The

induction in these pathways establishes a connection in the observed mild tumor phenotype and the reduced expression of Selectins in response to cholesterol. Cholesterol induced changes in bacterial communities can thus be identified as drivers for the reduced tumorigenesis in this mouse model of intestinal tumors.

4. Discussion

The association of shifts in the gut microbial communities with several human diseases is a well-established and accepted concept. Functional changes of the gut microbiota are associated with metabolic diseases like obesity (Liu *et al.*, 2017) and related co-morbidities like CVD (Witkowski, Weeks and Hazen, 2020), NAFLD (Aron-Wisnewsky *et al.*, 2020) or T2D (Canfora *et al.*, 2019). Obesity is further considered as one of the main risk factors for colorectal cancer in specific and also for this malignancy changes in gut microbial communities are outlined (Keum and Giovannucci, 2019; Wong and Yu, 2019). Where at first correlation were made on observational findings recent research underwent transition into defining mechanisms of microbiota-host interactions in the pathogenesis of these diseases.

The present study investigates the impact of the lipid cholesterol as a dietary component on host metabolism in relevant disease models. In order to highlight the importance of cholesterol - gut microbiota interactions feeding regimes have been performed in GF and SPF conditions in a comparative manner. Especially with regard to the proposed resistance to obesity in GF mice (Bäckhed *et al.*, 2004, 2007; Rabot *et al.*, 2010) and the identified role of cholesterol (Kübeck *et al.*, 2016) identification of interactions of lipids and the gut microbiota would widen our understanding of the disease pathology. Indeed, the resistance to diet-induced obesity (DIO) was inducible by cholesterol in a dose-specific manner. In the following comparative study the investigation of metabolic changes lead to the identification of an altered bile acid pool and specific cholesterol related microbial signatures, especially in the small intestine. These findings bring further insight into the underlying mechanism of a resistance to DIO in GF mice.

Obesity additionally is one of the main risk factors for colorectal cancer (CRC, Siegel, Miller and Jemal, 2019). This strong interconnection is also directly investigated by the inclusion of a disease model, which adds yet another layer. Further shared features of obesity and CRC are gut microbial shifts. An increased cholesterol intake is additionally considered a risk factor for CRC (Hu *et al.*, 2012). Interestingly, this study identified a lowered tumor burden as results of cholesterol supplementation, which alleviated the effect of HFD induced tumorigenesis. Investigation into the genetic program of the tumors identified general metabolic and immunological changes in GF and Conv derived neoplastic lesions. The cholesterol itself had a more specific effect and reduced the HFD elevated expression levels of the Selectins P & E only in the presence of gut microbiota. In the gut microbial

communities adjacent to these lesions, metabolic pathways producing legionaminate and degrading chondroitin were enriched, both able to interact with Selectins. The relevance of the identification of such a mechanism in a murine model system to widen our understanding of the role gut microbiota in colorectal cancer will be evaluated.

4.1. Protection to diet-induced obesity in germ free mice - a still unresolved puzzle?

Since its first discovery in 2004 (Bäckhed *et al.*, 2004) many studies were conducted to find an underlying mechanism for the resistance to DIO in GF mice, however so far nobody convincingly and reproducibly achieved this. Where some were able to successfully reproduce the original results (Rabot *et al.*, 2010) recent studies failed to a DIO resistant phenotype at all (Logan *et al.*, 2020; Moretti *et al.*, 2021). More specific studies investigating DIO in germ free conditions have focused on dietary quality and composition (Fleissner *et al.*, 2010; Kübeck *et al.*, 2016). Based on the finding by Kübeck et al. where the authors identified the dietary fat type as the primary driver and associated it with global changes in cholesterol homeostasis this study was conducted to directly investigate the impact of dietary cholesterol.

The dose response experiment performed in this study was intended to identify a cholesterol dose, which induces resistance to DIO most efficiently. In GF mice, a cholesterol supplementation of 0.01% was ineffective to induce resistance to DIO, which compares to the cholesterol dose identified in the Kübeck study (0.011 %). This is possibly caused by the counteracting mechanism of phytosterols present exclusively in plant material and influencing cholesterol uptake (Brauner *et al.*, 2012; Gylling and Simonen, 2015). On the contrary, a cholesterol supplementation of 0.05 % led to lowered fat mass as indicated by NMR. It has to be stated, however, that NMR measurements are error prone in GF mice. (Krisko *et al.*, 2020). Regardless, the iWAT fat depot size of the HFD + 0.05 fed mice proved to be decreased in mass after ANCOVA-correction (Kleinert *et al.*, 2018). In combination these measurements indicate a certain degree of resistance to DIO most pronounced in the HFD + 0.05 group.

GF mice are considered gold standard in microbiome research, however the lack of gut microbiota also induces a number of physiological changes (Clavel *et al.*, 2016). AbX treated mice, which have a reduced microbial diversity, have thus been included as a second model. The antibiotic treatment proved to be very efficient in these mice, indicated

by a dramatically decreased bacterial diversity in all metrics evaluated. Fat depot size in these mice showed a trend towards lower mass in the HFD + 0.05 group as observed in the GF mice, albeit non-significant. In addition, the AbX mice exhibited no susceptibility to DIO at all, which indicates that the treatment had systemic offside effects. As a result this model has been excluded from the further experiments performed in this study. Nevertheless, the outcome from the AbX treated mice can still be rated as confirmatory. In both the GF and the AbX mice, a palm-HFD with a supplemented cholesterol concentration of 0.05 % was most efficient in inducing resistance to DIO.

The next experimental step comprised a functional comparison of the 0.05 % cholesterol supplemented to the HFD. In GF mice, the HFD+ 0.05 % cholesterol group exhibited a lower weight gain and iWAT size compared to the group without supplemented cholesterol (HFD +0.00). In contrast, cholesterol induced no significant difference in the final body mass. This is likely caused by the increased number of obese mice in the HFD + 0.00 group, which died before reaching the end of the study and thus biased the data (Fig. S1). Investigation of these deaths yielded an increased number of cecal torsions, a malignancy which is described in GF mice (Djurickovic, Ediger and Hong, 1978; Bolsega *et al.*, 2023). It can therefore be hypothesized that an increased accumulation of body fat favors the occurrence cecal torsions in GF mice. Nonetheless, these results present a clear separation from the same feeding experiment in Conv mice. HF-DIO was induced here irrespective of the cholesterol concentration as visible in body mass and fat depots and final body weight. This definitely hints towards gut microbiome-cholesterol interactions, which counteract the resistance to DIO in response to cholesterol.

Interestingly an effect of cholesterol on obesity development is completely absent in the Apc^{1638N} tumor mice. In this model, both HFDs induce DIO in Conv mice and fail to do so in GF mice. Only a slight difference in body mass is detectable in GF conditions and fat depot masses fail to exhibit a difference. This indicates a general resistance to DIO in GF Apc^{1638N} mice. So far, no literature regarding the susceptibility to DIO in this model in GF conditions exist. It can be assumed that the genetic background is involved. The heterozygous KO of the APC gene leads to a reduced protein level of the APC protein resulting in increased β-catenin signaling. Besides its implication in cancer, the Wnt/ β-catenin pathway has critical and various role in embryonic development and adult tissue homeostasis (Liu *et al.*, 2022). Further studies also identified a role Wnt/ β-catenin in the development of obesity (Wang *et al.*, 2013; Loh *et al.*, 2015). It can thus be hypothesized that disturbance in Wnt/ β-catenin signaling leads to the resistance to DIO in the GF Apc^{1638N} mice. The underlying mechanism

remains elusive so far. Either the absence of gut microbiota or other physiological ablations in the GF model are potential factors further studies would be required.

In conclusion, the hypothesis that dietary cholesterol induces resistance to DIO in a dose and microbiome dependent manner can be confirmed. This adds yet another layer to the discussion of the resistance to DIO in GF mice by confirming the results from Kübeck et al.(Kübeck *et al.*, 2016, GF mice are DIO resistant), and opposing others (Logan *et al.*, 2020; Moretti *et al.*, 2021, GF mice are not DIO resistant). More recent studies have specifically investigated the role of the gut microbiome in obesity related features like energy absorption (Martinez-Guryn *et al.*, 2018; Petersen *et al.*, 2019), appetite regulation (Federico *et al.*, 2016; Jia *et al.*, 2017) and chronic inflammation (Jia *et al.*, 2017). In contrast, this study focuses on defining an obese state under the influence of dietary cholesterol. The next step is thus to include obesity-related features by testing glucose-homeostasis, liver function and atherosclerotic plaque formation. This paves the way to define the role of cholesterol dependent resistance to DIO in GF animals and subsequent implications of the gut microbiome in obesity.

4.1.1. Fatty acid assimilation is not influenced by cholesterol

Obesity develops from an imbalance of higher energy intake than energy expenditure. Ingested energy can either be used by metabolic processes and converted to heat, stored in the body in the form of fat depots or excreted via feces. In previous studies, the resistance to DIO in GF mice has been attributed to an increased fecal output resulting from reduced nutrient absorption (Kübeck *et al.*, 2016). This observation was further enforced by the identification of a HFD induced jejunal bacterial signature, which was able to boost luminal uptake of fatty acids (Martinez-Guryn *et al.*, 2018).

In the present study, cholesterol supplementation to a HFD resulted in an increased fecal energy content in GF mice compared to their Conv counterparts. Although this was, to a lower extent, true in Conv mice this finding was well in line with the observed resistance to DIO in GF mice. In humans, up to 41 % of the fecal energy is contributed by fat, which additionally is higher in germ free mice due to the absence of bacterial mass (Murphy *et al.*, 1991; Martinez-Guryn *et al.*, 2018). Especially with respects to the important role of cholesterol in fatty acid metabolism, a reduced luminal fatty acid uptake in germ free mice fed dietary cholesterol presented an interesting target.

Stable isotope labelling using labelled triglycerides and FFAs presents a comprehensive and targeted approach to analyze luminal fatty acid uptake (Ecker *et al.*, 2012). After 1h, plasma level of both labels yielded no difference in concentration indicating no difference in luminal fatty acid uptake in all groups. Even though this suggests that a decreased uptake of fatty acids can be excluded as potential driver of obesity resistance, the analysis covers only one measurement point. The timeframe of 60 minutes is well suited to track lipid uptake into plasma, yet fails to detect differences in the kinetic character of luminal lipid uptake (Ochiai, 2020). The inclusion of further measurement points would be required to get a comprehensive of the complete luminal fatty acid. In the scope of this study, this was not feasible due to a limited isolator capacity. Especially given the fact, that HFD + 0.05 fed mice excrete feces with higher energy content compared to the HFD + 0.00 group, differences in longer term fatty acid uptake are likely.

4.1.2. Cholesterol- gut microbiota interactions define bile acid profiles

In close connection to the luminal fatty acid uptake are bile acids (BAs), which act as emulsifiers and thus facilitate fatty uptake. Cholesterol induced a 3-fold increase of total BA pool size in the cecum and altered the gall bladder BA pool composition in Conv mice. However, this did not affect the absorption of fatty acids. Besides their role in lipid ingestion, bile acids are important metabolic regulators (Staels and Fonseca, 2009), account for more than 50 % of cholesterol turnover (Lefebvre *et al.*, 2009) and are modified by the gut bacteria (Collins *et al.*, 2023). Since 95% of secreted bile acids are reabsorbed in the ileum, increased cecal BAs indicate a wide range of possible metabolic consequences. Bile acids in Ileum and colon activate the receptors FXR (farnesoid X receptor) and TGR5 (takeda g protein coupled receptor 5) and can influence the central nervous system, the liver, and adipose tissue among others (Wahlström *et al.*, 2016; Mertens *et al.*, 2017). Gut bacteria modify the bile acid pool by dehydration, epimerization and oxidation, which renders their action as important influencers of metabolism (Wahlström *et al.*, 2016; Collins *et al.*, 2023).

While these are just some of the possible metabolic effects of BAs, the vast multitude of possible action leaves wide room for interpretation. Further testing like analysis of gene and protein expression patterns in ileum, colon and liver or systemic metabolomics in response to cholesterol-microbiota interactions are required to decipher the systemic effects of bile acids in this model. Nevertheless, combining FA stable isotope labelling and targeted BA metabolomics defines a direction towards BA signaling and is an important step into elucidating the underlying mechanism of cholesterol-induced resistance to DIO in GF mice.

4.1.3. Glyoxylate shunt- a gut microbial player in obesity?

Gut bacteria are able to affect lipid metabolism (Araújo *et al.*, 2020) and directly modify luminal fatty acid uptake (Miyamoto *et al.*, 2019) and bile acids (Wahlström *et al.*, 2016). Additionally, gut microbial signatures are impacted in an obese state (Canfora *et al.*, 2019). The obesity resistant phenotype, which depends on cholesterol-gut microbiota interactions further renders strong interest in changes in gut microbial communities.

Whereas in humans the highest microbial numbers are found in the colon, in the mouse model the cecum is the place with the highest abundance in the mouse. Analysis of cecal bacterial communities revealed only minor changes in the composition induced by cholesterol. Also on a functional, level no differences in bacterial pathways were detectable, which in conclusion means, that interactions of cecal gut microbiota and cholesterol play a subordinate role in the development of DIO here.

In consequence, focus was shifted on small intestinal microbiota. Even though the microbial diversity and abundance is lower compared to the large bowel and subject to a fast changing environment, small intestinal bacteria play an important role due to the high metabolic activity of the small intestine (Kastl *et al.*, 2020). Interestingly, dietary cholesterol induced segment specific changes in the communities, with either reduced or elevated diversity. On a functional level, communities found in the ileum adaption towards an increased fatty acid synthesis and an alteration in the TCA cycle, the glyoxylate bypass.

The glyoxylate bypass or shunt is a metabolic adaption of bacteria required for growth on fatty acids or acetate (Eoh and Rhee, 2014). In mice, enrichment of this pathway in gut microbiota has been previously reported in HFD feeding (Nicolas *et al.*, 2017). Additionally, gut microbiota also show an adaption towards increased fatty acid synthesis in the Ileum. The increased synthesis of fatty acids here is a possible explanation for the increased energy content of the feces in the HFD + 0.05 group. Furthermore, the glyoxylate shunt has been associated with metabolic disease in general (Proffitt *et al.*, 2022) and with the accumulation of visceral fat in specific (Beaumont *et al.*, 2016). In order to connect these changes in microbial metabolism to the increased cholesterol levels it can be hypothesized that cholesterol is used as primary carbon source for bacterial growth. Bacterial pathways for cholesterol degradation are described and such adaptions, including the glyoxylate shunt have been described in *Mycobacterium tuberculosis* (García, Uhía and Galán, 2012; Serafini *et al.*, 2019). Another possible factor are increased levels of bile acids in the ileum,

which itself have a bactericidal action and regulate gut microbial communities (Collins *et al.*, 2023).

The next question in deciphering the underlying mechanism of the cholesterol-induced resistance to DIO is how the host metabolism is directly shaped by these adaptions. The interplay of increased cholesterol in the gut lumen, increased bile acid levels and resulting changes in the microbial ecosystem represents an interesting finding in response to cholesterol supplementation. The present research highlights the gut microbial glyoxylate bypass as player in metabolic disease and adds an interesting new concept to the role of gut microbiota in obesity.

4.2. Cholesterol-gut microbiota interactions and colorectal cancer

The interplay of dietary fat, cholesterol and the gut microbiota investigated in this study delivers interesting new information in the development of obesity. Obesity itself is further regarded as a primary risk factor for the development of colorectal cancer (Siegel, Miller and Jemal, 2019). Taking a deeper look at the characteristics of colorectal cancer, excessive fat intake (Keum and Giovannucci, 2019) and dietary cholesterol (Hu *et al.*, 2012) are additional related risk factors and are in close connection with an observed microbial dysbiosis in this malignancy. The present setup thus presents a comprehensive and suitable opportunity to study the interplay of these risk factors in the emergence and progressing of colorectal cancer.

4.2.1. The selection of a suitable experimental model

Murine models of intestinal cancer harboring a truncating germline mutation of APC have been used for decades in preclinical research (Jackstadt and Sansom, 2016). A mutation in this gene resembles the human disease of FAP (familial adenomatous coli), but also 80-90% of sporadic CRC cases harbor a mutation in this gene (Powell *et al.*, 1992). Even though development of transgenic models has progressed a lot in recent years, Apc^{min}, the oldest model, is still the most commonly used (Bürtin, Mullins and Linnebacher, 2020).

For this study, the Apc^{1638N} model was chosen. The heterozygous deletion insertion at position 1638 in the Apc gene results in tumor formation after a lag of about 6 months in up to 100 % of the mice (Fodde *et al.*, 1994). One of the main advantages of this model in comparison to the widely used Apc^{min} mouse model is the increased mucosal and submucosal invasion, which also leads to the progression to adenocarcinomas.

Additionally, even though a lag phase of about 6 months produces prolonged experimental periods, this is closer to the human situation, where tumor formation and progression is a matter of years. Especially with this background, a HFD intervention with or without cholesterol can increasingly influence tumor formation after longer intervention periods.

In contrast to the human situation, the Apc^{1638N} mice develop a majority of lesion in the small intestine. This is especially a disadvantage in translating gut-microbiome-host interactions, however can serve a model organism to study cholesterol- gut microbiome interactions.. Another aspect, which has to be considered, is the suitability of a mouse model for germ free studies. There are conflicting results regarding the susceptibility to intestinal tumors with some studies identifying higher (Mizutani *et al.*, 1984; Zhan *et al.*, 2013) tumor incidence in GF or microbiome deficient mice and some lower (Kaur *et al.*, 2018) in different models. In this study, GF animals displayed a clearly elevated tumor burden, which was attributed to a decreased immune infiltration and an elevated metabolic activity. Confounding factors contributing to this discrepancy are first of all the use of different tumor models. Another interesting confounding factor is the diet fed to the animals. Comparing a regular chow diet to the control diet fed in this study, a dramatic increase in tumor burden can be observed in chow feeding (Fig. S2). This emphasizes on the use of purified and defined diets in the study of colorectal cancer as a critical standardization requirement.

Altogether, the investigated interplay of dietary lipids and gut microbiota unites several characteristics relevant to colorectal cancer, which is thus included into this study. Despite the different location of tumor incidence compared to the human situation, the Apc^{1638N} mouse model was chosen. This model enables studying specific interactions of dietary fat and cholesterol and the gut microbiota in a Conv and GF setting and thus is a suitable model.

4.2.2. Cholesterol reduces intestinal tumor formation

A central question in this study is the contribution of obesity and the gut microbiota to the development of intestinal tumors. As there is a close connection in factors contributing to obesity on the one hand and intestinal tumors on the other, dissecting the role of a single factor is challenging. The setup of this study allows an investigation of this interplay, with a special focus on the role of the gut microbiota.

In Conv mice, the feeding of a HFD efficiently induced DIO in the Apc^{1638N}, irrespectively of the cholesterol content. The tumor burden, however, was only significantly increased in

mice fed a HFD without cholesterol, along with HFD and cholesterol specific changes in tumor bearing regions of the GIT. When comparing these findings now to the GF setting, no dietary effect on tumorigenesis can be detected, induced neither by a HFD, nor by cholesterol supplementation. Consequently, a HFD induced elevated tumorigenesis is dependent on the presence of the gut microbiota, which is in line with recent reports (Yang *et al.*, 2022). Interestingly, supplementing cholesterol to this HFD completely ameliorated the HFD induced tumorigenesis. This was especially surprising, since dietary cholesterol intake is considered to be a risk factor for colorectal cancer in humans and that tumors in general require increased cholesterol levels for growth (Hu *et al.*, 2012; Mok and Lee, 2020). This phenotype was specific to Conv mice and absent in germ free mice, it is thus very likely cholesterol-gut microbiota interactions directly influence intestinal tumorigenesis.

In contrast to Conv mice, the absence of microbiota led to an overall increased tumor burden in GF mice. The analysis of gene expression of the bulk tumors yielded a decreased activity of the host immune system on the one hand and an increased metabolic activity in the lesion on the other hand. Both are potential drivers contributing to the increased tumor burden detected in the GF tumors. The reduced activity of the immune system can be attributed to the absence of the gut bacteria, which are well known and important factors in immune system development, maturation and regulation (Wu and Wu, 2012; Zheng, Liwinski and Elinav, 2020). Interestingly, GF tumors showed a higher metabolic activity, with in particular elevated fatty acid metabolism. Fatty acid metabolism is altered in colorectal cancer (Coleman, Ecker and Haller, 2022) and it is widely accepted that an increased availability of fatty acids support tumorigenesis and cancer progression (Koundouros and Poulogiannis, 2020)

4.2.3. Absence of gut microbiota increases tumors dependence on fatty acids

Following this finding, fatty acid uptake into the tumors was directly tracked using a stable isotope labelling approach. Here, two interesting observations were made: First, all tumors analyzed had a reduced uptake of fatty acids compared to healthy tissue. Given the fact that tumors occurred in the small intestine, where also fatty acid uptake is facilitated, this is especially interesting. It indicates, that intestinal tumors fuel their energy needs not via luminal fatty acid uptake but by a systemic supply route. Whereas this was true for both GF and Conv derived tumors, GF mice showed higher uptake of luminal fatty acids in healthy and malignant tissue, which is in conflict with previous reports (Martinez-Guryn *et al.*, 2018). Absence of gut microbiota promoted uptake of saturated fatty acids into malignant as well as healthy tissue, resulting in increased fatty acid related metabolic activity. The metabolic

activity in absence of gut microbiota included several pathways of fatty acid metabolism and in specific and increased activity of fatty acid desaturation. This was unveiled directly by the increased expression of SCD1, the key enzyme of fatty acid desaturation and the increased levels of MUFAs in these tumors. The desaturation of fatty acids presents a key process in cancer metabolism, required for growth and progression of tumors (Vriens *et al.*, 2019).It can thus be hypothesized that increased SCD1 dependent fatty acid desaturation due to a higher availability of fatty acids is the driving factor for the elevated tumor phenotype in GF mice compared to Conv mice

In synopsis of these findings the gut microbiota can be identified as necessary for the HFD and DIO related induction of tumorigenesis, confirming prior findings (Yang *et al.*, 2022). Absence of the gut microbiota resulted in no obesity or HFD related tumor phenotype, but in an overall increased tumor burden and elevated fatty acid metabolism. Stable isotope labelling revealed an increased uptake of saturated fatty acid into primarily healthy tissue. This resulted in higher fatty acid desaturation in the tumors and can thus be identified as driver for the increased tumorigenesis in GF mice.

4.2.4. Selectins and Selectin regulation in colorectal cancer

Following the investigation of differences between GF and Conv derived tumors, special focus was placed on the analysis of Conv tumors, since dietary differences here directly identified dampened tumorigenesis in response to cholesterol-gut microbiome interactions. Feeding the HFD + 0.00 resulted in an increase in tumor burden in the mice compared to feeding the CD. The supplementation of 0.05 % cholesterol to this HFD completely ameliorated this induction, which is one of the most striking and surprising findings of this study.

Dietary cholesterol is generally regarded as a risk factor for colorectal cancer (Järvinen *et al.*, 2001; Hu *et al.*, 2012), so the present result are surprising. A problem about dietary cholesterol as a risk factor is, however, that cholesterol is nearly exclusively contained in dietary products like meat, eggs or seafood. Each of these products contains other components that are considered dietary risk factors for colorectal cancer, which makes assessing the influence of a single component hard and further emphasizes on the need for targeted approaches (O'Keefe, 2016). This study focused on cholesterol as a supplemented component and thus the unbiased effect on tumorigenesis in search of an underlying mechanism.

The absence of dietary cholesterol in the HFD resulted in differential gene expression, and most remarkably, Selectin E and Selectin P were elevated in the tumors. The Selectins are a family of transmembrane proteins comprising three members (E, P & L) named after the cell type in which they are expressed. These are endothelial cells (Selectin E), platelets (Selectin P) and leukocytes (Selectin L), although the Selectins are not exclusively expressed in their respective cell type. Besides their primary role as mediators of cell adhesion all of them have been implicated in cancer immunity (Borsig, 2018). During carcinogenesis, selectins promote various steps in the interactions with tumor cells and blood constituents like platelets and immune cells. With respect to intestinal tumors, Selectin-E mediated binding of colon cancer cells correlates with metastatic potential (Sawada, Tsuboi and Fukuda, 1994). The role of Selectin-P in tumorigenesis is better defined. Selectin-P facilitates platelet adhesion at the site of the tumor and thus promoting angiogenesis (Qi *et al.*, 2015), coagulation (Galmiche *et al.*, 2022) and epithelial-mesenchymal transition (EMT), all of them hallmarks of tumor growth and metastasis formation.

An emerging question here is if the contribution of an increased Selectin expression can explain the elevated tumor phenotype observed in the HFD 0.00 feeding groups. The imminent role of Selectin-P in intestinal tumorigenesis and colorectal cancer has recently been addressed (Cariello *et al.*, 2021). Cariello and colleagues investigated intestinal tumorigenesis in mice carrying a full body knockout of Selectin-P (Selp $^{-/-}$). The formation of tumors was induced either by azoxymethane (AOM) treatment, or by crossing with Apc^{min} mice and thus covers formation of small intestinal tumors as well as tumors in the colon. Knockout of Selectin-P resulted in reduced tumor formation and growth in both models in the small intestine as well as in the colon. This very well resembles the observed tumor phenotype in the absence of cholesterol in this study and confirms elevated Selectin expression as driver of intestinal tumorigenesis, which is further not only relevant in the small intestine but also in the colon of mice.

4.2.5. Connecting dots-Selectin expression and the gut microbiota

After specifying the role of Selectins in colorectal cancer, a question that still remains is the connection between altered gut microbiota and elevated expression of Selectin E & P. 16S sequencing yielded significantly higher diversity in close proximity of the tumors induced by cholesterol. Functional assessment of the consequences of these changes yielded pathways enriched in response to cholesterol. Two of these pathways, the CMP-legionaminate biosynthesis and the chondroitin sulfate degradation were identified to be

able to interact with Selectins and thus present the most interesting changes with respect to the lowered tumorigenesis.

Legionaminate or legionaminic acid is a bacterial derived sialic acid like sugar, which was named after the pathogenic *Legionella pneumophila*. Generally regarded a virulence associated factor, it shares high similarities in absolute configuration to sialic acid, which are required for the binding of glycoproteins to the Selectins (Schoenhofen *et al.*, 2009). The relevance of hypersialation for tumor growth and progression is also known for a long time and well established. (Smith and Bertozzi, 2021) Thus, it can be hypothesized that bacterial synthesis of this sialic acid homologue influences binding properties of the Selectins. This can then further impede binding of platelets to Selectin-P, which is required for tumor growth and progression in colorectal and intestinal cancers (Cariello *et al.*, 2021). This very concise finding exhibits the imminent impact of legionaminic acid binding to Selectin-P on tumor relevant mechanisms like coagulation or EMT.

Another bacterial pathway, which is in close connection to Selectins, is the chondroitin sulfate degradation. Chondroitin sulfate is a sulfated glycosaminoglycan, which is usually found attached to extracellular proteins, thus forming proteoglycans. Upon cancer progression, tumor cells adapt the composition of their glycocalyx and accumulation of chondroitin sulfate has been discovered in squamous cell carcinoma (Chen *et al.*, 2022), prostate cancer (Al-Nakouzi *et al.*, 2022) and breast cancer (Nadanaka, Tamura and Kitagawa, 2022). In breast cancer, it has further been demonstrated that chondroitin sulfate directly interacts with Selectin-P to facilitate metastasis (Monzavi-Karbassi *et al.*, 2007; Cooney *et al.*, 2011). Degradation of cell surface chondrotitin by bacteria could thus inhibit the tumors ability to grow and form metastasis. A chondroitin sulfate chain consists of numerous sugars, which can be sulfated in various quantities and positions. Interestingly, a recent study shows the capability of gut bacteria to utilize cholesterol as a sulfate acceptor (Le *et al.*, 2022). By using a bio-orthogonal labelling approach, the authors demonstrated the distinct ability of commensal gut bacteria to transfer endogenous sulfate to cholesterol as a direct response to dietary cholesterol. Several bacterial genera are implicated in this action and particularly the *Bacteroides* genus shows high sulfotransferase activity. In line with this study, *Bacteroides* are highly enriched in response to dietary cholesterol and nearly not present in the cholesterol – free HFD in tumor bearing sections. Sulfatation patterns of chondroitin, which are functioning as binding motifs, could thus serve as endogenous source of sulfates and in consequence bacterial sulfate degradation changes cancer dependent binding properties of chondroitin.

The cholesterol induced reduced tumorigenesis and the discovery of these pathways calls for further investigation of the direct interaction of gut bacteria and Selectins and chondroitin in colorectal cancer. Careful considerations have to be taken regarding the experimental model system and setup to comprehensively assess these interactions in a meaningful manner. Selectins expression is elevated in colorectal tumors but this fails to be seen in typical model systems like intestinal tumor cell lines or tumor derived organoids. In addition, cholesterol is largely absorbed in the small intestine and only to a much lower extent present in the large intestine, the location, where colorectal cancer typically occurs. A possible solution for this problem is the application of Ezetimibe, a selective inhibitor of NPL1C1. Ezetimibe effectively reduces luminal uptake of cholesterol and in consequence, cholesterol levels in the colon. Moreover, Ezetimibe is shown to increase *Bacteroides* levels in the feces of mice (Jin *et al.*, 2022) and implicated as a potential candidate in colorectal cancer therapy (Gu *et al.*, 2022). Whereas this is mainly attributed to the systemic effect of Ezetimibe, the present proposed mechanism could add another layer to the mechanism of action. Altogether further in vitro and in vivo experiments are required to define the exact mechanism in the cholesterol – gut microbiota dependent tumor suppression.

4.3.Conclusion & Outlook

The present study evaluated the impact of the interplay of dietary lipid and commensal gut microbiota on host metabolism in health and disease. Special focus was placed on interactions with cholesterol, a lipid molecule that can be consumed either with the diet or by endogenous synthesis, with numerous implications in health and disease. By making efficient use of mouse models in conventional and germ free settings consequences of cholesterol-gut microbiota interactions with relevance to the development of obesity and intestinal cancer were investigated.

Previous reports of the involvement of dietary cholesterol in the resistance to DIO observed in GF mice could be confirmed. Employing a dose-response experiment, an optimal concentration of dietary cholesterol was determined, which efficiently induced resistance to DIO in GF and AbX mice. This marks the first major finding of the present study and shows that a single dietary component, the cholesterol, can induce resistance to diet induced obesity in germ free mice. In consequence, metabolic deviations in the host were analyzed to find an underlying mechanism. Even though fatty acid uptake seemingly can be excluded here, future studies should focus on how gut microbiota interacting with lipid species influence intestinal fat uptake. An effect here is in agreement with increased energy and the feces, elevated bile acid levels and the microbial signature identified. This signature is

defined by the glyoxylate bypass, which was already identified to be present in metabolic disease. Further research in this direction should focus on moving from correlations to mechanisms and define the role of the glyoxylate bypass in the gut microbiota. Entangling this interplay can widen our understanding of the role of cholesterol and the gut microbiota in obesity and connected metabolic diseases like NAFLD, T2D and cardiovascular diseases.

In order to investigate the impact of the obesity relevant interplay of gut microbiota and cholesterol, which is not only relevant to obesity but also combines several known risk factors for colorectal cancer analysis has been expanded. By employing a mouse model for intestinal tumors, dietary cholesterol was able to ameliorate HFD induced tumorigenesis only in presence of the gut microbiome. This surprising and striking new finding shows the direct influence of gut microbiome-cholesterol interactions on intestinal tumorigenesis. A combination of high throughput transcriptomic and 16S amplicon sequencing identified the interaction of the Selectins E & P and the gut microbial metabolites legionaminate and the degradation of chondroitin as target inhibitors of tumor growth. This establishes a direct causal link, starting with dietary cholesterol over enrichment of bacterial pathways in response to cholesterol that then in turn influence binding properties of the Selectins P and E, which are required for intestinal and colorectal cancer formation and progression. Further experiments should focus on reproducing and translating these findings to a colon setting to resemble the human situation and redefine the role of gut microbiota and the interaction of lipid species in the progression and growth of colorectal tumors.

References

Al-Nakouzi, N. *et al.* (2022) 'Reformation of the chondroitin sulfate glycocalyx enables progression of AR-independent prostate cancer', *Nature Communications*, 13(1), p. 4760. Available at: https://doi.org/10.1038/s41467-022-32530-7.

Araújo, J.R. *et al.* (2020) 'Fermentation Products of Commensal Bacteria Alter Enterocyte Lipid Metabolism', *Cell Host & Microbe*, 27(3), pp. 358-375.e7. Available at: https://doi.org/10.1016/j.chom.2020.01.028.

Arnold, M. *et al.* (2017) 'Global patterns and trends in colorectal cancer incidence and mortality', *Gut*, 66(4), pp. 683–691. Available at: https://doi.org/10.1136/gutjnl-2015-310912.

Aron-Wisnewsky, J. *et al.* (2020) 'Gut microbiota and human NAFLD: disentangling microbial signatures from metabolic disorders', *Nature Reviews Gastroenterology & Hepatology*, 17(5), pp. 279–297. Available at: https://doi.org/10.1038/s41575-020-0269-9.

Ashton, T.M. *et al.* (2018) 'Oxidative Phosphorylation as an Emerging Target in Cancer Therapy', *Clinical Cancer Research*, 24(11), pp. 2482–2490. Available at: https://doi.org/10.1158/1078-0432.CCR-17-3070.

Bäckhed, F. *et al.* (2004) 'The gut microbiota as an environmental factor that regulates fat storage', *Proceedings of the National Academy of Sciences*, 101(44), pp. 15718–15723. Available at: https://doi.org/10.1073/pnas.0407076101.

Bäckhed, F. *et al.* (2007) 'Mechanisms underlying the resistance to diet-induced obesity in germ-free mice', *Proceedings of the National Academy of Sciences*, 104(3), pp. 979–984. Available at: https://doi.org/10.1073/pnas.0605374104.

Bayer, F. *et al.* (2019) 'Antibiotic Treatment Protocols and Germ-Free Mouse Models in Vascular Research', *Frontiers in Immunology*, 10, p. 2174. Available at: https://doi.org/10.3389/fimmu.2019.02174.

Baynes, J.W. (2014) *Medical biochemistry*. 4. ed. Edinburgh: Saunders Elsevier.

Beaumont, M. *et al.* (2016) 'Heritable components of the human fecal microbiome are associated with visceral fat', *Genome Biology*, 17(1), p. 189. Available at: https://doi.org/10.1186/s13059-016-1052-7.

Benjamini, Y. and Hochberg, Y. (1995) 'Controlling the False Discovery Rate: A Practical and Powerful Approach to Multiple Testing', *Journal of the Royal Statistical Society: Series B (Methodological)*, 57(1), pp. 289–300. Available at: https://doi.org/10.1111/j.2517-6161.1995.tb02031.x.

Bolsega, S. *et al.* (2023) 'The Genetic Background Is Shaping Cecal Enlargement in the Absence of Intestinal Microbiota', *Nutrients*, 15(3), p. 636. Available at: https://doi.org/10.3390/nu15030636.

Bonnet, M. *et al.* (2014) 'Colonization of the Human Gut by E. coli and Colorectal Cancer Risk', *Clinical Cancer Research*, 20(4), pp. 859–867. Available at: https://doi.org/10.1158/1078-0432.CCR-13-1343.

Borsig, L. (2018) ‘Selectins in cancer immunity’, *Glycobiology*, 28(9), pp. 648–655. Available at: https://doi.org/10.1093/glycob/cwx105.

Brauner, R. *et al.* (2012) ‘Phytosterols Reduce Cholesterol Absorption by Inhibition of 27-Hydroxycholesterol Generation, Liver X Receptor α Activation, and Expression of the Basolateral Sterol Exporter ATP-Binding Cassette A1 in Caco-2 Enterocytes’, *The Journal of Nutrition*, 142(6), pp. 981–989. Available at: https://doi.org/10.3945/jn.111.157198.

Bürtin, F., Mullins, C.S. and Linnebacher, M. (2020) ‘Mouse models of colorectal cancer: Past, present and future perspectives’, *World Journal of Gastroenterology*, 26(13), pp. 1394–1426. Available at: https://doi.org/10.3748/wjg.v26.i13.1394.

Bus, K. and Szterk, A. (2021) ‘Relationship between Structure and Biological Activity of Various Vitamin K Forms’, *Foods*, 10(12), p. 3136. Available at: https://doi.org/10.3390/foods10123136.

Calle, E.E. *et al.* (2003) ‘Overweight, obesity, and mortality from cancer in a prospectively studied cohort of U.S. adults’, *The New England Journal of Medicine*, 348(17), pp. 1625–1638. Available at: https://doi.org/10.1056/NEJMoa021423.

Calle, E.E. and Kaaks, R. (2004) ‘Overweight, obesity and cancer: epidemiological evidence and proposed mechanisms’, *Nature Reviews. Cancer*, 4(8), pp. 579–591. Available at: https://doi.org/10.1038/nrc1408.

Canfora, E.E. *et al.* (2019) ‘Gut microbial metabolites in obesity, NAFLD and T2DM’, *Nature Reviews Endocrinology*, 15(5), pp. 261–273. Available at: https://doi.org/10.1038/s41574-019-0156-z.

Cani, P.D. and Jordan, B.F. (2018) ‘Gut microbiota-mediated inflammation in obesity: a link with gastrointestinal cancer’, *Nature Reviews Gastroenterology & Hepatology*, 15(11), pp. 671–682. Available at: https://doi.org/10.1038/s41575-018-0025-6.

Cariello, M. *et al.* (2021) ‘Adhesion of Platelets to Colon Cancer Cells Is Necessary to Promote Tumor Development in Xenograft, Genetic and Inflammation Models’, *Cancers*, 13(16), p. 4243. Available at: https://doi.org/10.3390/cancers13164243.

Carmody, R.N. and Bisanz, J.E. (2023) ‘Roles of the gut microbiome in weight management’, *Nature Reviews Microbiology*, pp. 1–16. Available at: https://doi.org/10.1038/s41579-023-00888-0.

Castro, F. *et al.* (2018) ‘Interferon-Gamma at the Crossroads of Tumor Immune Surveillance or Evasion’, *Frontiers in Immunology*, 9, p. 847. Available at: https://doi.org/10.3389/fimmu.2018.00847.

Chakaroun, R., Massier, L. and Kovacs, P. (2020) ‘Gut Microbiome, Intestinal Permeability, and Tissue Bacteria in Metabolic Disease: Perpetrators or Bystanders?’, *Nutrients*, 12(4), p. 1082. Available at: https://doi.org/10.3390/nu12041082.

Chang, P.V. *et al.* (2014) ‘The microbial metabolite butyrate regulates intestinal macrophage function via histone deacetylase inhibition’, *Proceedings of the National Academy of Sciences*, 111(6), pp. 2247–2252. Available at: https://doi.org/10.1073/pnas.1322269111.

Chen, K. *et al.* (2022) ‘Chondroitin Sulfate Proteoglycan 4 as a Marker for Aggressive Squamous Cell Carcinoma’, *Cancers*, 14(22), p. 5564. Available at: https://doi.org/10.3390/cancers14225564.

Cheon, H. *et al.* (2023) ‘How cancer cells make and respond to interferon-I’, *Trends in Cancer*, 9(1), pp. 83–92. Available at: https://doi.org/10.1016/j.trecan.2022.09.003.

Chomzynski, P. (1987) ‘Single-Step Method of RNA Isolation by Acid Guanidinium Thiocyanate–Phenol–Chloroform Extraction’, *Analytical Biochemistry*, 162(1), pp. 156–159. Available at: https://doi.org/10.1006/abio.1987.9999.

Clavel, T. *et al.* (2016) ‘The mouse gut microbiome revisited: From complex diversity to model ecosystems’, *International Journal of Medical Microbiology*, 306(5), pp. 316–327. Available at: https://doi.org/10.1016/j.ijmm.2016.03.002.

Coleman, O., Ecker, M. and Haller, D. (2022) ‘Dysregulated lipid metabolism in colorectal cancer’, *Current Opinion in Gastroenterology*, 38(2), pp. 162–167. Available at: https://doi.org/10.1097/MOG.0000000000000811.

Collins, S.L. *et al.* (2023) ‘Bile acids and the gut microbiota: metabolic interactions and impacts on disease’, *Nature Reviews Microbiology*, 21(4), pp. 236–247. Available at: https://doi.org/10.1038/s41579-022-00805-x.

Cooney, C.A. *et al.* (2011) ‘Chondroitin sulfates play a major role in breast cancer metastasis: a role for CSPG4 and CHST11gene expression in forming surface P-selectin ligands in aggressive breast cancer cells’, *Breast Cancer Research*, 13(3), p. R58. Available at: https://doi.org/10.1186/bcr2895.

Dalile, B. *et al.* (2019) ‘The role of short-chain fatty acids in microbiota–gut–brain communication’, *Nature Reviews Gastroenterology & Hepatology*, 16(8), pp. 461–478. Available at: https://doi.org/10.1038/s41575-019-0157-3.

Dawson, P.A. and Rudel, L.L. (1999) ‘Intestinal cholesterol absorption’, *Current Opinion in Lipidology*, 10(4), pp. 315–320. Available at: https://doi.org/10.1097/00041433-199908000-00005.

Depommier, C. *et al.* (2019) ‘Supplementation with Akkermansia muciniphila in overweight and obese human volunteers: a proof-of-concept exploratory study’, *Nature Medicine*, 25(7), pp. 1096–1103. Available at: https://doi.org/10.1038/s41591-019-0495-2.

Dietrich, A. *et al.* (2022) ‘Namco: a microbiome explorer’, *Microbial Genomics*, 8(8). Available at: https://doi.org/10.1099/mgen.0.000852.

Djurickovic, S.M., Ediger, R.D. and Hong, C.C. (1978) ‘Volvulus at the i1eocaecal junction in germfree mice’, *Laboratory Animals*, 12(4), pp. 219–220. Available at: https://doi.org/10.1258/002367778781088585.

Dobie, C. and Skropeta, D. (2021) ‘Insights into the role of sialylation in cancer progression and metastasis’, *British Journal of Cancer*, 124(1), pp. 76–90. Available at: https://doi.org/10.1038/s41416-020-01126-7.

Douglas, G.M. *et al.* (2020) ‘PICRUSt2 for prediction of metagenome functions’, *Nature Biotechnology*, 38(6), pp. 685–688. Available at: https://doi.org/10.1038/s41587-020-0548-6.

Drover, V.A. *et al.* (2005) ‘CD36 deficiency impairs intestinal lipid secretion and clearance of chylomicrons from the blood’, *Journal of Clinical Investigation*, 115(5), pp. 1290–1297. Available at: https://doi.org/10.1172/JCI21514.

Ecker, J. *et al.* (2012) 'A rapid GC–MS method for quantification of positional and geometric isomers of fatty acid methyl esters', *Journal of Chromatography B*, 897, pp. 98–104. Available at: https://doi.org/10.1016/j.jchromb.2012.04.015.

Ecker, J. *et al.* (2021) 'The Colorectal Cancer Lipidome: Identification of a Robust Tumor-Specific Lipid Species Signature', *Gastroenterology*, 161(3), pp. 910-923.e19. Available at: https://doi.org/10.1053/j.gastro.2021.05.009.

Eoh, H. and Rhee, K.Y. (2014) 'Methylcitrate cycle defines the bactericidal essentiality of isocitrate lyase for survival of *Mycobacterium tuberculosis* on fatty acids', *Proceedings of the National Academy of Sciences*, 111(13), pp. 4976–4981. Available at: https://doi.org/10.1073/pnas.1400390111.

Fan, Y. and Pedersen, O. (2021) 'Gut microbiota in human metabolic health and disease', *Nature Reviews Microbiology*, 19(1), pp. 55–71. Available at: https://doi.org/10.1038/s41579-020-0433-9.

Federico, A. *et al.* (2016) 'Gastrointestinal Hormones, Intestinal Microbiota and Metabolic Homeostasis in Obese Patients: Effect of Bariatric Surgery', *In Vivo (Athens, Greece)*, 30(3), pp. 321–330.

Flanagan, L. *et al.* (2014) 'Fusobacterium nucleatum associates with stages of colorectal neoplasia development, colorectal cancer and disease outcome', *European Journal of Clinical Microbiology & Infectious Diseases*, 33(8), pp. 1381–1390. Available at: https://doi.org/10.1007/s10096-014-2081-3.

Fleissner, C.K. *et al.* (2010) 'Absence of intestinal microbiota does not protect mice from diet-induced obesity', *British Journal of Nutrition*, 104(6), pp. 919–929. Available at: https://doi.org/10.1017/S0007114510001303.

Fodde, R. *et al.* (1994) 'A targeted chain-termination mutation in the mouse Apc gene results in multiple intestinal tumors.', *Proceedings of the National Academy of Sciences*, 91(19), pp. 8969–8973. Available at: https://doi.org/10.1073/pnas.91.19.8969.

Furusawa, Y. *et al.* (2013) 'Commensal microbe-derived butyrate induces the differentiation of colonic regulatory T cells', *Nature*, 504(7480), pp. 446–450. Available at: https://doi.org/10.1038/nature12721.

Galmiche, A. *et al.* (2022) 'Coagulome and the tumor microenvironment: an actionable interplay', *Trends in Cancer*, 8(5), pp. 369–383. Available at: https://doi.org/10.1016/j.trecan.2021.12.008.

García, J.L., Uhía, I. and Galán, B. (2012) 'Catabolism and biotechnological applications of cholesterol degrading bacteria: Cholesterol degradation', *Microbial Biotechnology*, 5(6), pp. 679–699. Available at: https://doi.org/10.1111/j.1751-7915.2012.00331.x.

Gill, C.I.R. and Rowland, I.R. (2002) 'Diet and cancer: assessing the risk', *The British Journal of Nutrition*, 88 Suppl 1, pp. S73-87. Available at: https://doi.org/10.1079/BJN2002632.

Goedhart, J. and Luijsterburg, M.S. (2020) 'VolcaNoseR is a web app for creating, exploring, labeling and sharing volcano plots', *Scientific Reports*, 10(1), p. 20560. Available at: https://doi.org/10.1038/s41598-020-76603-3.

Gong, J. *et al.* (2020) 'Reprogramming of lipid metabolism in cancer-associated fibroblasts potentiates migration of colorectal cancer cells', *Cell Death & Disease*, 11(4), pp. 1–15. Available at: https://doi.org/10.1038/s41419-020-2434-z.

Gower, J.C. (1966) 'Some Distance Properties of Latent Root and Vector Methods Used in Multivariate Analysis', *Biometrika*, 53(3/4), p. 325. Available at: https://doi.org/10.2307/2333639.

Gu, J. *et al.* (2022) 'Ezetimibe and Cancer: Is There a Connection?', *Frontiers in Pharmacology*, 13, p. 831657. Available at: https://doi.org/10.3389/fphar.2022.831657.

Gylling, H. and Simonen, P. (2015) 'Phytosterols, Phytostanols, and Lipoprotein Metabolism', *Nutrients*, 7(9), pp. 7965–7977. Available at: https://doi.org/10.3390/nu7095374.

Hamosh, M. *et al.* (1981) 'Fat digestion in the newborn. Characterization of lipase in gastric aspirates of premature and term infants', *The Journal of Clinical Investigation*, 67(3), pp. 838–846. Available at: https://doi.org/10.1172/jci110101.

Haslam, D.W. and James, W.P.T. (2005) 'Obesity', *The Lancet*, 366(9492), pp. 1197–1209. Available at: https://doi.org/10.1016/S0140-6736(05)67483-1.

Heumüller-Klug, S. (2015) 'Degradation of intestinal mRNA: A matter of treatment', *World Journal of Gastroenterology*, 21(12), p. 3499. Available at: https://doi.org/10.3748/wjg.v21.i12.3499.

Hu, J. *et al.* (2012) 'Dietary cholesterol intake and cancer', *Annals of Oncology*, 23(2), pp. 491–500. Available at: https://doi.org/10.1093/annonc/mdr155.

Huang, B., Song, B. and Xu, C. (2020) 'Cholesterol metabolism in cancer: mechanisms and therapeutic opportunities', *Nature Metabolism*, 2(2), pp. 132–141. Available at: https://doi.org/10.1038/s42255-020-0174-0.

Jackstadt, R. and Sansom, O.J. (2016) 'Mouse models of intestinal cancer', *The Journal of Pathology*, 238(2), pp. 141–151. Available at: https://doi.org/10.1002/path.4645.

Jakulj, L. *et al.* (2016) 'Transintestinal Cholesterol Transport Is Active in Mice and Humans and Controls Ezetimibe-Induced Fecal Neutral Sterol Excretion', *Cell Metabolism*, 24(6), pp. 783–794. Available at: https://doi.org/10.1016/j.cmet.2016.10.001.

Järvinen, R. *et al.* (2001) 'Dietary fat, cholesterol and colorectal cancer in a prospective study', *British Journal of Cancer*, 85(3), pp. 357–361. Available at: https://doi.org/10.1054/bjoc.2001.1906.

Jia, L., Betters, J.L. and Yu, L. (2011) 'Niemann-pick C1-like 1 (NPC1L1) protein in intestinal and hepatic cholesterol transport', *Annual Review of Physiology*, 73, pp. 239–259. Available at: https://doi.org/10.1146/annurev-physiol-012110-142233.

Jia, Y. *et al.* (2017) 'Butyrate stimulates adipose lipolysis and mitochondrial oxidative phosphorylation through histone hyperacetylation-associated β3 -adrenergic receptor activation in high-fat diet-induced obese mice', *Experimental Physiology*, 102(2), pp. 273–281. Available at: https://doi.org/10.1113/EP086114.

Jin, J. *et al.* (2022) 'Orlistat and ezetimibe could differently alleviate the high-fat diet-induced obesity phenotype by modulating the gut microbiota', *Frontiers in Microbiology*, 13, p. 908327. Available at: https://doi.org/10.3389/fmicb.2022.908327.

Jorgovanovic, D. *et al.* (2020) 'Roles of IFN-γ in tumor progression and regression: a review', *Biomarker Research*, 8(1), p. 49. Available at: https://doi.org/10.1186/s40364-020-00228-x.

Jost, L. (2007) 'PARTITIONING DIVERSITY INTO INDEPENDENT ALPHA AND BETA COMPONENTS', *Ecology*, 88(10), pp. 2427–2439. Available at: https://doi.org/10.1890/06-1736.1.

Juste, C. and Gérard, P. (2021) 'Cholesterol-to-Coprostanol Conversion by the Gut Microbiota: What We Know, Suspect, and Ignore', *Microorganisms*, 9(9), p. 1881. Available at: https://doi.org/10.3390/microorganisms9091881.

Kang, S.-A. *et al.* (2016) 'The effect of soluble E-selectin on tumor progression and metastasis', *BMC Cancer*, 16(1), p. 331. Available at: https://doi.org/10.1186/s12885-016-2366-2.

Karp, P.D. (2002) 'The MetaCyc Database', *Nucleic Acids Research*, 30(1), pp. 59–61. Available at: https://doi.org/10.1093/nar/30.1.59.

Karp, P.D. *et al.* (2019) 'The BioCyc collection of microbial genomes and metabolic pathways', *Briefings in Bioinformatics*, 20(4), pp. 1085–1093. Available at: https://doi.org/10.1093/bib/bbx085.

Kastl, A.J. *et al.* (2020) 'The Structure and Function of the Human Small Intestinal Microbiota: Current Understanding and Future Directions', *Cellular and Molecular Gastroenterology and Hepatology*, 9(1), pp. 33–45. Available at: https://doi.org/10.1016/j.jcmgh.2019.07.006.

Kaur, K. *et al.* (2018) 'Antibiotic-mediated bacteriome depletion in Apc $^{Min/+}$ mice is associated with reduction in mucus-producing goblet cells and increased colorectal cancer progression', *Cancer Medicine*, 7(5), pp. 2003–2012. Available at: https://doi.org/10.1002/cam4.1460.

Kennedy, E.A., King, K.Y. and Baldridge, M.T. (2018) 'Mouse Microbiota Models: Comparing Germ-Free Mice and Antibiotics Treatment as Tools for Modifying Gut Bacteria', *Frontiers in Physiology*, 9, p. 1534. Available at: https://doi.org/10.3389/fphys.2018.01534.

Kenny, D.J. *et al.* (2020) 'Cholesterol Metabolism by Uncultured Human Gut Bacteria Influences Host Cholesterol Level', *Cell Host & Microbe*, 28(2), pp. 245-257.e6. Available at: https://doi.org/10.1016/j.chom.2020.05.013.

Keum, N. and Giovannucci, E. (2019) 'Global burden of colorectal cancer: emerging trends, risk factors and prevention strategies', *Nature Reviews Gastroenterology & Hepatology*, 16(12), pp. 713–732. Available at: https://doi.org/10.1038/s41575-019-0189-8.

Kim, D. *et al.* (2019) 'Graph-based genome alignment and genotyping with HISAT2 and HISAT-genotype', *Nature Biotechnology*, 37(8), pp. 907–915. Available at: https://doi.org/10.1038/s41587-019-0201-4.

Kim, Y.J. *et al.* (1998) 'P-selectin deficiency attenuates tumor growth and metastasis', *Proceedings of the National Academy of Sciences*, 95(16), pp. 9325–9330. Available at: https://doi.org/10.1073/pnas.95.16.9325.

Kindt, A. *et al.* (2018) 'The gut microbiota promotes hepatic fatty acid desaturation and elongation in mice', *Nature Communications*, 9(1), p. 3760. Available at: https://doi.org/10.1038/s41467-018-05767-4.

Kinzler, K.W. and Vogelstein, B. (1996) 'Lessons from Hereditary Colorectal Cancer', *Cell*, 87(2), pp. 159–170. Available at: https://doi.org/10.1016/S0092-8674(00)81333-1.

Kleinert, M. *et al.* (2018) 'Animal models of obesity and diabetes mellitus', *Nature Reviews Endocrinology*, 14(3), pp. 140–162. Available at: https://doi.org/10.1038/nrendo.2017.161.

Ko, C.-W. *et al.* (2020) 'Regulation of intestinal lipid metabolism: current concepts and relevance to disease', *Nature Reviews Gastroenterology & Hepatology*, 17(3), pp. 169–183. Available at: https://doi.org/10.1038/s41575-019-0250-7.

Kojima, Y. *et al.* (2019) 'Stromal iodothyronine deiodinase 2 (DIO 2) promotes the growth of intestinal tumors in *Apc* $^{\Delta 716}$ mutant mice', *Cancer Science*, 110(8), pp. 2520–2528. Available at: https://doi.org/10.1111/cas.14100.

Koundouros, N. and Poulogiannis, G. (2020) 'Reprogramming of fatty acid metabolism in cancer', *British Journal of Cancer*, 122(1), pp. 4–22. Available at: https://doi.org/10.1038/s41416-019-0650-z.

Krisko, T.I. *et al.* (2020) 'Dissociation of Adaptive Thermogenesis from Glucose Homeostasis in Microbiome-Deficient Mice', *Cell Metabolism*, 31(3), pp. 592-604.e9. Available at: https://doi.org/10.1016/j.cmet.2020.01.012.

Kübeck, R. *et al.* (2016) 'Dietary fat and gut microbiota interactions determine diet-induced obesity in mice', *Molecular Metabolism*, 5(12), pp. 1162–1174. Available at: https://doi.org/10.1016/j.molmet.2016.10.001.

Lagkouvardos, I. *et al.* (2016) 'IMNGS: A comprehensive open resource of processed 16S rRNA microbial profiles for ecology and diversity studies', *Scientific Reports*, 6(1), p. 33721. Available at: https://doi.org/10.1038/srep33721.

Lampreht Tratar, U., Horvat, S. and Cemazar, M. (2018) 'Transgenic Mouse Models in Cancer Research', *Frontiers in Oncology*, 8, p. 268. Available at: https://doi.org/10.3389/fonc.2018.00268.

Laqueur, G.L., McDaniel, E.G. and Matsumoto, H. (1967) 'Tumor induction in germfree rats with methylazoxymethanol (MAM) and synthetic MAM acetate', *Journal of the National Cancer Institute*, 39(2), pp. 355–371.

Le, H.H. *et al.* (2022) 'Characterization of interactions of dietary cholesterol with the murine and human gut microbiome', *Nature Microbiology*, 7(9), pp. 1390–1403. Available at: https://doi.org/10.1038/s41564-022-01195-9.

Lefebvre, P. *et al.* (2009) 'Role of Bile Acids and Bile Acid Receptors in Metabolic Regulation', *Physiological Reviews*, 89(1), pp. 147–191. Available at: https://doi.org/10.1152/physrev.00010.2008.

Leystra, A.A. and Clapper, M.L. (2019) 'Gut Microbiota Influences Experimental Outcomes in Mouse Models of Colorectal Cancer', *Genes*, 10(11), p. 900. Available at: https://doi.org/10.3390/genes10110900.

Liao, W. *et al.* (2019) 'KRAS-IRF2 Axis Drives Immune Suppression and Immune Therapy Resistance in Colorectal Cancer', *Cancer Cell*, 35(4), pp. 559-572.e7. Available at: https://doi.org/10.1016/j.ccell.2019.02.008.

Liao, Y., Smyth, G.K. and Shi, W. (2014) 'featureCounts: an efficient general purpose program for assigning sequence reads to genomic features', *Bioinformatics*, 30(7), pp. 923–930. Available at: https://doi.org/10.1093/bioinformatics/btt656.

Liberzon, A. *et al.* (2015) 'The Molecular Signatures Database Hallmark Gene Set Collection', *Cell Systems*, 1(6), pp. 417–425. Available at: https://doi.org/10.1016/j.cels.2015.12.004.

Lichtenstein, P. *et al.* (2000) 'Environmental and Heritable Factors in the Causation of Cancer — Analyses of Cohorts of Twins from Sweden, Denmark, and Finland', *New England Journal of Medicine*, 343(2), pp. 78–85. Available at: https://doi.org/10.1056/NEJM200007133430201.

Liebisch, G. *et al.* (2021) 'The effect of gut microbiota on the intestinal lipidome of mice', *International Journal of Medical Microbiology*, 311(3), p. 151488. Available at: https://doi.org/10.1016/j.ijmm.2021.151488.

Liu, J. *et al.* (2022) 'Wnt/β-catenin signalling: function, biological mechanisms, and therapeutic opportunities', *Signal Transduction and Targeted Therapy*, 7(1), p. 3. Available at: https://doi.org/10.1038/s41392-021-00762-6.

Liu, R. *et al.* (2017) 'Gut microbiome and serum metabolome alterations in obesity and after weight-loss intervention', *Nature Medicine*, 23(7), pp. 859–868. Available at: https://doi.org/10.1038/nm.4358.

Lloyd-Price, J. *et al.* (2017) 'Strains, functions and dynamics in the expanded Human Microbiome Project', *Nature*, 550(7674), pp. 61–66. Available at: https://doi.org/10.1038/nature23889.

Logan, I.E. *et al.* (2020) 'Germ-Free Swiss Webster Mice on a High-Fat Diet Develop Obesity, Hyperglycemia, and Dyslipidemia', *Microorganisms*, 8(4), p. 520. Available at: https://doi.org/10.3390/microorganisms8040520.

Loh, N.Y. *et al.* (2015) 'LRP5 Regulates Human Body Fat Distribution by Modulating Adipose Progenitor Biology in a Dose- and Depot-Specific Fashion', *Cell Metabolism*, 21(2), pp. 262–273. Available at: https://doi.org/10.1016/j.cmet.2015.01.009.

Louis, P., Hold, G.L. and Flint, H.J. (2014) 'The gut microbiota, bacterial metabolites and colorectal cancer', *Nature Reviews Microbiology*, 12(10), pp. 661–672. Available at: https://doi.org/10.1038/nrmicro3344.

Love, M.I., Huber, W. and Anders, S. (2014) 'Moderated estimation of fold change and dispersion for RNA-seq data with DESeq2', *Genome Biology*, 15(12), p. 550. Available at: https://doi.org/10.1186/s13059-014-0550-8.

Lugano, R., Ramachandran, M. and Dimberg, A. (2020) 'Tumor angiogenesis: causes, consequences, challenges and opportunities', *Cellular and Molecular Life Sciences*, 77(9), pp. 1745–1770. Available at: https://doi.org/10.1007/s00018-019-03351-7.

Mardones, P. *et al.* (2001) 'Hepatic cholesterol and bile acid metabolism and intestinal cholesterol absorption in scavenger receptor class B type I-deficient mice', *Journal of Lipid Research*, 42(2), pp. 170–180.

Marquet, P. *et al.* (2009) 'Lactate has the potential to promote hydrogen sulphide formation in the human colon', *FEMS Microbiology Letters*, 299(2), pp. 128–134. Available at: https://doi.org/10.1111/j.1574-6968.2009.01750.x.

Martin, M. (2011) ‘Cutadapt removes adapter sequences from high-throughput sequencing reads’, *EMBnet.journal*, 17(1), p. 10. Available at: https://doi.org/10.14806/ej.17.1.200.

Martinez-Guryn, K. *et al.* (2018) ‘Small Intestine Microbiota Regulate Host Digestive and Absorptive Adaptive Responses to Dietary Lipids’, *Cell Host & Microbe*, 23(4), pp. 458-469.e5. Available at: https://doi.org/10.1016/j.chom.2018.03.011.

McMurdie, P.J. and Holmes, S. (2013) ‘phyloseq: An R Package for Reproducible Interactive Analysis and Graphics of Microbiome Census Data’, *PLoS ONE*. Edited by M. Watson, 8(4), p. e61217. Available at: https://doi.org/10.1371/journal.pone.0061217.

McMurdie, P.J. and Holmes, S. (2014) ‘Waste Not, Want Not: Why Rarefying Microbiome Data Is Inadmissible’, *PLoS Computational Biology*. Edited by A.C. McHardy, 10(4), p. e1003531. Available at: https://doi.org/10.1371/journal.pcbi.1003531.

Mertens, K.L. *et al.* (2017) ‘Bile Acid Signaling Pathways from the Enterohepatic Circulation to the Central Nervous System’, *Frontiers in Neuroscience*, 11, p. 617. Available at: https://doi.org/10.3389/fnins.2017.00617.

Mima, K. *et al.* (2016) ‘Fusobacterium nucleatum in colorectal carcinoma tissue and patient prognosis’, *Gut*, 65(12), pp. 1973–1980. Available at: https://doi.org/10.1136/gutjnl-2015-310101.

Miyamoto, J. *et al.* (2019) ‘Gut microbiota confers host resistance to obesity by metabolizing dietary polyunsaturated fatty acids’, *Nature Communications*, 10(1), p. 4007. Available at: https://doi.org/10.1038/s41467-019-11978-0.

Mizutani, T. *et al.* (1984) ‘Spontaneous polyposis in the small intestine of germ-free and conventionalized BALB/c mice’, *Cancer Letters*, 25(1), pp. 19–23. Available at: https://doi.org/10.1016/S0304-3835(84)80021-X.

Mok, E.H.K. and Lee, T.K.W. (2020) ‘The Pivotal Role of the Dysregulation of Cholesterol Homeostasis in Cancer: Implications for Therapeutic Targets’, *Cancers*, 12(6), p. 1410. Available at: https://doi.org/10.3390/cancers12061410.

Monzavi-Karbassi, B. *et al.* (2007) ‘Chondroitin sulfate glycosaminoglycans as major P-selectin ligands on metastatic breast cancer cell lines’, *International Journal of Cancer*, 120(6), pp. 1179–1191. Available at: https://doi.org/10.1002/ijc.22424.

Moretti, C.H. *et al.* (2021) ‘Germ-free mice are not protected against diet-induced obesity and metabolic dysfunction’, *Acta Physiologica*, 231(3). Available at: https://doi.org/10.1111/apha.13581.

Morrison, K.E. *et al.* (2020) ‘It’s the fiber, not the fat: significant effects of dietary challenge on the gut microbiome’, *Microbiome*, 8(1), p. 15. Available at: https://doi.org/10.1186/s40168-020-0791-6.

Murphy, J.L. *et al.* (1991) ‘Energy content of stools in normal healthy controls and patients with cystic fibrosis.’, *Archives of Disease in Childhood*, 66(4), pp. 495–500. Available at: https://doi.org/10.1136/adc.66.4.495.

Nadanaka, S., Tamura, J. and Kitagawa, H. (2022) ‘Chondroitin Sulfates Control Invasiveness of the Basal-Like Breast Cancer Cell Line MDA-MB-231 Through ROR1’, *Frontiers in Oncology*, 12, p. 914838. Available at: https://doi.org/10.3389/fonc.2022.914838.

Nicolas, S. *et al.* (2017) 'Transfer of dysbiotic gut microbiota has beneficial effects on host liver metabolism', *Molecular Systems Biology*, 13(3), p. 921. Available at: https://doi.org/10.15252/msb.20167356.

Nilsell, K. *et al.* (1983) 'Comparative effects of ursodeoxycholic acid and chenodeoxycholic acid on bile acid kinetics and biliary lipid secretion in humans. Evidence for different modes of action on bile acid synthesis', *Gastroenterology*, 85(6), pp. 1248–1256.

Obesity and overweight (2023). Available at: https://www.who.int/news-room/fact-sheets/detail/obesity-and-overweight (Accessed: 30 May 2023).

Ochiai, M. (2020) 'Evaluating the appropriate oral lipid tolerance test model for investigating plasma triglyceride elevation in mice', *PLoS ONE*, 15(10), p. e0235875. Available at: https://doi.org/10.1371/journal.pone.0235875.

O'Keefe, S.J.D. (2016) 'Diet, microorganisms and their metabolites, and colon cancer', *Nature Reviews Gastroenterology & Hepatology*, 13(12), pp. 691–706. Available at: https://doi.org/10.1038/nrgastro.2016.165.

Ostlund, R.E. (2004) 'Phytosterols and cholesterol metabolism':, *Current Opinion in Lipidology*, 15(1), pp. 37–41. Available at: https://doi.org/10.1097/00041433-200402000-00008.

Pang, Z. *et al.* (2021) 'MetaboAnalyst 5.0: narrowing the gap between raw spectra and functional insights', *Nucleic Acids Research*, 49(W1), pp. W388–W396. Available at: https://doi.org/10.1093/nar/gkab382.

Parker, B.S., Rautela, J. and Hertzog, P.J. (2016) 'Antitumour actions of interferons: implications for cancer therapy', *Nature Reviews Cancer*, 16(3), pp. 131–144. Available at: https://doi.org/10.1038/nrc.2016.14.

Petersen, C. *et al.* (2019) 'T cell–mediated regulation of the microbiota protects against obesity', *Science*, 365(6451), p. eaat9351. Available at: https://doi.org/10.1126/science.aat9351.

Porporato, P.E. *et al.* (2018) 'Mitochondrial metabolism and cancer', *Cell Research*, 28(3), pp. 265–280. Available at: https://doi.org/10.1038/cr.2017.155.

Powell, S.M. *et al.* (1992) 'APC mutations occur early during colorectal tumorigenesis', *Nature*, 359(6392), pp. 235–237. Available at: https://doi.org/10.1038/359235a0.

Proffitt, C. *et al.* (2022) 'Genome-scale metabolic modelling of the human gut microbiome reveals changes in the glyoxylate and dicarboxylate metabolism in metabolic disorders', *iScience*, 25(7), p. 104513. Available at: https://doi.org/10.1016/j.isci.2022.104513.

Qi, C. *et al.* (2015) 'P-selectin-mediated platelet adhesion promotes tumor growth', *Oncotarget*, 6(9), pp. 6584–6596. Available at: https://doi.org/10.18632/oncotarget.3164.

Quail, D.F. and Dannenberg, A.J. (2019) 'The obese adipose tissue microenvironment in cancer development and progression', *Nature reviews. Endocrinology*, 15(3), pp. 139–154. Available at: https://doi.org/10.1038/s41574-018-0126-x.

Quintero-Fabián, S. *et al.* (2019) 'Role of Matrix Metalloproteinases in Angiogenesis and Cancer', *Frontiers in Oncology*, 9, p. 1370. Available at: https://doi.org/10.3389/fonc.2019.01370.

Rabot, S. *et al.* (2010) 'Germ-free C57BL/6J mice are resistant to high-fat-diet-induced insulin resistance and have altered cholesterol metabolism', *The FASEB Journal*, 24(12), pp. 4948–4959. Available at: https://doi.org/10.1096/fj.10-164921.

Ran, H. *et al.* (2018) 'Stearoyl-CoA desaturase-1 promotes colorectal cancer metastasis in response to glucose by suppressing PTEN', *Journal of Experimental & Clinical Cancer Research*, 37(1), p. 54. Available at: https://doi.org/10.1186/s13046-018-0711-9.

Reiter, S. *et al.* (2021) 'Targeted LC-MS/MS Profiling of Bile Acids in Various Animal Tissues', *Journal of Agricultural and Food Chemistry*, 69(36), pp. 10572–10580. Available at: https://doi.org/10.1021/acs.jafc.1c03433.

Reitmeier, S. *et al.* (2020) 'Comparing Circadian Rhythmicity in the Human Gut Microbiome', *STAR Protocols*, 1(3), p. 100148. Available at: https://doi.org/10.1016/j.xpro.2020.100148.

Ribatti, D., Tamma, R. and Annese, T. (2020) 'Epithelial-Mesenchymal Transition in Cancer: A Historical Overview', *Translational Oncology*, 13(6), p. 100773. Available at: https://doi.org/10.1016/j.tranon.2020.100773.

Riedl, R.A. *et al.* (2021) 'Gut Microbiota Represent a Major Thermogenic Biomass', *Function*, 2(3), p. zqab019. Available at: https://doi.org/10.1093/function/zqab019.

Risso, D. *et al.* (2014) 'Normalization of RNA-seq data using factor analysis of control genes or samples', *Nature Biotechnology*, 32(9), pp. 896–902. Available at: https://doi.org/10.1038/nbt.2931.

Röhrig, F. and Schulze, A. (2016) 'The multifaceted roles of fatty acid synthesis in cancer', *Nature Reviews Cancer*, 16(11), pp. 732–749. Available at: https://doi.org/10.1038/nrc.2016.89.

Sawada, R., Tsuboi, S. and Fukuda, M. (1994) 'Differential E-selectin-dependent adhesion efficiency in sublines of a human colon cancer exhibiting distinct metastatic potentials', *The Journal of Biological Chemistry*, 269(2), pp. 1425–1431.

Schoenhofen, I.C. *et al.* (2009) 'The CMP-legionaminic acid pathway in Campylobacter: Biosynthesis involving novel GDP-linked precursors', *Glycobiology*, 19(7), pp. 715–725. Available at: https://doi.org/10.1093/glycob/cwp039.

Sender, R., Fuchs, S. and Milo, R. (2016) 'Revised Estimates for the Number of Human and Bacteria Cells in the Body', *PLOS Biology*, 14(8), p. e1002533. Available at: https://doi.org/10.1371/journal.pbio.1002533.

Serafini, A. *et al.* (2019) 'Mycobacterium tuberculosis requires glyoxylate shunt and reverse methylcitrate cycle for lactate and pyruvate metabolism', *Molecular Microbiology*, 112(4), pp. 1284–1307. Available at: https://doi.org/10.1111/mmi.14362.

Sharonov, G.V. *et al.* (2020) 'B cells, plasma cells and antibody repertoires in the tumour microenvironment', *Nature Reviews Immunology*, 20(5), pp. 294–307. Available at: https://doi.org/10.1038/s41577-019-0257-x.

Shim, J. *et al.* (2009) 'Fatty acid transport protein 4 is dispensable for intestinal lipid absorption in mice', *Journal of Lipid Research*, 50(3), pp. 491–500. Available at: https://doi.org/10.1194/jlr.M800400-JLR200.

Sica, V. *et al.* (2020) 'Oxidative phosphorylation as a potential therapeutic target for cancer therapy', *International Journal of Cancer*, 146(1), pp. 10–17. Available at: https://doi.org/10.1002/ijc.32616.

Siegel, R.L., Miller, K.D. and Jemal, A. (2019) 'Cancer statistics, 2019', *CA: A Cancer Journal for Clinicians*, 69(1), pp. 7–34. Available at: https://doi.org/10.3322/caac.21551.

Smith, B.A.H. and Bertozzi, C.R. (2021) 'The clinical impact of glycobiology: targeting selectins, Siglecs and mammalian glycans', *Nature Reviews Drug Discovery*, 20(3), pp. 217–243. Available at: https://doi.org/10.1038/s41573-020-00093-1.

Snaebjornsson, M.T., Janaki-Raman, S. and Schulze, A. (2020) 'Greasing the Wheels of the Cancer Machine: The Role of Lipid Metabolism in Cancer', *Cell Metabolism*, 31(1), pp. 62–76. Available at: https://doi.org/10.1016/j.cmet.2019.11.010.

Staels, B. and Fonseca, V.A. (2009) 'Bile Acids and Metabolic Regulation', *Diabetes Care*, 32(suppl_2), pp. S237–S245. Available at: https://doi.org/10.2337/dc09-S355.

Steck, S.E. and Murphy, E.A. (2020) 'Dietary patterns and cancer risk', *Nature Reviews Cancer*, 20(2), pp. 125–138. Available at: https://doi.org/10.1038/s41568-019-0227-4.

Steinhart, Z. and Angers, S. (2018) 'Wnt signaling in development and tissue homeostasis', *Development*, 145(11), p. dev146589. Available at: https://doi.org/10.1242/dev.146589.

The Cancer Genome Atlas Network (2012) 'Comprehensive molecular characterization of human colon and rectal cancer', *Nature*, 487(7407), pp. 330–337. Available at: https://doi.org/10.1038/nature11252.

The Galaxy Community *et al.* (2022) 'The Galaxy platform for accessible, reproducible and collaborative biomedical analyses: 2022 update', *Nucleic Acids Research*, 50(W1), pp. W345–W351. Available at: https://doi.org/10.1093/nar/gkac247.

Tilg, H. *et al.* (2018) 'The Intestinal Microbiota in Colorectal Cancer', *Cancer Cell*, 33(6), pp. 954–964. Available at: https://doi.org/10.1016/j.ccell.2018.03.004.

Vriens, K. *et al.* (2019) 'Evidence for an alternative fatty acid desaturation pathway increasing cancer plasticity', *Nature*, 566(7744), pp. 403–406. Available at: https://doi.org/10.1038/s41586-019-0904-1.

Wahlström, A. *et al.* (2016) 'Intestinal Crosstalk between Bile Acids and Microbiota and Its Impact on Host Metabolism', *Cell Metabolism*, 24(1), pp. 41–50. Available at: https://doi.org/10.1016/j.cmet.2016.05.005.

Wang, D.Q.H. (2003) 'New Concepts of Mechanisms of Intestinal Cholesterol Absorption', *Annals of Hepatology*, 2(3), pp. 113–121. Available at: https://doi.org/10.1016/S1665-2681(19)32136-2.

Wang, J. *et al.* (2013) 'Ablation of LGR4 promotes energy expenditure by driving white-to-brown fat switch', *Nature Cell Biology*, 15(12), pp. 1455–1463. Available at: https://doi.org/10.1038/ncb2867.

Wang, T.-H., Hsia, S.-M. and Shieh, T.-M. (2016) 'Lysyl Oxidase and the Tumor Microenvironment', *International Journal of Molecular Sciences*, 18(1), p. 62. Available at: https://doi.org/10.3390/ijms18010062.

Wang, X. *et al.* (2022) 'Platelets involved tumor cell EMT during circulation: communications and interventions', *Cell Communication and Signaling*, 20(1), p. 82. Available at: https://doi.org/10.1186/s12964-022-00887-3.

Warburg, O. (1956) 'On the Origin of Cancer Cells', *Science*, 123(3191), pp. 309–314. Available at: https://doi.org/10.1126/science.123.3191.309.

Willem M de Vos *et al.* (2022) 'Gut microbiome and health: mechanistic insights', *Gut*, 71(5), p. 1020. Available at: https://doi.org/10.1136/gutjnl-2021-326789.

Wit, M. *et al.* (2022) 'When fat meets the gut—focus on intestinal lipid handling in metabolic health and disease', *EMBO Molecular Medicine*, 14(5), p. e14742. Available at: https://doi.org/10.15252/emmm.202114742.

Witkowski, M., Weeks, T.L. and Hazen, S.L. (2020) 'Gut Microbiota and Cardiovascular Disease', *Circulation Research*, 127(4), pp. 553–570. Available at: https://doi.org/10.1161/CIRCRESAHA.120.316242.

Wong, C.C. and Yu, J. (2023) 'Gut microbiota in colorectal cancer development and therapy', *Nature Reviews Clinical Oncology*, 20(7), pp. 429–452. Available at: https://doi.org/10.1038/s41571-023-00766-x.

Wong, S.H. and Yu, J. (2019) 'Gut microbiota in colorectal cancer: mechanisms of action and clinical applications', *Nature Reviews Gastroenterology & Hepatology*, 16(11), pp. 690–704. Available at: https://doi.org/10.1038/s41575-019-0209-8.

Wu, H.-J. and Wu, E. (2012) 'The role of gut microbiota in immune homeostasis and autoimmunity', *Gut Microbes*, 3(1), pp. 4–14. Available at: https://doi.org/10.4161/gmic.19320.

Xu, D. *et al.* (2022) 'Cholesterol sulfate alleviates ulcerative colitis by promoting cholesterol biosynthesis in colonic epithelial cells', *Nature Communications*, 13(1), p. 4428. Available at: https://doi.org/10.1038/s41467-022-32158-7.

Xu, Z., McClure, S. and Appel, L. (2018) 'Dietary Cholesterol Intake and Sources among U.S Adults: Results from National Health and Nutrition Examination Surveys (NHANES), 2001–2014', *Nutrients*, 10(6), p. 771. Available at: https://doi.org/10.3390/nu10060771.

Yang, J. *et al.* (2022) 'High-Fat Diet Promotes Colorectal Tumorigenesis Through Modulating Gut Microbiota and Metabolites', *Gastroenterology*, 162(1), pp. 135-149.e2. Available at: https://doi.org/10.1053/j.gastro.2021.08.041.

Yoon, S.-H. *et al.* (2017) 'Introducing EzBioCloud: a taxonomically united database of 16S rRNA gene sequences and whole-genome assemblies', *International Journal of Systematic and Evolutionary Microbiology*, 67(5), pp. 1613–1617. Available at: https://doi.org/10.1099/ijsem.0.001755.

Zeineldin, M. and Neufeld, K.L. (2013) 'More than two decades of Apc modeling in rodents', *Biochimica et Biophysica Acta (BBA) - Reviews on Cancer*, 1836(1), pp. 80–89. Available at: https://doi.org/10.1016/j.bbcan.2013.01.001.

Zhan, Y. *et al.* (2013) 'Gut microbiota protects against gastrointestinal tumorigenesis caused by epithelial injury', *Cancer Research*, 73(24), pp. 7199–7210. Available at: https://doi.org/10.1158/0008-5472.CAN-13-0827.

Zhang, X. *et al.* (2021) ‘Dietary cholesterol drives fatty liver-associated liver cancer by modulating gut microbiota and metabolites’, *Gut*, 70(4), pp. 761–774. Available at: https://doi.org/10.1136/gutjnl-2019-319664.

Zhang, Y. *et al.* (2014) ‘Effect of various antibiotics on modulation of intestinal microbiota and bile acid profile in mice’, *Toxicology and Applied Pharmacology*, 277(2), pp. 138–145. Available at: https://doi.org/10.1016/j.taap.2014.03.009.

Zheng, D., Liwinski, T. and Elinav, E. (2020) ‘Interaction between microbiota and immunity in health and disease’, *Cell Research*, 30(6), pp. 492–506. Available at: https://doi.org/10.1038/s41422-020-0332-7.

Zou, Z. *et al.* (2020) ‘mTOR signaling pathway and mTOR inhibitors in cancer: progress and challenges’, *Cell & Bioscience*, 10(1), p. 31. Available at: https://doi.org/10.1186/s13578-020-00396-1.

Appendix

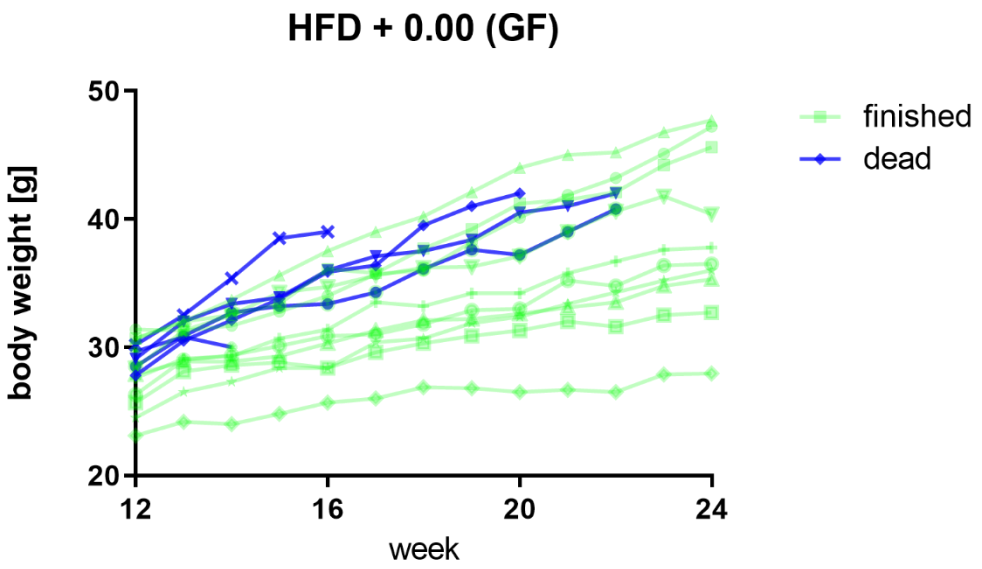

Figure S1 Individual body mass of GF mice fed the HFD + 0.00

Total body mass curves of all GF mice included into the study fed the HFD + 0.00. Every line represents a single mouse. Mice that failed to reach the end of the study are indicated in blue.

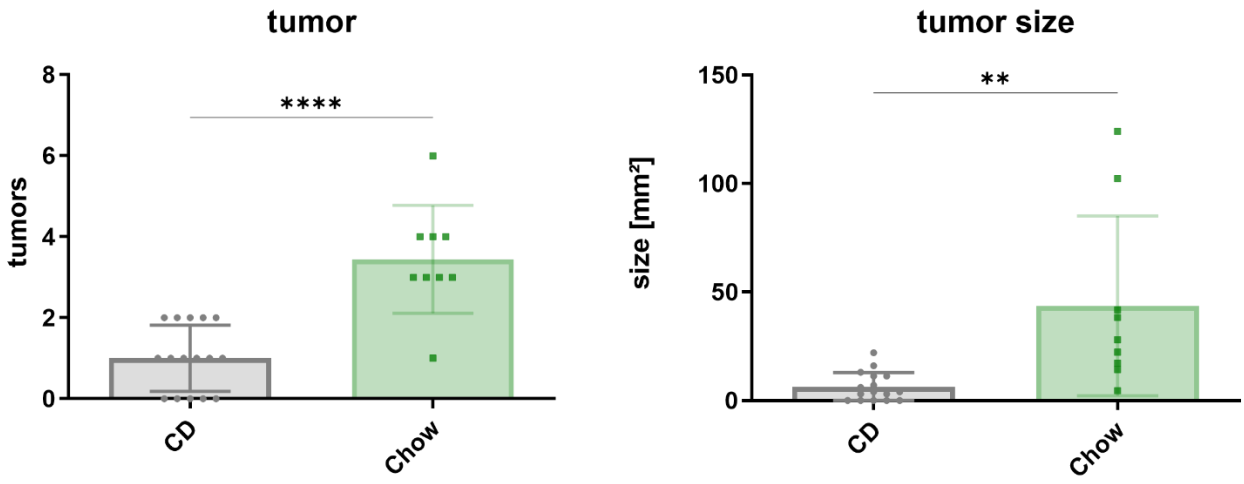

Figure S2 Tumor burden in conventional Apc^{1638N} mice

*Tumor burden of CD and chow fed mice at an age of 32 weeks. Mice were kept under identical conditions except for the diet fed. Males and females are represented in both groups in similar proportions. Mice were either littermates or from different litters of the same breeding pairs. n = 9 for Chow group and n = 16 for CD group. Statistically significant results are highlighted with asterisks: * = p < 0.05. ** = p < 0.01, *** = p < 0.001, **** = p < 0.0001*

Acknowledgements

Without the scientific, technical and mental support of my colleagues, friends and family, this work wouldn´t have been possible. I therefore want to express my deep gratitude.

First of all, I want to thank Prof. Martin Klingenspor for giving me the opportunity to do the underlying research work for this PhD thesis at his chair. He supported me in every aspect the best way he could, encouraged me with great enthusiasm and gave useful advice and guidance.

Further, I want to say thank you to the other group members of the Klingenspor lab. Dr. Tobias Fromme kindly and with great patience reviewed my abstracts and manuscripts like this work and giving advice on how to be a better scientist. Additionally I want to thank the people with whom I shared the office and workplaces at the time of my thesis. Kathi, Anni, Johanna, Josef and Kate supported me by giving me advice when encountering problems listening to all my complaints and motivating me in tough situations. Thanks also go to our technicians Sabine and Manu, who gave excellent technical support.

I also want thank our cooperation partners from the CRC 1371, who provided an excellent scientific environment for the investigation of gut microbiome-host interactions. A special mention here goes to Johannes Plagge, who spent a huge amount of his time dissecting mice with me and provided me with excellent knowledge and input in the lipidomics field.

Last but definitely not least, I want to express my deep gratitude to the persons who supported me off the court. I am incredibly fortunate to have such amazing parents who have made this journey possible with their financial support throughout my whole studies and always believed in me. The best thing that happened to me in this time however is my wonderful girlfriend Alexandra: Thank you for always being there, your presence in my life always brings me joy and strength every day more than words can express.

Publications

Trujillo-Viera, J., El-Merahbi, R., Schmidt, V., Karwen, T., Loza-Valdes, A., **Strohmeyer, A**., Reuter, S., Noh, M., Wit, M., Hawro, I. and Mocek, S., 2021. Protein Kinase D2 drives chylomicron-mediated lipid transport in the intestine and promotes obesity. *EMBO Molecular Medicine*, *13*(5), p.e13548.

Dieckmann, S., **Strohmeyer, A**., Willershäuser, M., Maurer, S.F., Wurst, W., Marschall, S., de Angelis, M.H., Kühn, R., Worthmann, A., Fuh, M.M. and Heeren, J., 2022. Susceptibility to diet-induced obesity at thermoneutral conditions is independent of UCP1. *American Journal of Physiology-Endocrinology and Metabolism*, *322*(2), pp.E85-E100.

Wit, M., Trujillo-Viera, J., **Strohmeyer, A**., Klingenspor, M., Hankir, M. and Sumara, G., 2022. When fat meets the gut—focus on intestinal lipid handling in metabolic health and disease. *EMBO Molecular Medicine*, *14*(5), p.e14742.